122. P. J. Olver, "Evolution equations possessing infinitely many summaries," J. Math. Phys., 18, No. 6, 1212-1215 (1977).
123. L. A. Peletier, "The porous media equation," in: Applications of Nonlinear Analysis in the Physical Sciences, Pitman, Boston–Melbourne (1981), pp. 229-241.
124. P. E. Sacks, "The initial and boundary value problem for a class of degenerate parabolic equations," Commun. Part. Diff. Eqs., 8, No. 7, 693-733 (1983).
125. P. E. Sacks, "Global behavior for a class of nonlinear evolution equations," SIAM J. Math. Anal., 16, No. 2, 233-250 (1985).
126. D. H. Sattinger, "On the total variation of solutions of parabolic equations," Math. Ann., 183, No. 1, 78-92 (1969).
127. M. Schatzman, "Stationary solutions and asymptotic behavior of a quasilinear degenerate parabolic equation," Indiana Univ. Math. J., 33, No. 1, 1-29 (1984).
128. F. B. Weissler, "Local existence and nonexistence for semilinear parabolic equations in L^p," Indiana Univ. Math. J., 29, No. 1, 79-102 (1980).
129. F. B. Weissler, "Single point blow-up for a semilinear initial value problem," J. Diff. Eqs., 55, No. 2, 204-224 (1984).
130. F. B. Weissler, "An L^∞ blow-up estimate for a nonlinear heat equation," Commun. Pure Appl. Math., 38, No. 3, 291-205 (1985).

CLASSIFICATION OF SOLUTIONS OF A SYSTEM OF NONLINEAR DIFFUSION EQUATIONS IN A NEIGHBORHOOD OF A BIFURCATION POINT

T. S. Akhromeeva, S. P. Kurdyumov,
G. G. Malinetskii, and A. A. Samarskii

UDC 517.958

The theory of reaction-diffusion systems in a neighborhood of a bifurcation point is considered. The basic types of space–time ordering, diffusion chaos in such systems, and sequences of bifurcations leading to complication of solutions are studied. A detailed discussion is given of a hierarchy of simplified models (one- and two-dimensional mappings, systems of ordinary differential equations, and others) which make it possible to carry out a qualitative analysis of the problem studied in the case of small regions. A number of generalizations of the equations studied and the simplest types of ordering in the two-dimensional case are described.

1. Two-Component Systems and the Classification Problem

In many systems which are studied in physics, chemistry, and biology there arise self-sustaining structures of various types [24, 32, 36, 40, 42, 62]. The question of the properties of nonlinear media where structures are formed and of the general regularities of their occurrence is one of the fundamental questions of modern science.

We shall characterize the deviation from equilibrium in the systems studied by a parameter λ ($\lambda = 0$ corresponds to the equilibrium state). It follows from classical thermodynamics that the evolution of such a system proceeds in the direction of increasing entropy; any order hereby vanishes. A necessary condition for the existence of stable structures is exchange with an external medium (the system must be open).

For small deviations ($0 < \lambda < \lambda_0$) concepts of linear nonequilibrium thermodynamics are applicable. This theory describes processes in a neighborhood of thermodynamic equilibrium and "... encompasses all cases where the flows (or velocities of irreversible processes) are linear functions of the "thermodynamic forces" (gradients of the temperature or concentrations)" [52]. It has been shown that in this range of parameters a stationary state of the system is close to the equilibrium state (for each value of λ it is unique and stable). It is therefore said that all such states lie on the thermodynamic branch.

Translated from Itogi Nauki i Tekhniki, Seriya Sovremennye Problemy Matematiki, Noveishie Dostizheniya, Vol. 28, 207-313, 1986.

 0090-4104/88/4105-1292$12.50

Off the thermodynamic branch ($\lambda > \lambda_0$) structures of various types can arise. Nonlinear effects play an essential role in their formation. This leads to the necessity of constructing and investigating nonlinear mathematical models. The principles of constructing such models and their connection with concepts of thermodynamics are discussed in the works [52, 70].

Structures arise in open systems to which energy is supplied from without. The energy is transformed and dispersed as a result of dissipative processes whose role turns out to be very large. They determine the number of types of structures, the coordination of processes in different parts of the system, etc. In order to emphasize this circumstance the structures in open, nonlinear systems arising off the thermodynamic branch are called dissipative structures.

The development of the theory of dissipative structures or synergetics has shown that it is possible to distinguish a number of general regularities in the behavior of open, nonlinear systems.

The mathematical models which describe concrete physical, chemical or biological systems may be very complex. In many cases there are systems of nonlinear parabolic equations depending on a number of parameters:

$$\begin{pmatrix} u_1 \\ \vdots \\ u_N \end{pmatrix}_t = \begin{pmatrix} D_1 & & 0 \\ & \ddots & \\ 0 & & D_N \end{pmatrix} \begin{pmatrix} u_1 \\ \vdots \\ u_N \end{pmatrix}_{xx} + \begin{pmatrix} Q_1(u_1, \ldots, u_N, \lambda_1, \ldots, \lambda_m) \\ \vdots \\ Q_N(u_1, \ldots, u_N, \lambda_1, \ldots, \lambda_m) \end{pmatrix}. \tag{1.1}$$

In them, however, it is frequently possible to distinguish a small number of controlling variables to which all others are tuned. The presence of such variables, which are usually order parameters, greatly simplifies the description of the processes. They usually make it possible to describe the behavior of the system at large or small characteristic times [42, 70].

Separation of the order parameters affords the possibility not only of simplifying the model used but in a number of cases of investigating many nonlinear processes within the framework of the same equations. They are usually called base models. One of the most important and widely used base models is the system of equations of the form

$$\begin{aligned} X_t &= D_1 X_{xx} + F_1(X, Y, \lambda), \\ Y_t &= D_2 Y_{xx} + F_2(X, Y, \lambda). \end{aligned} \tag{1.2}$$

Here F_1 and F_2 are nonlinear functions depending on the parameter λ. Equations (1.2), just as (1.1), are frequently called models of reaction-diffusion type.

In spite of the fact that the base model is much simpler than the original problem, it is a complex mathematical object. It is just for this reasons that computational experiment – the combination of a large series of calculations on a computer with extensive use of various analytic methods – plays a major role in the development of the theory of dissipative structures [51, 59, 62, 63]. It is possible to give a number of examples from plasma physics [41, 62, 67], the theory of nonlinear waves [7, 66, 68, 69, 125], biology [21, 36, 48, 56, 86] and other areas where investigation by means of numerical computational experiment preceded experimental discovery of new phenomena, the introduction of new concepts, or the creation of a rigorous mathematical theory.

1.1. Reaction-Diffusion Systems; Description in a Neighborhood of a Bifurcation Point. In recent decades the system of equation (1.2) has been used in modeling a large circle of phenomena in chemistry, ecology, the theory of morphogenesis, the physics of plasma, the theory of combustion, and many other areas. An enormous number of works have been devoted to this model.

The diversity of two-component systems of the form (1.2), the broad area of their application, the necessity of constructing approximate methods, and the performance of a large number of numerical calculations in their analysis lead to the formulation of two questions. First, do there exist common features in the behavior of solutions of Eqs. (1.2) for different right sides? This question is very complex, since the "number of qualitatively different solutions of these equations is so great that up until now no general method of classifying them has been found. In the best case it is possible to construct approximate expressions for some special solutions of the type of stationary solutions or periodic or almost periodic solutions, but without special assurance whether these solutions exhaust all possible bifurcations in the system" [52]).

The second question is whether it is possible to classify two-component systems according to some criteria. The importance of this problem can be judged from the significance classification problems had for the theory of ordinary differential equations and the theory of singularities of differentiable mappings [4, 5, 29]. Classification and separation of general features would make it possible to go over from the investigation of concrete models of special form to the creation of a theory of them and would assist in simplifying the analysis of each concrete problem.

A basic step in this direction was made in 1975 in the work of Kuramoto and Tsuzuki [103]. There exists an analogue of the thermodynamic branch for the majority of open dissipative systems considered in synergetics. For all values of the parameter the equations studied have a spatially homogeneous stationary solution. This solution is stable if $\lambda < \lambda_0$. The behavior of solutions after loss of stability of the thermodynamic branch ($\lambda > \lambda_0$) is determined by the spectrum of the linearized problem for Eq. (1.2) in a neighborhood of the bifurcation point λ_0 [49, 52, 70].

If for $\lambda = \lambda_0$ one simple eigenvalue passes through zero there arise spatially inhomogeneous stationary solutions. Such behavior in the system (1.2) was found by Turing in the investigation of a mathematical model of morphogenesis [120]; it is often called the Turing instability. A typical dependence of the amplitude of the stationary solution A on the parameter λ will be as shown in Fig. 1.

If for $\lambda = \lambda_0$ two complex conjugate eigenvalues intersect the imaginary axis in the $(\mathrm{Re}\mu, \mathrm{Im}\mu)$ plane, where μ is the eigenvalue, then a Hopf bifurcation occurs, and oscillations begin in the system [49].

The equation proposed by Kuramoto and Tsuzuki describes the behavior of both two-component systems in a neighborhood of the bifurcation point λ_0 [103]. It has the form

$$W_T = (\pm 1 + ic_0) W + (1 + ic_1) W_{RR} - (1 + ic_2) W |W|^2. \tag{1.3}$$

Here $W = u + iv$; c_0, c_1, c_2 are real constants whose values are determined on the basis of the coefficients D_1, D_2, the functions $Q_1(X, Y, \lambda)$, $Q_2(X, Y, \lambda)$, and their derivatives. The plus sign on the right side of Eq. (1.3) corresponds to the range of parameters $\lambda > \lambda_0$, while the minus sign corresponds to $\lambda < \lambda_0$.

We shall clarify the meaning of the variables W, R, T. The possibility of going over from systems of the form (1.2) to Eq. (1.3) is connected with the presence of a small parameter $\varepsilon \sim (\lambda - \lambda_0)^{1/2}$. A solution of Eq. (1.2) in this case can be written in the form

$$\begin{pmatrix} X \\ Y \end{pmatrix} = \begin{pmatrix} X_0 \\ Y_0 \end{pmatrix} + \varepsilon [W(R, T) \cdot f + \text{c.c.}] \begin{pmatrix} e_1 \\ e_2 \end{pmatrix}; \quad e_1, e_2 = \text{const}, \tag{1.4}$$

where $\{X_0, Y_0\}$ is the thermodynamic branch; W depends on the slow variables $R = \varepsilon x$, $T = \varepsilon^2 t$, $f = e^{ik_c x}$ in the case of a Turing instability; $f = e^{i\omega_0 t}$ if a Hopf bifurcation occurs. That is, R and T are slow variables determining the modulation in time and space of the simplest solutions f whose form follows from linear analysis.

The functions W(R, T) characterize the deviation of solutions of the system of equations (1.2) from a spatially homogeneous solution. Therefore, Eq. (1.3) describes only those cases when for $\lambda > \lambda_0$ the solution remains in a small neighborhood of the thermodynamic branch. This condition is violated, for example, when a jump occurs to another stable branch (the bifurcation is subcritical; see Fig. 2). Equation (1.3) also does not describe degenerate cases when more than two eigenvalues of the linearized problem intersect the imaginary axis simultaneously. Nevertheless, this equation is applicable to a very broad class of problems and is therefore of great interest. We consider just this equation below.

The study of Eq. (1.3) turns out to be closely related to the problem of classification of two-component systems in a neighborhood of a bifurcation point. Suppose the qualitative features of its solutions (the type of asymptotics, symmetry, etc.) are known for all values c_0, c_1, c_2 and length of the region ℓ. It is then possible to combine into one class all systems of the form (1.2) for which the solutions of Eq. (1.3) behave in a similar manner. This approach turns out to be still more useful if it is possible to set forth effective approximate and qualitative methods of analysis of solutions of different types.

We shall consider in more detail the algorithm of passing from a concrete system of the form (1.2) to Eq. (1.3), following the work [103].

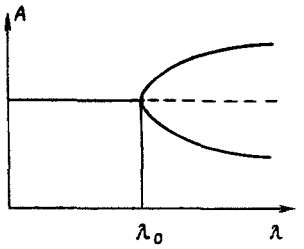

Fig. 1

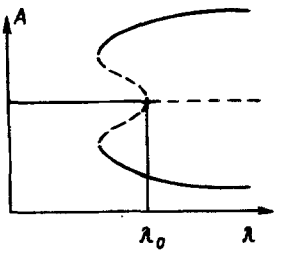

Fig. 2

We rewrite Eqs. (1.2) in vector form, denoting the spatial coordinate by r:

$$\frac{\partial}{\partial t}\mathbf{X}-\hat{\mathbf{D}}\nabla_r^2\mathbf{X}=\mathbf{F}(\mathbf{X}), \tag{1.5}$$

where $\mathbf{X}\equiv\begin{pmatrix}X\\Y\end{pmatrix}$, $\hat{\mathbf{D}}\equiv\begin{pmatrix}D_1&0\\0&D_2\end{pmatrix}$. We transform this equation to

$$\hat{\Gamma}\mathbf{x}=\mathbf{G}(\mathbf{x}), \tag{1.6}$$

where $\mathbf{x}=\mathbf{X}-\mathbf{X}_0$ ($\mathbf{X}_0$ is the thermodynamic branch), $\mathbf{x}\equiv\begin{pmatrix}x\\y\end{pmatrix}$,

$$\hat{\Gamma}\left(-i\frac{\partial}{\partial t},\ -i\nabla_r\right)\equiv\begin{pmatrix}\frac{\partial}{\partial t}+K_{xx}-D_1\nabla_r^2 & K_{xy}\\ K_{yx} & \frac{\partial}{\partial t}+K_{yy}-D_2\nabla_r^2\end{pmatrix}. \tag{1.7}$$

The function $\mathbf{G}\equiv\begin{pmatrix}P\\Q\end{pmatrix}$ in this notation contains only terms nonlinear in $\mathbf{x}$.

Equation (1.6) can be rewritten as

$$\mathscr{L}\mathbf{x}=\hat{\mathbf{L}}\mathbf{G},\quad \hat{\mathbf{L}}\left(-i\frac{\partial}{\partial t},\ -i\nabla_r\right)=\begin{pmatrix}\frac{\partial}{\partial t}+K_{yy}-D_2\nabla_r^2 & -K_{xy}\\ -K_{yx} & \frac{\partial}{\partial t}+K_{xx}-D_1\nabla_r^2\end{pmatrix}, \tag{1.8}$$

where

$$\mathscr{L}\left(-i\frac{\partial}{\partial t},\ -i\nabla_r\right)=\det\hat{\Gamma}. \tag{1.9}$$

Thus, after separation on the right sides of the system (1.2) of terms linear with respect to deviation from the thermodynamic branch, it can be brought to the form (1.6) or (1.8).

Suppose now that

$$\lambda=\lambda_0+\varepsilon^2\lambda_1. \tag{1.10}$$

In a neighborhood of a bifurcation point

$$\begin{pmatrix}K_{\alpha\beta}\\D_m\\\vdots\end{pmatrix}\to\begin{pmatrix}K'_{\alpha\beta}\\D'_m\\\vdots\end{pmatrix}+\varepsilon^2\begin{pmatrix}\gamma_{\alpha\beta}\\d_m\\\vdots\end{pmatrix}+\ldots \tag{1.11}$$

α and β can assume the values x or y, m = 1, 2. $K'_{\alpha\beta}$, D'_m do not depend on ε; we henceforth omit the prime on these terms.

Let

$$T=\varepsilon^2\xi t,\ (\xi>0);\quad R=\varepsilon\chi r \tag{1.12}$$

(χ is a real number),

$$f_\nu=\begin{cases}e^{i\nu k_c r} & \text{(case A, a Turing instability)},\\ e^{i\nu\omega_0 t} & \text{(case B, a Hopf bifurcation)}.\end{cases} \tag{1.13}$$

here $\nu = \pm1, \pm2, \ldots$ (The explicit formulas for ξ, χ, k_c, ω_0 will be derived later.)

The vector of deviations $\mathbf{x}$ can also be represented as a series

$$\mathbf{x}=\sum_{n=1}^{\infty}\varepsilon^n\mathbf{x}_n,\ \text{where}\ \ \mathbf{x}_n=\sum_{\nu=-\infty}^{\infty}\mathbf{x}_n^{(\nu)}(T,R)f_\nu. \tag{1.14}$$

Then for operators $\hat{\Gamma}$, $\mathscr{L}$, $\hat{\mathbf{L}}$, $\mathbf{G}$ we also obtain series:

$$\hat{\Gamma}=\hat{\Gamma}_0+\varepsilon\hat{\Gamma}_1+\ldots,\ \mathscr{L}=\mathscr{L}_0+\varepsilon\mathscr{L}_1+\varepsilon^2\mathscr{L}_2+\ldots,$$
$$\hat{\mathbf{L}}=\hat{\mathbf{L}}_0+\varepsilon\hat{\mathbf{L}}_1+\ldots,\ \mathbf{G}=\varepsilon^2\mathbf{G}_2+\varepsilon^3\mathbf{G}_3+\ldots. \tag{1.15}$$

The operators $\mathscr{L}_n=\mathscr{L}_n\left(-i\frac{\partial}{\partial t},\ -i\nabla_r\right)$ contain $-i\frac{\partial}{\partial t}$ and $-i\nabla_r$. We simplify their notation by setting

$$\mathscr{L}_n(\nu)=\begin{cases}\mathscr{L}_n(0,\ \nu k_c) & \text{(case A)},\\ \mathscr{L}_n(\nu\omega_0,\ 0) & \text{(case B)}.\end{cases} \tag{1.16}$$

The same goes for the operators $\hat{\mathbf{L}}$, $\hat{\Gamma}$, $\mathbf{G}$.

$$\mathbf{x}_1^{(1)}=\mathbf{x}_1^{(-1)*}=\mathbf{a}\xi W(R,\ T),$$
$$\mathbf{x}_1^{(\nu)}=0,\ \nu\neq\pm1, \tag{1.17}$$

where $\mathbf{a}=\begin{pmatrix}1\\ a\end{pmatrix}$

$$a=-\hat{\Gamma}_0(1)_{xx}/\hat{\Gamma}_0(1)_{xy}=-\hat{\Gamma}_0(1)_{yx}/\hat{\Gamma}_0(1)_{yy}=\hat{L}_0(1)_{yy}/\hat{L}_0(1)_{xy}=\hat{L}_0(1)_{yx}/\hat{L}_0(1)_{xx} \tag{1.18}$$

connects the Kuramoto–Tsuzuki equation for the function W(R, T) and the deviation x ($_{xx}$ is the upper left element in the matrix, $_{xy}$ is the second element in the first row, etc.).

The coefficients c_0, c_1, c_2 in Eq. (1.3) and ξ, χ, ζ in formulas (1.12), (1.17) are defined by the formula

$$c_0=\operatorname{Im}\tilde{\gamma}/|\operatorname{Re}\tilde{\gamma}|,\ c_1=\operatorname{Im}\tilde{D}/\operatorname{Re}\tilde{D},\ c_2=\operatorname{Im}\tilde{g}/\operatorname{Re}\tilde{g},$$
$$\xi=|\operatorname{Re}\tilde{\gamma}|,\ \chi^2=|\operatorname{Re}\tilde{\gamma}|/\operatorname{Re}\tilde{D},\ |\zeta|^2=|\operatorname{Re}\tilde{\gamma}|/\operatorname{Re}\tilde{g}, \tag{1.19}$$

where $\tilde{\gamma}$, $\tilde{D}$, and $\tilde{g}$ are defined differently for cases A and B.

Case A (a Turing instability). It follows from linear analysis that at a bifurcation point

$$(K_{xx}D_2-K_{yy}D_1)^2+4K_{xy}K_{yx}D_1D_2=0, \tag{1.20}$$
$$k_c^2=-(K_{xx}D_2+K_{yy}D_1)/(2D_1D_2). \tag{1.21}$$

We shall consider only the case $k_c\neq0$

$$\tilde{\gamma}=-\{(K_{xx}+D_1k_c^2)(\gamma_{yy}+d_2k_c^2)+(K_{yy}+D_2k_c^2)(\gamma_{xx}+d_1k_c^2)-(K_{yx}\gamma_{xy}+K_{xy}\gamma_{yx})\}/\{K_{xx}+K_{yy}+(D_1+D_2)k_c^2\},$$
$$\tilde{D}=-2(D_2K_{xx}+D_1K_{yy})/\{K_{xx}+K_{yy}+(D_1+D_2)k_c^2\}>0, \tag{1.22}$$
$$\tilde{g}=g/\{K_{xx}+K_{yy}+(D_2+D_1)k_c^2\},$$

the quantity g is defined by the formula

$$g=-\left[4\mathscr{L}_0^{-1}(0)\,\mathbf{a}^{\mathrm{T}}\hat{M}_2\hat{\mathbf{L}}_0(0)\begin{pmatrix}\mathbf{a}^{*\mathrm{T}}\hat{P}_2\mathbf{a}\\ \mathbf{a}^{*\mathrm{T}}\hat{Q}_2\mathbf{a}\end{pmatrix}+2\mathscr{L}_0^{-1}(2)\,\mathbf{a}^{*\mathrm{T}}\hat{\mathbf{M}}_2\hat{\mathbf{L}}_0(2)\begin{pmatrix}\mathbf{a}^{\mathrm{T}}\hat{P}_2\mathbf{a}\\ \mathbf{a}^{\mathrm{T}}\hat{Q}_2\mathbf{a}\end{pmatrix}+2\mathbf{a}^{\mathrm{T}}\hat{\mathbf{M}}_3\hat{a}a^*+\mathbf{a}^{*\mathrm{T}}\hat{\mathbf{M}}_3\hat{a}\mathbf{a}\right], \tag{1.23}$$

where $\hat{a}\equiv\begin{pmatrix}1&0\\0&a\end{pmatrix}$, * corresponds to complex conjugation, and $^{\mathrm{T}}$ is transposition.

The terms contained in g are determined from the relations

$$\mathscr{L}_0(0)=K_{xx}K_{yy}-K_{xy}K_{yx},$$
$$\mathscr{L}_0(2)=(K_{xx}+4D_1k_c^2)(K_{yy}+4D_2k_c^2)-K_{xy}K_{yx},$$
$$\hat{\mathbf{L}}_0(0)=\begin{pmatrix}K_{yy}&-K_{xy}\\-K_{yx}&K_{xx}\end{pmatrix},\ \hat{\mathbf{L}}_0(2)=\begin{pmatrix}K_{yy}+4D_2k_c^2&-K_{xy}\\-K_{yx}&K_{xx}+4D_1k_c^2\end{pmatrix}, \tag{1.24}$$
$$\hat{\mathbf{M}}_{2,3}=(K_{yy}+D_2k_c^2)\hat{P}_{2,3}-K_{xy}\hat{Q}_{2,3},$$
$$a=-\frac{K_{xx}+D_1k_c^2}{K_{xy}}=-\frac{K_{yx}}{K_{yy}+D_2k_c^2}.$$

Case B (Hopf bifurcation). At the bifurcation point there are the equalities

$$K_{xx}+K_{yy}=0, \quad \omega_0=\sqrt{K_{xx}K_{yy}-K_{xy}K_{yx}}, \tag{1.25}$$

$\tilde{\gamma}$, $\tilde{D}$, and $\tilde{g}$ are determined by the relations

$$\tilde{\gamma}=-\frac{1}{2}(\gamma_{xx}+\gamma_{yy})+\frac{i}{2\omega_0}\{K_{xx}(\gamma_{yy}-\gamma_{xx})-(K_{xy}\gamma_{yx}+K_{yx}\gamma_{xy})\}, \tag{1.26}$$

$$\tilde{D}=D_+ + iK_{xx}D_-/\omega_0, \quad D_\pm=\frac{1}{2}(D_1\pm D_2), \quad \tilde{g}=-ig/2\omega_0.$$

The quantity g is determined by formula (1.23), and $\mathcal{L}_0(0)$ and $\hat{\mathbf{L}}_0(0)$ are the same as in formulas (1.24). For the other terms contained in g we have the relations

$$\mathcal{L}_0(2)=(2i\omega_0+K_{xx})(2i\omega_0+K_{yy})-K_{xy}K_{yx},$$
$$\hat{\mathbf{L}}_0(2)=\begin{pmatrix}2i\omega_0+K_{yy} & -K_{xy}\\ -K_{yx} & 2i\omega_0+K_{xx}\end{pmatrix}, \quad \hat{\mathbf{M}}_{2,3}=(i\omega_0+K_{yy})\hat{P}_{2,3}- \tag{1.27}$$
$$-K_{xy}\hat{Q}_{2,3}, \quad a=-\frac{(i\omega_0+K_{xx})}{K_{xy}}=-K_{yx}/(i\omega_0+K_{yy}).$$

We shall list the basic steps in going from a concrete system (1.2) to equation (1.3). 1. Separation in Eq. (1.2) of the part linear in the deviation, and reduction to the form (1.6) and (1.8). 2. Expansion in the small parameter ε [formulas (1.11) and (1.15)]. Determination of the values γ_{xx}, γ_{yx}, γ_{xy}, γ_{yy}, d_1, d_2 and $\hat{P}_2$, $\hat{P}_3$, $\hat{Q}_2$, $\hat{Q}_3$. 3. In case A, when relation (1.20) is satisfied, k_c^2, c_0, c_1, c_2 are found in accordance with formulas (1.21)-(1.24) and (1.19). In case B, when relation (1.25) is satisfied, the values of ω_0, c_0, c_1, c_2 are found according to formulas (1.25), (1.26), (1.23), (1.27).

An example of the use of this algorithm for the Brussalator model [$F_1 = A - (B + 1)X + X^2Y$, $F_2 = BX - X^2Y$ in formulas (1.2)], which is widely used in the theory of dissipative structures, is presented in the work [102].

We focus attention on the difference of this approach connected with multiscale expansions from traditional methods of bifurcation theory [39]. In that theory solutions of known form (stationary or periodic) are usually investigated in a neighborhood of an analogue of the thermodynamic branch. Here an equation is obtained which generates such solutions. This method can be compared with the results of Chapman and Enskog on the derivation of the equations of hydrodynamics from the Boltzmann equation [98].

1.2. Other Problems Leading to the Kuramoto-Tsuzuki Equation. The range of applicability of Eq. (1.3) is not exhausted by the analysis of two-component systems of the form (1.2). It is of great interest in many physical problems. In particular, in the work [2] for the investigation of wind waves on water the following equation was suggested:

$$a_t-i\varkappa a_{xx}-iqa_{yy}-i\alpha|a|^2a=\gamma_0 a+i\delta a_t+\beta a_{xx}+\nu a_{yy}-\rho|a|^2a.$$

Special cases of it were considered for Poiseuille flow [115], for ion-sonic waves in a plasma [55], and also for Tollmin-Schliching waves [92]. A number of important and interestimg effects can be investigated by studying its one-dimensional analogue which coincides with (1.3).

In many problems of nonlinear optics and hydrodynamics, in particular, in the theory of waves of finite amplitude on the surface of a deep liquid the Schrödinger equation with a cubic nonlinearity is used [66, 68, 125]. This equation has an infinite number of conservation laws; typical solutions of it are solitons [68]. In those cases where it is necessary to consider dissipative processes, sources, and sinks Eq. (1.3) occurs; solutions of it may behave in a completely different manner.

Equation (1.3) was used in the analysis of order arising in active biological media [21, 97] and for the investigation of autowave processes in oscillating chemical reactions [90]. There is reason to suppose that the behavior of perturbations in many nonequilibrium processes for small supercriticality is described by this equation. The importance and generality of this approach are indicated by the authors of the work [2] in which an analogy is drawn between problems of hydrodynamics and plasma physics.

Various names are used for Eq. (1.3) in the literature. In the works [22, 109] it is called TDGL (time-dependent Ginzburg-Landau equation). In the work [97] it is assigned to

$\lambda-\omega$ systems. It has also been called the Kuramoto–Tsuzuki equation [7-19], since it was just the authors of the work [103] whose proposed using it for the analysis of a broad class of two-component systems. For brevity and convenience we shall use this name below.

2. General Properties of the Equation and the Basic Types of Solutions

2.1. Basic Properties of the Kuramoto–Tsuzuki Equation and Its Simplest Solutions.

Equation (1.3) is a complex mathematical object. Analysis of it began from the construction of various classes of special solutions.

In Eq. (1.3) it is possible to set $c_0 = 0$ with no loss of generality. This can be seen by making the change of variables $W = W' \exp(ic_0 t)$. We shall henceforth assume that such a change has already been made.

In the majority of cases the second boundary value problem is a major interest with the condition that the fluxes on the boundaries are equal to zero:

$$\begin{gathered} W_t = \pm W + (1+ic_1) W_{xx} - (1+ic_2) W |W|^2, \\ 0 \leqslant x \leqslant l,\ 0 < t < \infty,\ W(x,\ 0) = W_0(x), \\ W_x(0,\ t) = W_x(l,\ t) = 0. \end{gathered} \tag{2.1}$$

The simplest solution of this problem is the zero solution

$$W(x,\ t) = 0 \tag{2.2}$$

and the spatially homogeneous solution

$$W(x,\ t) = \exp(-ic_2 t + i\alpha),\ \alpha = \text{const}. \tag{2.3}$$

All spatially homogeneous solutions are described by the dynamical system

$$\frac{d}{dt}\begin{pmatrix} u \\ v \end{pmatrix} = \pm \begin{pmatrix} u \\ v \end{pmatrix} - \begin{pmatrix} 1 & -c_2 \\ c_2 & 1 \end{pmatrix} \begin{pmatrix} u \\ v \end{pmatrix} (u^2+v^2). \tag{2.4}$$

When the minus sign is chosen on the right side, in its phase plane there is one singular point – the stable node (0, 0). If the plus sign is chosen, then (0, 0) is an unstable node, and in the phase plane there is a stable limit cycle (2.3). For nonzero initial data solutions of Eq. (2.4) tend to it as $t \to \infty$.

If in Eq. (2.1) the minus sign is chosen, then $\int_0^l (u^2+v^2)\,dx \to 0$ as $t \to \infty$. We write problem (2.1) in the form of a system of equations for u and v. We multiply the first equation by u, the second by v, add them, and integrate over the length of the segment. After integration by parts with consideration of the boundary conditions we obtain

$$\frac{1}{2}\frac{\partial}{\partial t}\int_0^l (u^2+v^2)\,dx = -\int_0^l (u_x^2+v_x^2)\,dx - \int_0^l (u^2+v^2)\,dx - \int_0^l (u^2+v^2)^2\,dx. \tag{2.5}$$

If $u \neq 0$, $v \neq 0$ for $0 \leqslant x \leqslant l$, then the right side of equality (2.5) is negative. This implies that for any initial data $\int_0^l |W|^2\,dx \to 0$, $t \to \infty$. We therefore consider henceforth only the case where the plus sign is chosen on the right side of Eqs. (2.1).

In this case for $\int_0^l |W|^2\,dx$ there is the relation

$$\frac{1}{2}\frac{\partial}{\partial t}\int_0^l (u^2+v^2)\,dx = -\int_0^l (u_x^2+v_x^2)\,dx - \int_0^l (u^2+v^2)^2\,dx + \int_0^l (u^2+v^2)\,dx. \tag{2.6}$$

The first term is nonpositive, and the second can be estimated by using the Cauchy–Bunyakovskii inequality for the functions $u^2 + v^2$ and 1:

$$\int_0^l (u^2+v^2)\,dx \leqslant \left(\int_0^l (u^2+v^2)^2\,dx\right)^{1/2} \left(\int_0^l dx\right)^{1/2}.$$

As a result we obtain the inequality

$$\frac{1}{2}\frac{\partial}{\partial t}\int_0^l (u^2+v^2)\,dx \leqslant \int_0^l (u^2+v^2)\,dx - \frac{1}{l}\left[\int_0^l (u^2+v^2)\,dx\right]^2,$$

from which we obtain the estimate

$$\int_0^l (u^2+v^2)\,dx \leqslant l/[1+A_1\exp(-t)], \tag{2.7}$$

where A_1 depends on the initial data. Thus, the solution of problem (2.1) is bounded in the norm of L_2.

We note that all that has been said is valid also in the case of a problem with periodic boundary conditions.

We shall specify those values of the parameters for which it is necessary to investigate problem (2.1). We first go over to the variables ρ, φ:

$$\rho_t=\rho-\rho^3+\rho_{xx}-\rho\varphi_x^2-2c_1\rho_x\varphi_x-c_1\rho\varphi_{xx},$$
$$\rho\varphi_t=-c_2\rho^3+2\rho_x\varphi_x+c_1\rho_{xx}-c_1\rho\varphi_x^2+\rho\varphi_{xx},\quad u=\rho\cos\varphi,\quad v=\rho\sin\varphi. \tag{2.8}$$

Suppose $\{\rho(x, t), \varphi(x, t)\}$ is a solution of (2.8) and hence also of (2.1); then the functions $\{\rho(x, t), -\varphi(x, t)\}$ will also be a solution of this system if the values of the parameters c_1, c_2 are replaced by $-c_1$, $-c_2$.

The validity of this assertion can be verified by direct substitution. It implies that it suffices to consider the range of parameters $c_1 \geqslant 0$.

From the form of the equation it is clear that the transformation $W \to -W$ and $W(x, t) \to W(\ell - x, t)$ takes solutions into other solutions. Symmetry with respect to the transformation

$$W \to We^{i\alpha}, \tag{2.9}$$

where α is a real constant, plays an important role.

By carrying out a linear analysis of the stability of the solution (2.3), it can be shown that it will be stable relative to small perturbations of the n-th harmonic under the condition [103]

$$(c_1^2+1)k^4+2k^2(1+c_1c_2)>0,\quad k=\pi n/l,\quad n=1, 2, \ldots \tag{2.10}$$

Inequality (2.10) is valid for any values of k if

$$1+c_1c_2>0. \tag{2.11}$$

It is natural to expect that if inequality (2.11) is not satisfied, then the solution of problem (2.1) will be spatially inhomogeneous.

2.2. Basic Types of Regimes and Problems Arising in Their Analysis. A group-invariant analysis carried out for Eq. (1.3) showed that it can have a spatially inhomogeneous, self-similar solution of the form [22]:

$$W(x, t)=R(x)\exp[i\omega t+ia(x)]. \tag{2.12}$$

In order to construct such solutions in problem (2.1) it is necessary to solve a nonlinear boundary value problem for the functions R(x) and a(x) depending on the parameter ω whose value must be found from the boundary conditions.

Spiral waves are studied theoretically in many active media [34, 36, 90]. To model them it is necessary to solve a multidimensional problem. The two-dimensional analogue of the Kuramoto–Tsuzuki equation can also describe spiral waves. To them there correspond self-similar solutions of the form

$$W(r, t)=R(r)\exp[i(\omega t+m\varphi-S(r))],\quad r^2=x^2+y^2,\quad x=r\cos\varphi,$$
$$y=r\sin\varphi,\quad m=0, 1, 2, \ldots \tag{2.13}$$

Here the following conditions are imposed on the functions R and S [90, 95]: $R(r) \to 0$, $S_r \to 0$ as $r \to 0$; $R \to R^\infty = \text{const}$, $S_r \to \text{const}$ as $r \to \infty$. Solutions with $m > 1$ have received the name many-loop waves. Their asymptotics as $r \to 0$ is as follows:

$$W \sim r^m\exp(i\omega t+im\varphi+iS).$$

To construct the functions R, S it is again necessary to solve a nonlinear boundary value problem for different values of ω from which it is also necessary to determine the value of ω. An extensive bibliography devoted to the investigation of numerical and analytic methods in this problem is presented in the works [34, 90].

In the work [96] it was shown that spiral waves in many two-component systems do not depend on the details of the kinetics and can be described by the same averaged equations. Results concerning such solutions were carried over to the simplest spatially inhomogeneous media for which $c = c_2(r)$ [123].

Having written the solution (2.13) in the form $W = R(r)e^{i\theta}$, it can be seen that the value of the phase θ for $r = 0$ is not defined. Such points have received the name of phase singularities. In the book [121] the thought was expressed that they play a basic role in the occurrence of order in a large class of systems of different nature.

Earlier cases were investigated where spiral wavs lose stability. In the work [101] results are presented of a numerical calculation in which phase singularities were created in pairs and then a turbulent regime ensued.

We shall point out difficulties connected with the investigation of spiral waves. These solutions are considered in the Cauchy problem. However, their numerical modeling is carried out in a bounded, usually small region. There arises the question of how the solutions of these problems are related. Explicit schemes and grids with large step sizes in spaces are frequently used in calculations in order to investigate spiral waves in the largest possible region. It would be an important problem to clarify what techniques in this case make it possible to convey the basic characteristics of the solutions studied.

In the study of Eq. (1.3) major attention is devoted to the search for periodic solutions of it (they have received the name of diffusion chaos). Such regimes are of great theoretical interest and can be related to models of many concrete processes [98-100, 105], in particular, to the occurrence of complex, apparently oscillatory, nonperiodic regimes in the Belousov–Zhabotinskii reaction [31]. This question is also interesting in that the behavior of spatially homogeneous solutions which are described by the dynamical system (2.4) turns out to be very simple. Therefore, the complex behavior is occasioned only by the influence of the spatial inhomogeneity and diffusion processes.

Computational experiment is a main source of information regarding stochastic regimes in problem (2.1). This made stringent demands on the technique of calculation. Therefore, the results of a number of works [100, 101, 105], where solutions are described which remain nonperiodic for a certain time, cannot with total certainty be interpreted as diffusion chaos (large step sizes in space, insufficient time of the calculations). Below we shall consider questions of the technique and results of investigating nonperiodic solutions in more detail.

The study of diffusion chaos posed still another important question. After the work of Lorenz [47] and also Ruelle and Takens investigations of chaos in dynamical systems and the study of strange attractors were broadly developed. A general question was posed of whether it is possible to relate stochastic regimes in a distributed system having infinitely many degrees of freedom with the presence of a strange attractor in a system of a small number of ordinary differential equations representing a simplified mathematical model of the processes.

In application to problem (2.1) this question was posed in the work of Kuramoto: "An important problem which is so far unsolved is to find a connection of diffusion chaos with some known type of chaos in systems with several degrees of freedom" [99].

We shall summarize what has been said and formulate questions which we shall consider in more detail below.

1. Equation (1.3) is a complex object. An ideal situation would be one in which we could predict the qualitative and basic quantitative characteristics of solutions for all values c_1, c_2, and ℓ. A path to the solution of this problem is connected with the construction of a hierarchy of simplified models (systems of several ordinary differential equations, etc.). Such models should be simple and nevertheless reflect the most important features of the original problem in various cases.

It is natural to excpect that the construction of such a hierarchy requires invoking various mathematical methods and broad use of computational experiment.

2. It would be important to clarify whether, aside from self-similar solutions, there exist other types of solutions describing space–time order in the system.

3. The question of the existence of nonperiodic solutions (diffusion chaos). Are such regimes connected with the presence of strange attractors in some dynamical system of low dimension? What is the mechanism for passing to chaos?

4. For many dissipative systems passage from an entire class of initial data to one and the same solution as $t \to \infty$ is characteristic [52, 70]. It is interesting to clarify whether different initial data in problem (2.1) can lead to a different asymptotic behavior as $t \to \infty$.

5. Investigation of properties of the two-dimensional analogue of problem (2.1). Analysis of the simplest types of order in the multidimensional case.

6. Methodological questions. Choice of the most effective algorithms for numerical investigation of Eq. (1.3) and for different simplified models.

Such are the basic questions which arise in the investigation of two-component systems in a neighborhood of a bifurcation point. We now proceed to analyze them.

3. Symmetric Solutions of the Kuramoto–Tsuzuki Equation

3.1. Solutions Preserving Spatial Symmetry. Investigation of the asymptotics of solutions of problem (2.1) for different initial data $W_0(x)$ is a major interest. Regarding the latter, in the work [105] it was conjectured that the initial data are of no consequence and the system "forgets" them for large characteristic times. We shall show that in the case of problem (2.1) this is not so: there exist certain symmetric initial data whose evolution as $t \to \infty$ is qualitatively different from the behavior of other solutions.

We point out that a closely related situation occurred in the case of the nonlinear heat equation with a volumetric source [30, 42, 43, 61] and in media with trigger properties [45].

We represent the solution of problem (2.1) as series

$$u(x,t)=\sum_{m=0}^{\infty} a_m(t)\cos\frac{\pi m x}{l},\quad v(x,t)=\sum_{m=0}^{\infty} b_m(t)\cos\frac{\pi m x}{l},$$

where $W = u + iv$. We assume that the boundary condition at the initial time are satisfied and the corresponding series converge. It can then be verified that the functions $a_m(t)$ and $b_m(t)$ are connected by the relations

$$\begin{aligned}
\dot a_0 &= a_0-\frac{1}{2}\left[r_0(a_0-c_2b_0)+\sum_{m=0}^{\infty} r_m(a_m-c_2b_m)\right],\\
\dot b_0 &= b_0-\frac{1}{2}\left[r_0(c_2a_0+b_0)+\sum_{m=0}^{\infty} r_m(c_2a_m+b_m)\right],\\
\dot a_p &= a_p-k^2p^2(a_p-c_1b_p)-0{,}5\left[\sum_{m=0}^{p} r_m(a_{p-m}-c_2b_{p-m})+\right.\\
&\left.+\sum_{m=0}^{\infty} r_m(a_{p+m}-c_2b_{p+m})+\sum_{m=0}^{\infty} r_{p+m}(a_m-c_2b_m)\right],\\
\dot b_p &= b_p-k^2p^2(c_1a_p+b_p)-0{,}5\left[\sum_{m=0}^{p} r_m(c_2a_{p-m}+b_{p-m})+\right.\\
&\left.+\sum_{m=0}^{\infty} r_m(c_2a_{p+m}+b_{p+m})+\sum_{m=0}^{\infty} r_{p+m}(c_2a_m+b_m)\right],\quad p=1,2,\ldots,
\end{aligned}\tag{3.1}$$

where $k=\pi/l$, $r_0=0{,}5\left[a_0^2+b_0^2+\sum_{m=0}^{\infty}(a_m^2+b_m^2)\right]$, $r_n=\sum_{m=0}^{\infty}(a_ma_{m+n}+b_mb_{m+n})+0{,}5\sum_{m=0}^{n}(a_ma_{n-m}+b_mb_{n-m})$. We also introduce the notation $\rho_m=(a_m^2+b_m^2)^{1/2}$.

It is possible to formulate conditions under which part of the Fourier coefficients of solutions of problem (2.1) are equal to zero during the entire process $0 < t < \infty$. We assign to the initial distributions $u_0(x)$ and $v_0(x)$ a sequence of integers $\{L\}$ in the following manner: if $n \bar\in \{L\}$, then $\rho_n(0) = 0$. In other words, $\{L\}$ contains all indices of harmonics with nonzero amplitude.

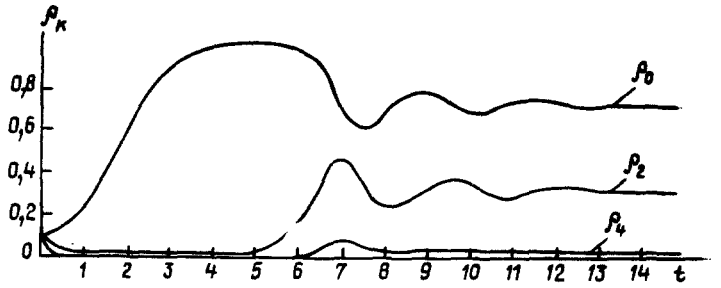

a $L=\{0,2,4,6....\}$; $C_1=1$, $C_2=-8$, $\ell=\pi$

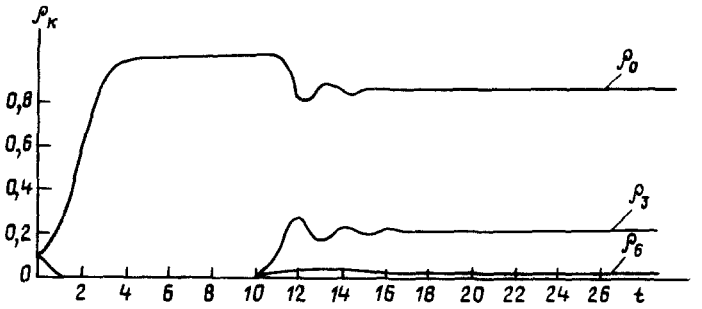

b $L=\{0,3,6,9,...\}$; $C_1=1$, $C_2=-13$, $\ell=\pi$

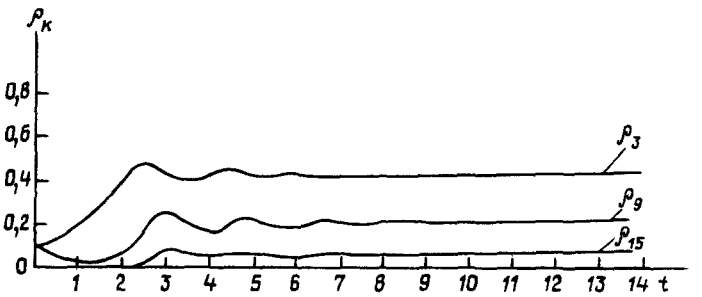

c $L=\{3,9,15,21,...\}$; $C_1=1$, $C_2=-13$, $\ell=6\pi$

Fig. 3. Examples of evolution of symmetric solutions.

We shall prove the following assertions.

LEMMA 1. If the sequence {L} is such that for any numbers $m\in\{L\}$, $n\bar{\in}\{L\}$ the condition $m\pm n\bar{\in}\{L\}$, holds, then all Fourier coefficients of solutions of problem (2.1) with indices $n\bar{\in}\{L\}$ are equal to zero for $0\leqslant t<\infty$.

Proof. It can be verified that under the conditions of the lemma all $r_n = 0$ if $n\bar{\in}\{L\}$. But then for all $p\bar{\in}\{L\}$, $a_p=0$, which follows from the form of the right sides of the system of equation (3.1).

Example 1. Taking the sequence {L} = {0, 2, 4, 6,...}, we obtain solutions symmetric with respect to the midpoint of the segment $x = \ell/2$. An example of passage to a nontrivial spatially inhomogeneous even solution is shown in Fig. 3a. We point out that all quantities $\rho_n(t)$ tend to constant values as $t \to \infty$.

The sequences {0, m, 2m,...}, where m is any natural number, also satisfy the condition of Lemma 1. An example of a solution with m = 3 is presented in Fig. 3b. We note that all sequences satisfying the conditions of the lemma must contain zero. Otherwise ($0\bar{\in}\{L\}$) the conditions $k\in\{L\}$ and $k\pm 0\bar{\in}\{L\}$ must be satisfied simultaneously.

LEMMA 2. If the sequence {L} is such that

1) for all $m, n\in\{L\}$ we have $m\pm n\bar{\in}\{L\}$;

2) for all $m, n\bar{\in}\{L\}$ we have $m\pm n\bar{\in}\{L\}$,

then all the Fourier coefficients of solutions of problem (2.1) with indices $n \bar{\in} \{L\}$ are equal to zero for $0 \leqslant t < \infty$.

Proof. It can be verified directly that $r_n = 0$ if $n \in \{L\}$. From this, as in the preceding case, it follows that for all $p \bar{\in} \{L\}$ $\dot{a}_p = 0$.

Example 2. The sequence of odd numbers {1, 3, 5, 7,...} gives an example of such a sequence.

We mention that $0 \bar{\in} \{L\}$ for all sequences {L} satisfying the second lemma.

The assertions proved turn out to be useful also in a more general case. Suppose, for example, that {L} = {3, 9, 15, 21,...}. This sequence does not satisfy the conditions of Lemmas 1 and 2. However, it is entirely contained both in $\{L_1\}$ = {0, 3, 6, 9, 12,...} and in $\{L_2\}$ = {1, 3, 5, 7, 9,...}; $\{L_1\}$ satisfies the first lemma, and $\{L_2\}$ satisfies the second. Therefore, the solution of the problem in partial derivatives will contain only modes with indices $n \in \{L_1\} \cap \{L_2\} = \{L\}$. An example of a numerical computation corresponding to a solution of this type is shown in Fig. 3c.

Suppose a nonzero sequence of initial data satisfies Lemma $1, 0 \in \{L\}$, and m is the next element of this sequence. If the spatially homogeneous solution (2.3) is unstable relative to perturbations of the form $\cos(\pi m x/\ell)$, then as $t \to \infty$ the solution of problem (2.1) remains spatially inhomogeneous. A necessary condition for this follows from formula (2.10):

$$(\pi m/l)^2 < -2(1+c_1c_2)/(1+c_1^2). \tag{3.2}$$

The greater the length of the region ℓ, the more numbers m satisfy inequality (3.2), and hence the more different types of symmetric initial data lead to the appearance of spatially inhomogeneous solutions.

Numerical investigation of problem (2.1) shows that the symmetric solutions constructed in many cases are unstable relative to perturbations of general form. However, below we shall consider a range of parameters where precisely such solutions determine the behavior of the system in the case of initial data of general form.

3.2. A Class of Odd Solutions. We shall consider as an example a class of odd solutions of the Kuramoto–Tsuzuki equation corresponding to the nonzero sequence {L} = {1, 3, 5,...}.

Suppose $c_1 = 0$ and that the initial data are nonmonotonic in space and are not symmetric. In calculations it is possible to distinguish a complex transitional regime; it is connected with the appearance and vanishing of extrema and with restructuring of the profiles of u(x, t) and v(x, t). However, the nonmonotonicity is then smoothed out and passage to the spatially homogeneous solution (2.3) occurs.

We now choose odd initial data. The equation contains only odd powers of functions and even derivatives with respect to the coordinates. It is therefore clear that if a point, located at first at the midpoint of the segment at which u(x, t) = 0 or v(x, t) = 0, were displaced, then this would ruin the symmetry of the positive and negative parts of the solution. This conclusion follows from Lemma 2.

The picture of the process differs qualitatively from that observed in the case of initial data of general form (see Fig. 4). The functions u(x, t) and v(x, t) vary in a complex manner. However, their Fourier coefficients $a_k(t)$, $b_k(t)$ decay rapidly with increasing index and depend on time in a rather simple way. For $t > 65$ the amplitude of the zeroth harmonic increases, and symmetry is lost.

The last circumstance is connected with features of the algorithms used and the computers. They contribute small perturbations to the even harmonics and therefore are unable in full measure to convey the properties of problem (2.1). This calculation nevertheless shows that an odd solution will be unstable and it makes it possible to estimate its increment. If the length of the region is changed while the other parameters remain fixed, then in large regions odd solutions have larger amplitude, smaller period, and smaller increment. Moreover, a nontrivial odd solution occurs only for $\ell \gtrsim 3$; in smaller regions $\rho_n(t) \to 0$ as $t \to \infty$ (this solution is also unstable relative to the zero harmonic).

We note that odd initial data of different form lead to the same asymptotic behavior as $t \to \infty$. It is important to clarify how the period of the limit solution and its amplitude depend on the parameters c_1, c_2, and ℓ. In order to answer this question we consider an

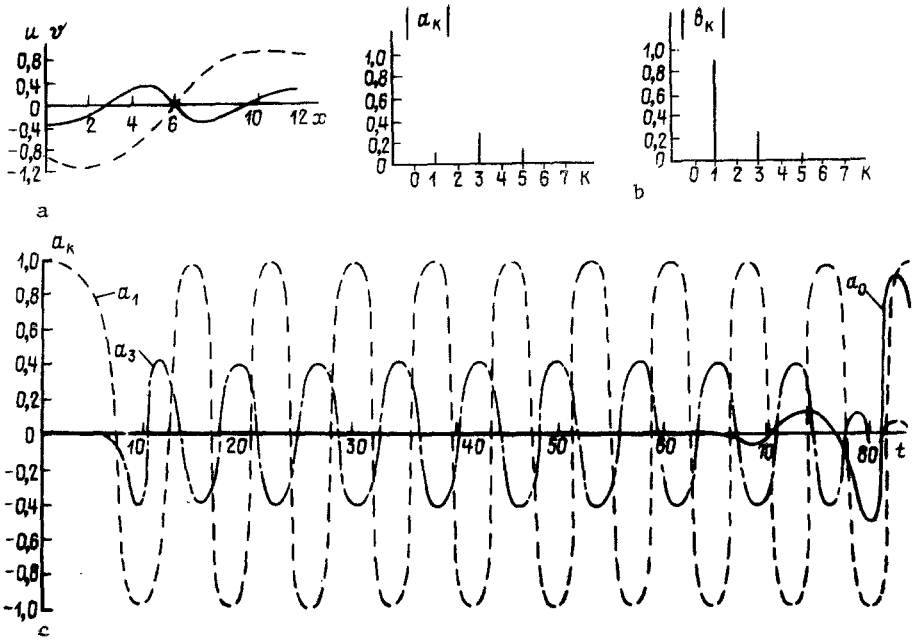

Fig. 4. Evolution of an odd solution for $c_1 = 0$, $c_2 = 1$, $\ell = 11.9$: a) the form of the functions u and v at one moment of time; b) amplitude of their Fourier coefficients; c) law of variation of $a_n(t)$.

approximate method of analysis of the system in question.

3.3. A Simplified Model. Since the Fourier coefficients of solutions decay rapidly with increasing index, an approximate method should at least give the law of variation of several first harmonics. We suppose that there are only two modes in the solution studied:

$$\begin{pmatrix} u \\ v \end{pmatrix} = \begin{pmatrix} x_0 \\ y_0 \end{pmatrix} + \begin{pmatrix} x_1 \\ y_1 \end{pmatrix} \cos kx, \tag{3.3}$$

and we choose k so that the boundary conditions of problem (2.1) are satisfied. As a rule, k will be equal to π/ℓ which determines the first harmonic. We substitute (3.3) into formula (2.1) and drop all terms containing $\cos(\pi mx/\ell)$, $m > 1$, assuming that they are negligibly small. This leads to a closed system of ordinary differential equations

$$\begin{aligned}
\dot{x}_0 &= x_0 - (x_0 - c_2 y_0)(\rho_0^2 + \rho_1^2/2) - s(x_1 - c_2 y_1), \\
\dot{y}_0 &= y_0 - (c_2 x_0 + y_0)(\rho_0^2 + \rho_1^2/2) - s(c_2 x_1 + y_1), \\
\dot{x}_1 &= x_1 - (x_1 - c_2 y_1)(\rho_0^2 + 3\rho_1^2/4) - 2s(x_0 - c_2 y_0) - k^2(x_1 - c_1 y_1), \\
\dot{y}_1 &= y_1 - (c_2 x_1 + y_1)(\rho_0^2 + 3\rho_1^2/4) - 2s(c_2 x_0 + y_0) - k^2(c_1 x_1 + y_1),
\end{aligned} \tag{3.4}$$

where $\rho_0^2 = x_0^2 + y_0^2$, $\rho_1^2 = x_1^2 + y_1^2$, $s = x_0 x_1 + y_0 y_1$. We rewrite this system in a form more convenient for subsequent analysis. If we set $x_0 = \rho_0 \cos\varphi_0$, $y_0 = \rho_0 \sin\varphi_0$, $x_1 = \rho_1 \cos\varphi_1$, $y_1 = \rho_1 \sin\varphi_1$, then we obtain the relations

$$\begin{aligned}
\dot{\rho}_0 &= \rho_0 - \rho_0(\rho_0^2 + \rho_1^2/2) - \rho_0\rho_1^2 \cos\Psi[\cos\Psi + c_2 \sin\Psi], \\
\dot{\rho}_1 &= \rho_1 - \rho_1(\rho_0^2 + 3\rho_1^2/4) - 2\rho_0^2\rho_1 \cos\Psi[\cos\Psi - c_2 \sin\Psi] - k^2\rho_1, \\
\dot{\varphi}_0 &= -c_2(\rho_0^2 + \rho_1^2/2) + \rho_1^2 \cos\Psi[\sin\Psi - c_2 \cos\Psi], \\
\dot{\varphi}_1 &= -c_2(\rho_0^2 + 3\rho_1^2/4) - 2\rho_0^2 \cos\Psi[\sin\Psi + c_2 \cos\Psi] - c_1 k^2,
\end{aligned} \tag{3.5}$$

where $\Psi = \varphi_0 - \varphi_1$. From (3.5) it is possible to go over to the system of three equations

$$\begin{aligned}
\dot{\xi} &= 2\xi - 2\xi(\xi + \eta) - \xi\eta(\cos\theta + c_2 \sin\theta), \\
\dot{\eta} &= 2\eta - 2\eta(2\xi + 3\eta/4) - 2\xi\eta(\cos\theta - c_2 \sin\theta) - 2k^2\eta, \\
\dot{\theta} &= c_2(2\xi - \eta/2) + \sin\theta(2\xi + \eta) + c_2 \cos\theta(2\xi - \eta) + 2c_1 k^2.
\end{aligned} \tag{3.6}$$

The connection between the variables ξ, η, θ and ρ_0, ρ_1, φ_0, φ_1 is determined by the relations

$$\xi=\rho_0^2,\quad \eta=\rho_1^2,\quad \varphi_0-\varphi_1=\theta/2,$$
$$\dot{\varphi}_0=-c_2(\xi+\eta)+0{,}5\eta(\sin\theta-c_2\cos\theta). \tag{3.7}$$

The possibility of going over to the system of three equations is connected with the symmetry (2.9) which the original system possesses. We shall be interested in the asymptotic behavior of the simplified two-mode system as $t\to\infty$. We consider the simplest solutions of it.

The first solution is the unstable node in the system (3.4)

$$x_0=0,\ y_0=0,\ x_1=0,\ y_1=0, \tag{3.8}$$

to which there corresponds the invariant line in the dynamical system (3.6)

$$\xi=0,\ \eta=0,\ \theta=2c_1k^2t+\text{const}. \tag{3.9}$$

Another solution can be obtained by setting $x_1 = 0$, $y_1 = 0$:

$$x_0=\cos(-c_2t+\alpha),\ y_0=\sin(-c_2t+\alpha),\ x_1=0,\ y_1=0, \tag{3.10}$$

where α is a real constant. In Eqs. (3.6) there corresponds to it the stable invariant line $\xi = 1$, $\eta = 0$, $\theta = \theta(t)$ if the following inequality holds:

$$c_1^2k^4+2c_1c_2k^2-1>0. \tag{3.11}$$

A pair of singular points $\xi = 1$, $\eta = 0$ – a saddle point and an unstable node – generated on the curve $c_1^2k^4 + 2c_1c_2k^2 - 1 = 0$. The node loses stability on the line

$$(c_1^2+1)k^4+2k^2(1+c_1c_2)=0. \tag{3.12}$$

It is natural to compare solutions with $\xi = 1$, $\eta = 0$ to spatially homogeneous solutions of the problem in partial derivatives. The limit cycle (3.10) also loses stability on the line (3.12).

Suppose now that $\rho_0(0) = 0$; then $\rho_0(t)=0$, $0\leqslant t<\infty$. From (3.5) we find that $\rho_1\to\rho$, $\dot{\varphi}_1\to\omega_1$ as $t\to\infty$, and

$$\bar{\rho}=\begin{cases}\sqrt{4(1-k^2)/3}, & k\leqslant 1,\\ 0, & k>1,\end{cases}\quad \omega_1=-3c_2\bar{\rho}^2/4-c_1k^2. \tag{3.13}$$

An analogue of such a solution in the system (3.6) may be the invariant line $\xi = 0$, $\eta = \bar{\rho}^2$, $\theta = \theta(t)$ or a pair of singular points. The condition for the existence of singular points is the inequality

$$P(c_1, c_2, k)\leqslant 0,\quad k<1,$$

where $P(c_1, c_2, k)=(9c_1^2+6c_1c_2-4-3c_2^2)k^4-2k^2(3c_1c_2-4-3c_2^2)-(4+3c_2^2)$. One of these points is stable if

$$-(4k^2-1)^2<P(c_1, c_2, k).$$

The solution with $\xi = 0$ is an invariant line when

$$P(c_1, c_2, k)>0.$$

This line is stable for $k < 1/2$.

If an analogy is drawn between odd solutions of the problem in partial derivatives and solutions of the system (3.5) with $\rho_0 = 0$, then it is possible to make the following qualitative predictions. For odd initial data the quantity $\rho_1=(a_1^2+b_1^2)^{1/2}$ is constant, and apparently the quantities $\rho_n=(a_n^2+b_n^2)^{1/2}$, $n = 2m + 1$, $m + 1, 2, 3,\ldots$ are also constant as $t\to\infty$. Passage to one and the same solution occurs from an entire class of odd initial data. Nontrivial odd solutions arise only in regions whose length exceeds some critical length [from (3.13) an estimate of it is $\ell_c = \pi$].

The calculations carried out for problem (2.1) completely corroborate these predictions [10]. In the example shown in Fig. 4 the amplitude of the first harmonic is ≈ 1.1, and the period of the solution is $T \approx 7.5$. It follows from formulas (3.13) that $\rho = 1.11$, $T = 2\pi/\omega_1 = 6.75$. In this case it is possible to speak not only of a qualitative but a quantitative correspondence of these characteristics. For odd initial data a fair correspondence is observed for $\ell < 4\pi - 5\pi$ [10].

Thus, Eqs. (3.4) turn out to be a useful simplified model, and we shall consider them in more detail below.

4. Two-Mode System and Its Properties

4.1. Simplest Properties of Solutions. We shall consider the simplest properties of the dynamical system (3.6).

Boundedness of Solutions. Using the first two equations of the system (3.6), we consider how the quantity $2\xi + \eta$ changes:

$$2\dot{\xi}+\dot{\eta}=2(2\xi+\eta)-(2\xi+\eta)^2-\eta^2/2-2k^2\eta-4\xi\eta(1+\cos\theta)\leqslant 2(2\xi+\eta)-(2\xi+\eta)^2. \tag{4.1}$$

From the last inequality it follows that $2\xi+\eta\leqslant z$, where z(t) is a solution of the equation

$$\dot{z}=2z-z^2, \quad z(0)=2\xi(0)+\eta(0)\geqslant 0. \tag{4.2}$$

Since z(t) is bounded and $\xi\geqslant 0$, $\eta\geqslant 0$, each of the functions $\xi(t)$, $\eta(t)$ is also bounded.

Dissipativeness of the System. The quantity Ω, which determines the rate of variation of a small volume in phase space on motion along trajectories, $\dot{V} = \Omega V$, is an important characteristic of the dynamical system. This quantity characterizes the dissipativeness of the system and shows how fast its solutions converge to an attractor. In our case

$$\Omega=\partial\dot{\xi}/\partial\xi+\partial\dot{\eta}/\partial\eta+\partial\dot{\theta}/\partial\theta=4-2k^2-8\xi-5\eta. \tag{4.3}$$

The quantity Ω does not depend explicitly on the parameters c_1, c_2 and one the variable θ. In the case $k > \sqrt{2}$ (sufficiently small values of ℓ) the system is dissipative everywhere. For $k < \sqrt{k}$ in phase space there appears a region where $\Omega > 0$. Neither stable singular points nor stable limit cycles can lie in this region. This region is located below the line $8\xi + 5\eta = 4 - 2k^2$, that is, rather near to the origin. In the majority of systems which have so far been investigated the quantity Ω is constant in all of phase space. In this sense Eqs. (3.6) constitute a complex object.

4.2. Singular Points. Above we considered the simplest solutions of the dynamical system for which $\xi = 0$ or $\eta = 0$. We now assume that $\xi \neq 0$, $\eta \neq 0$. From (3.6) we then obtain the system of equations

$$\begin{gathered}2-2(\xi+\eta)-\eta(\cos\theta+c_2\sin\theta)=0,\\ 2-2(2\xi+3\eta/4)-2\xi(\cos\theta-c_2\sin\theta)-2k^2=0,\\ c_2(2\xi-\eta/2)+\sin\theta(2\xi+\eta)+c_2\cos\theta(2\xi-\eta)+2c_1k^2=0.\end{gathered} \tag{4.4}$$

The first two equations make it possible to express ξ and η in terms of $\cos\theta$ and $\sin\theta$. Substituting these expressions into the third equation and setting $\varepsilon=(c_2^2+1)/[k^2(c_1-c_2)]$, $y=\tan(\theta/2)-\varepsilon/2$, we obtain the equality

$$\begin{gathered}y^4+by^2+cy+d=0,\ b=-1{,}5\varepsilon^2+8\varepsilon c_1k^2-14,\\ c=\varepsilon(\varepsilon^2-8\varepsilon c_1k^2+8k^2),\ d=-3\varepsilon^4/16+2c_1k^2\varepsilon^3+\varepsilon^2(3{,}5-4k^2)-15.\end{gathered} \tag{4.5}$$

The coordinates of the singular point are determined by the relations

$$\begin{gathered}\xi=\frac{(1+2k^2)x^2+4c_2(k^2-1)x+(6k^2-3)}{x^4+(8c_2^2-6)x^2-15}(1+x^2),\quad x=y+\varepsilon/2,\\ \eta=\frac{4(1+x^2)(-k^2x^2+2c_2x-k^2-2)}{x^4+(8c_2^2-6)x^2-15},\quad \cos\theta=\frac{1-x^2}{1+x^2},\quad \sin\theta=\frac{2x}{1+x^2}\end{gathered} \tag{4.6}$$

From the form of Eq. (4.5) it follows that for all $c \neq c_2$ it has at least two real roots. Indeed, the function on the left side of (4.5) is continuous, for $y = -\varepsilon/2$ it is equal to -15, and as $y \to \pm\infty$ its values are positive. Writing out the equation of fourth degree for the quantity x, it can be seen that its free term is always negative. From this it follows that Eq. (4.5) cannot have a fourfold root. It has a twofold root if

$$\begin{gathered}\sqrt{-b\pm\sqrt{b^2+12d}}\,[2b\pm\sqrt{b^2+12d}\,]=+3\sqrt{3/2}\,c,\\ \sqrt{-b\pm\sqrt{b^2+12d}}\,[2b\pm\sqrt{b^2+12d}\,]=-3\sqrt{3/2}\,c\end{gathered} \tag{4.7}$$

and a root of multiplicity three if

$$\begin{gathered}b^2+12d=0,\\ -8b^3=27c^2.\end{gathered} \tag{4.8}$$

The singular point with coordinates $\{\xi, \eta, \theta\}$ which is determined by relations (4.5), (4.6) is stable if the real parts of all eigenvalues of the following matrix are negative:

$$A=\begin{vmatrix} 2-4\xi-\eta(2+\cos\theta+c_2\sin\theta) & -\xi(2+\cos\theta+c_2\sin\theta) & \xi\eta(\sin\theta-c_2\cos\theta) \\ -2\eta(2+\cos\theta-c_2\sin\theta) & 2(1-k^2)-3\eta-2\xi(2+\cos\theta-c_2\sin\theta) & 2\xi\eta(\sin\theta+c_2\cos\theta) \\ 2(c_1+\sin\theta+c_2\cos\theta) & -c_2/2+\sin\theta-c_2\cos\theta & (2\xi+\eta)\cos\theta-c_2(2\xi-\eta)\sin\theta \end{vmatrix}. \tag{4.9}$$

Formulas (4.4)-(4.9) give complete information regarding each singular point of the system of equations (3.6). We shall consider what conclusions can be drawn from these relations.

We consider the basic regularities in the example of systems with $k = 1$. We turn to Eq. (4.5). Results of its investigation are shown in Figs. 5-8. Calculations show that for all values of c_1 and c_2 Eq. (4.5) for $k = 1$ has at least one root determining a singular point with $\eta < 0$. Figure 5 shows the number of points for which $\xi > 0$, $\eta > 0$ in different regions of the parameters. The number of such points can change on passing across the lines ABD and DMEQF in the $\{c_1, c_2\}$ plane.

The curve ABC is determined by relation (3.12) for $c_1 \to \infty$; it has the asymptotics $c_2 = -0.5c_1k^2$. Above and to the left of this curve (including for all $c_1 < 0$) the singular point $\xi = 1$, $\eta = 0$ (or the singular line) is stable. It determines the asymptotics of the system. On the line ABC the point $\xi = 1$, $\eta = 0$ loses stability. One of the eigenvalues of the matrix A becomes equal to zero. Simultaneously with this a point from the region $\xi > 0$, $\eta < 0$ goes over into the region $\xi > 0$, $\eta > 0$ and becomes stable.

The line DMEQF is the line of multiple roots. It is determined by formulas (4.7). Two states of equilibrium appear or disappear on this curve. On the segment QF it is close to a line; we find its asymptotics for $|c_2| \gg 1$ by setting $|c_1| \sim |c_2| \sim |\varepsilon| \to \infty$. Leaving the leading terms in the expressions for the coefficients b, c, d, we have from (4.7)

$$3\sqrt{3/2}\,\varepsilon(-\varepsilon^2+8\varepsilon c_1k^2)+\ldots=3\sqrt{3/2}\,\varepsilon(\varepsilon^2-8\varepsilon c_1k^2)+\ldots, \tag{4.10}$$

which is equivalent to the equation

$$\varepsilon=8c_1k^2 \text{ for } \frac{c_2}{c_1}=-4k^4\pm\sqrt{16k^8+8k^4}. \tag{4.11}$$

In our case from (4.11) we obtain

$$c_2/c_1=-4-2\sqrt{6}\approx-8{,}9,$$

which coincides with the dependence observed in calculations. Such are the equations which describe the boundaries of regions with a different number of singular points. Stable points which determine the asymptotics of the process are of greatest interest.

Figures 7 and 8 show the number of stable singular points of the system of equations (3.6) as a function of the parameters c_1 and c_2. The curves ABC and DMEQF are the same as in Figs. 5 and 6. Aside from these, the line MQNF on which a Hopf bifurcation occurs gives important information regarding stability. On this line the matrix A has two purely imaginary eigenvalues; one of the singular points of the system loses stability on it. In the region bounded by the lines FQNP there are no stable singular points. The attractors are limit cycles or have a more complex structure. We also note that in the region MEQ on the $\{c_1, c_2\}$ plane the system (3.6) has two stable singular points.

We shall clarify how the system of equations (3.6) behaves as $|c_2| \to \infty$. Can it be asserted that in this region of parameters it has stable singular points? What are their characteristics? These questions were considered in the works [6, 11, 113].

The results of the analysis carried out are contained in Table 1. From it it is evident that in the region there is always at least one stable point $\{\xi^*, \eta^*\}$. Moreover, $\xi^* \xrightarrow[|c_2|\to\infty]{} 1$, $\eta^* \xrightarrow[|c_2|\to\infty]{} 0$. There is a range of parameters where still another point can be stable. This is the situation, for example, if $k = 3$, $c_1 = 3$, $c_2 \to -\infty$.

The behavior of the dynamical system (3.6) for c_2 close to zero determines a solution with $\xi = 1$, $\eta = 0$. Calculations show that as c_2 decreases the attractor becomes more complicated, and other points, limit cycles, and nonperiodic solutions appear. However, the system possesses an interesting feature: for $c_2 \to -\infty$ a stabilization of processes occurs in it. Solutions corresponding to the point $\{\xi^*, \eta^*\}$ again determine the asymptotics. Moreover

TABLE 1. Asymptotic Behavior of Singular Points of the System of Equations (3.6) for $c_2 \to \infty$. Only Leading Terms Are Written in the Matrix of the Linearized System

Roots of the equation of fourth degree	Singular points of system (3.6)	Matrix of the linearized system of equations (3.6)	Equation for the eigenvalues of the matrix	Condition for stability of the singular point, $c_2 \to \infty$
$x_1 = \frac{15}{(8\kappa^2-14)\varepsilon}$ $x_1 \to 0$ $c_2 \to \infty$	$\xi_1 = \frac{7-4\kappa^2}{35}$ $\eta_1 = \frac{8}{3}\frac{7-4\kappa^2}{35}$ $\theta_1 = 2\pi n$ $n = 0, \pm 1 \ldots$	$\begin{pmatrix} \frac{8\kappa^2-14}{35} & -\frac{3\kappa^2+21}{35} & -c_2\frac{8}{3}\frac{(7-4\kappa^2)^2}{35^2} \\ \frac{16(9\kappa^2-7)}{35} & \frac{4(4\kappa^2-7)}{35} & c_2\frac{16}{3}\frac{(7-4\kappa^2)^2}{35^2} \\ 4c_2 & -3c_2/2 & \frac{2(49-13\kappa^2)}{105} \end{pmatrix}$	$\lambda^3 + \frac{28-46\kappa^2}{105}\lambda^2 + \frac{56}{3}c_2^2\frac{(7-4\kappa^2)^2}{35^2}\lambda + \frac{16}{3}c_2^2\frac{(7-4\kappa^2)^3}{35^2} = 0$	Unstable if $\xi_1 > 0$ $\eta_1 > 0$
$x_2 = -2\varepsilon + 4c_1\kappa^2$ $x_2 \to \infty$ $c_2 \to \infty$	$\xi_2 = 1$ $\eta_2 = \frac{-8c_1\kappa^6}{c_2(1+2\kappa^4)}$ $\eta_2 \to 0, c_2 \to \infty$ $\theta_2 = \pi + 2\pi n$ $n = 0, \pm 1 \ldots$	$\begin{pmatrix} -2 & -1-\kappa^2 & -\frac{8c_1\kappa^6}{1+2\kappa^4} \\ 0 & 0 & \frac{16c_1\kappa^6}{1+2\kappa^4} \\ 0 & c_2/2 & -2(1+\kappa^2) \end{pmatrix}$	$(\lambda+2)(\lambda^2 + 2(1+\kappa^2)\lambda - \frac{8c_1c_2\kappa^6}{1+2\kappa^4}) = 0$	$c_1c_2 < 0$
$x_{3,4} = -2c_1\kappa^2 \pm \sqrt{4c_1^2\kappa^4 - 4\kappa^2 + 7}$	$\xi_{3,4} = \frac{(\kappa^2-1)(1+x_{3,4}^2)}{2c_2x_{3,4}}$ $\eta_{3,4} = \frac{1+x_{3,4}^2}{c_2x_{3,4}}$ $\sin\theta_{3,4} = \frac{2x_{3,4}}{1+x_{3,4}^2}$ $\cos\theta_{3,4} = \frac{1-x_{3,4}^2}{1+x_{3,4}^2}$	$\begin{pmatrix} 0 & 1-\kappa^2 & -\frac{(1-x_{3,4}^4)(\kappa^2-1)}{2c_2x_{3,4}^2} \\ 4 & 0 & \frac{(1-x_{3,4}^4)(\kappa^2-1)}{c_2x_{3,4}^2} \\ \frac{4c_2}{1+x_{3,4}^2} & \frac{c_2(x_{3,4}^2-3)}{2(1+x_{3,4}^2)} & 4-2\kappa^2 \end{pmatrix}$	$\lambda^3 + (2\kappa^2-4)\lambda^2 + \frac{\kappa^2-1}{2x_{3,4}^2}(x_{3,4}^4+7)\lambda - \frac{\kappa^2-1}{x_{3,4}^2}(x_{3,4}^2+1)\cdot(x_{3,4}^2-4\kappa^2+7) = 0$	either $\begin{cases} \kappa^2 > 2 \\ x_{3,4}^2 < 4\kappa^2 - 7 \\ x_{3,4}^2 < \min\left[1, \frac{3\kappa^2-7}{\kappa^2-1}\right] \end{cases}$ or $\begin{cases} \kappa^2 > 2 \\ x_{3,4}^2 < 4\kappa^2 - 7 \\ x_{3,4}^2 > \max\left[1, \frac{3\kappa^2-7}{\kappa^2-1}\right] \end{cases}$

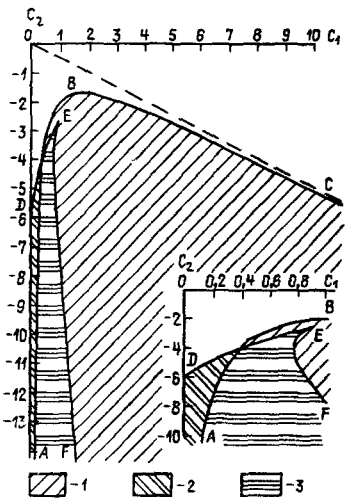

Fig. 5

Fig. 6

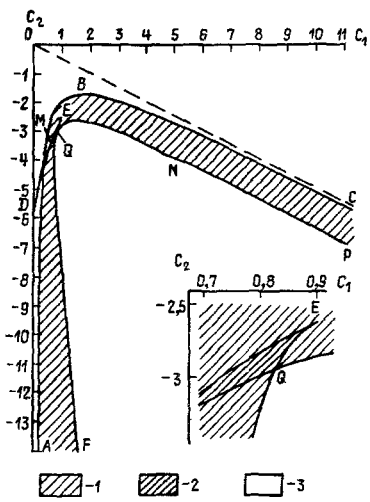

Fig. 7

Fig. 8

Figs. 5, 6. The number of singular points of the system (3.6) for k = 1: 1) 1 point, 2) 2 points, 3) 3 points.

Figs. 7, 8. The number of stable singular points for k = 1: 1) a point, 2) 2 points, 3) no stable points.

$\xi^* \to 1$, $\eta^* \to 0$ when $c_2 \to -\infty$. Thus, the processes in the system for $c_2 \to 0$ and $c_2 \to -\infty$ are qualitatively similar.

We shall consider features of the occurrence of states of equilibrium. On the curve DMEQF the system has two singular points. Calculations show that on the segment ME one of them is stable, while on the segment DM both are unstable. A particular situation is realized depending on the eigenvalues of the matrix A on the curve of multiple roots. One of the eigenvalues on the line DMEQF is always equal to zero. If at least one of the two others has a positive real part, then both states of equilibrium which arise are unstable. If the real parts of both eigenvalues are negative, then one stable and one unstable singular point occur.

Figure 9 gives a graphic representation of the occurrence of states of equilibrium. We fix a value of c_1 and reduce the parameter c_2. The variation of the quantity $\rho_0 = \xi^{1/2}$ for

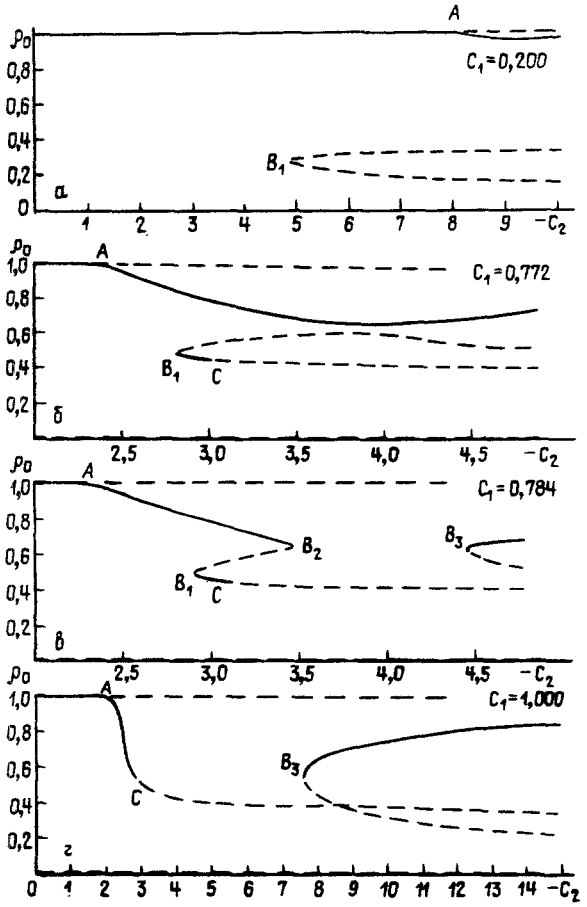

Fig. 9. Picture of the behavior of singular points with $\xi>0$, $\eta\geqslant 0$ for different values of c_1. ——) Indicates a stable point, – – –) indicates an unstable point.

all singular points with $\xi > 0$, $\eta > 0$ and $\xi = 1$, $\eta = 0$ obtained in the calculations for different values of c_1 is shown in the figure. Those values of the parameter c_2 for which the number of singular points or their stability changes are denoted by the letters A, B_1, B_2, B_3, C.

The point A lies on the line ABC, and the point C lies on the line of Hopf bifurcation. B_1, B_2, B_3 are determined by the line of multiple roots. At the points B_1 and B_3 two new states of equilibrium occur in the system (3.6). At the point B_2 the two states of equilibrium vanish.

If $|c_1| \ll 1$, then the system always has one stable singular point (a typical situation is shown in Fig. 9a). When $|c_1| \gtrsim 1$ there are not stable points in a certain range of parameters (see Fig. 9d). In the intermediate case the picture may be more complex; it is illustrated in Fig. 9b and c. It is evident that here two stable points exist simultaneously, and the dynamical system (3.6) hereby possesses trigger properties.

We note that one of the states of equilibrium arising on the line of multiple roots is stable. This is especially interesting. Complication of the system on change of the parameter in synergetics is usually associated with sequences of bifurcations, and branching theory is the main tool used [52, 70]. An altogether different behavior is observed in the model studied: the stable point determining the asymptotics of the system does not occur as a result of the branching of solutions present earlier. Apparently this situation is rather common. Analysis of it requires invoking other methods (for example, ideas from catastrophe theory [5, 29]) and further developing of existing concepts.

4.3. Stable Limit Cycles. We shall consider periodic solutions of Eqs. (3.6). Suppose the functions $\xi(t)$, $\eta(t)$, $\theta(t)$ satisfy this dynamical system and that $\xi(t + T) = \xi(t)$, $\eta(t + T) = \eta(t)$. It can then be verified that

$$\theta(t+T)-\theta(t)=2\pi m,\ m=0,\ \pm 1,\ \pm 2,\ldots \qquad (4.12)$$

Solutions with $m = 0$ correspond to ordinary limit cycles which are closed trajectories in the space of ξ, η, θ ($0\leqslant\xi<\infty$, $0\leqslant\eta<\infty$, $-\infty<\theta<\infty$). If $m \neq 0$, then the functions $\{\xi(t), \eta(t), \theta(t)\}$ define spirals. In the literature they are called limit cycles of the second kind

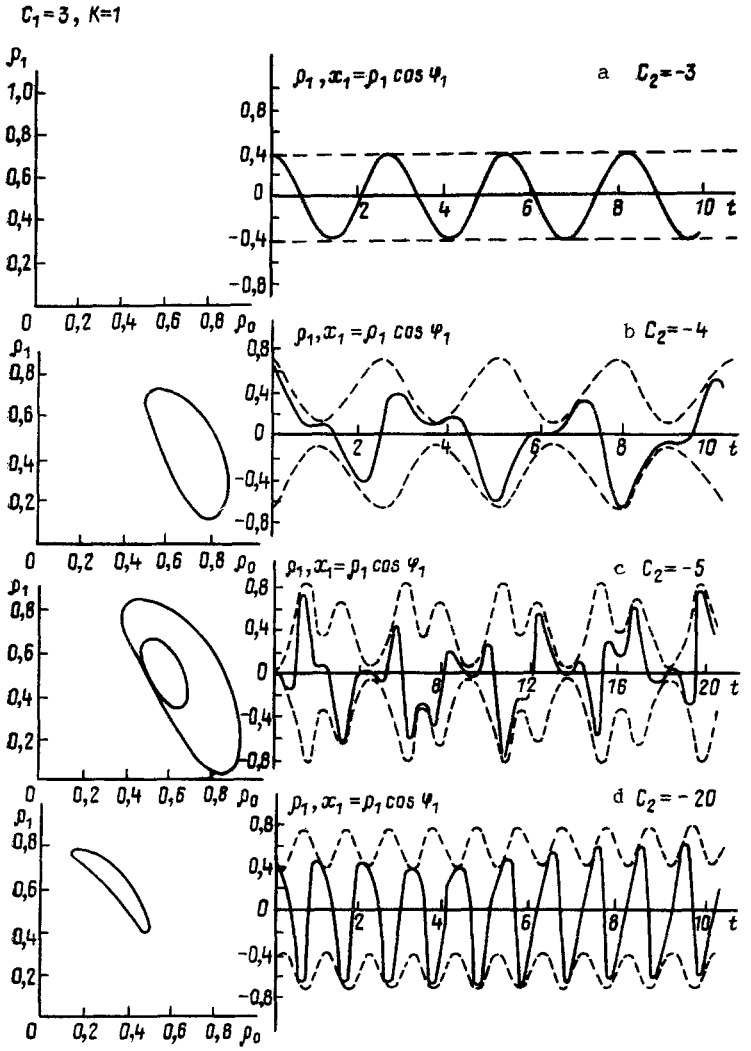

Fig. 10. Self-oscillations corresponding to different types of attractors of the system (3.6). Solutions of the system (3.4) are shown by the solid line in the figures.

in contrast to solutions with m = 0 which are called limit cycles of the first kind. For brevity we call both solutions cycles.

It is convenient to distinguish cycles according to the number of turns which the projection of the point $\{\xi, \eta, \theta\}$ onto the plane $\{\xi, \eta\}$ makes about some central region while returning to the original position [11]. Cycles which are characterized by the numbers m and n we denote by S_m^n. We call cycles S_m^1 simple.

We shall consider the connection between solutions of the two-mode system (3.4) and the system (3.6). A periodic solution in the model (3.4) corresponds to a singular point in Eqs. (3.6) (see Fig. 10). To limit cycles of different types there correspond double frequency regimes in which the functions x_0, x_1, y_0, y_1 may be nonperiodic [19]. Passing from (3.4) to (3.6) makes it possible to simplify the description. Below in speaking of cycles in the simplified model, we have in mind the periodicity of the functions $\rho_0(t)$ and $\rho_1(t)$ (respectively, ξ and η).

We shall consider periodic solutions of the system (3.6) for which k = 1. We distinguish the most interesting qualitative properties of the solutions and note their common features.

Figure 11 shows the decomposition of the plane of the parameters $\{c_1, c_2\}$ into regions in which the attractors of the system (3.6) have different type. On the curve QNP (see Figs. 7, 8) the singular point determining the asymptotics of the system loses stability. Bifurcation of the creation of the limit cycle S_0^1 occurs — a Hopf bifurcation. The cycle arising is

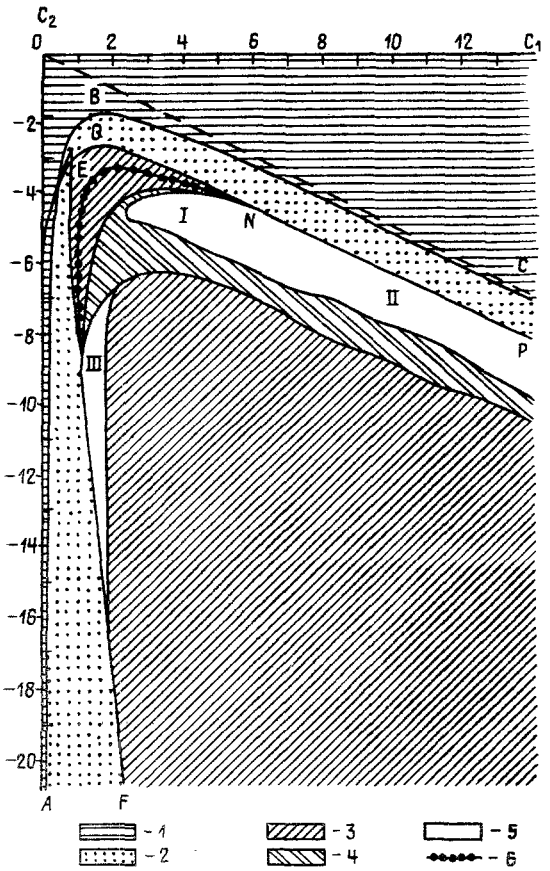

Fig. 11

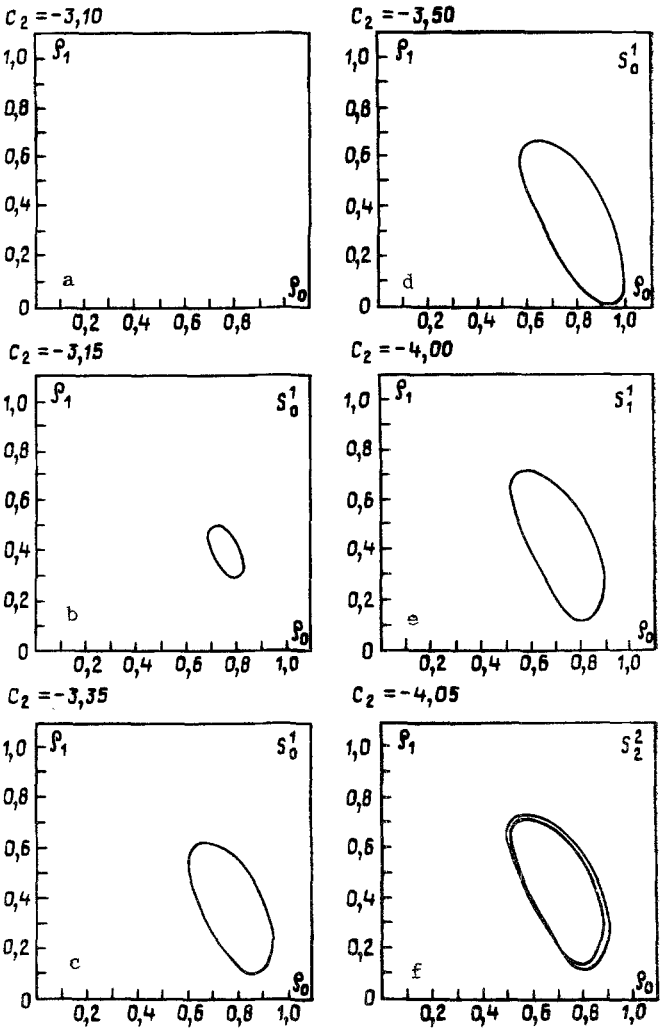

Fig. 12

Fig. 11. Types of attractors for the system of equations (3.6) for k = 1: 1) the point $\xi = 1$, $\eta = 0$, 2) singular point with $\xi > 0$, $\eta > 0$, 3) simple cycle, 4) the cycle S^2, 5) more complex solutions, 6) the line on which the transition $S_0^1 \to S_1^1$ occurs; QNP is the line of Hopf bifurcation. The picture was obtained as a result of numerical solution of Eqs. (3.6). The step size in the parameter c_1 is $h_1 = 1.0$ and in the parameter c_2 is $h_2 = 0.5$. In a neighborhood of the boundaries between regions the step size was reduced to 0.1. The initial data for the problem with parameters $\{c_1, c_2 - h_2\}$ below the line ABC were provided by a point belonging to the attractor of the system for the values $\{c_1, c_2\}$.

Fig. 12. Complication of the attractors of the dynamical system (3.6) as the parameter c_2 is reduced; k = 1, $c_1 = 3$.

stable on the segment QN. On the segment NP nonperiodic solutions arise on passing across the line QNP with a jump [13].

The amplitude of the stable cycle S_0^1 increases with decreasing c_2. Beginning from some value of this parameter, the asymptotics of the system is determined by the cycle S_1^1. As the transition point c_2^* is approached the cycle approaches one of the saddle points $\xi = 1$, $\eta = 0$ (see Fig. 12). After the transition, $c_2 < c_2^*$, the cycle passes away from it. For $c_2 = c_2^*$ the cycle passes through the saddle. It is natural to expect that $T(c_2) \to \infty$, $c_2 \to c_2^*$. Just this dependence is observed in calculations (see Fig. 14). The line on which the type of the cycle changes is shown in Table 11.

There exists a region of parameters in the $\{c_1, c_2\}$ plane where complication of periodic solutions occurs (see Fig. 11). In this region a sequence of bifurcations with doubling the period is observed, the theory of which is being intensively developed at the present time

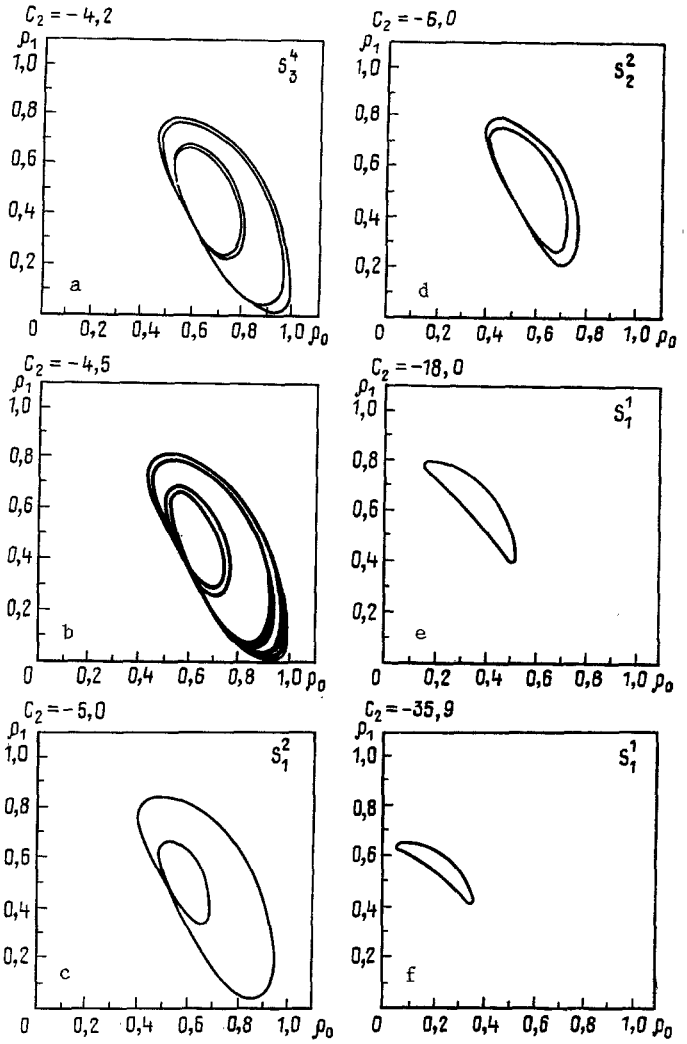

Fig. 13. Change of attractors on further reduction of c_2.

[27, 84, 85]. A cycle of the type S_m^n hereby goes over into S_{2m}^{2n}, and its period is doubled. Figures 12 and 13 show the picture of this process for $c_1 = 3$. After several bifurcations $S_m^n \to S_{2m}^{2n}$ nonperiodic solutions are observed in the computations (see Fig. 13b) examples of which we consider below. Bifurcations $S_{2m}^{2n} \to S_m^n$ occur when c_2 is reduced further (see Fig. 13) as a result of which simple cycles again arise.

Figure 11 shows that in a broad range of parameters the cycle S_1^1 determines the asymptotics of the solutions. We shall consider some features of them. We consider the dependence of the period T on the parameter c_2. Figure 15 shows that over a broad range of variation of c_2 ($|c_2| \gg 1$) the period does not depend on this parameter, while the remaining characteristics of the cycle vary strongly (see Fig. 13e and f). The calculations showed that for $|c_2| \gg 1$, $k = 1$ there is the following dependence:

$$T = 3/c_1.$$

In the work [1] this phenomenon was called the effect of constancy of the period. Another regularity is observed for the cycles S^1: although the variable $\theta(t)$ changes in a complex fashion and rapid segments on this curve alternate with slow segments, the laws of variation of the quantities ξ and η are close to harmonic.

In many works where dissipative structures are investigated the dependence of the structures arising on many parameters and their correspondence to intrinsic properties of the system are emphasized. Their dependence on the initial data ("forgetting" details of the initial data [1, 52, 70]) and on the boundary conditions (effects of localization of processes [28, 33, 42, 60, 61]) has been frequently emphasized. Here we see a new type of independence of a parameter. The magnitude of c_2 determines the frequency of oscillations of

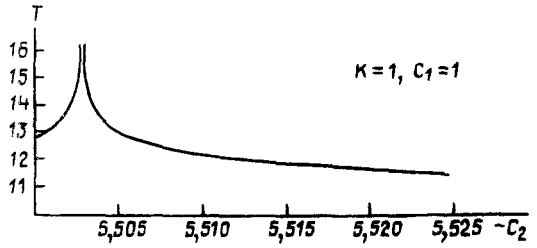

Fig. 14. Dependence of the period of limit cycles on the parameter c_2. The markers correspond to solutions of problem (2.1).

the homogeneous solution (2.3). Dissipative processes lead to the situation that the frequency of oscillations of the quantities ξ and η does not depend on c_2.

The most complex periodic solutions are observed for small values of c_1: $1 \leqslant c_1 \leqslant 2$. A number of their properties were considered in the works [13, 19]. On the line $c_1 = 1.5$ examples of stable cycles S_2^2, S_4^4, S_8^8, S_{16}^{16} were constructed numerically. Several further examples of limit cycles are shown in Fig. 16. They differ considerably from all solutions considered above. This difference consists in the fact that the number of maxima of $\rho_0(t)$ may not coincide with the number of turns of the cycle on the $\{\rho_0, \rho_1\}$ plane. We shall compare the solutions shown in Fig. 16a and b. As c_2 is reduced the cycle practically does not change. However, the first solution has three maxima of ρ_0 while the second has four.

This can be explained as follows. In a nearby region of parameters the system (3.6) has a stable singular point. Restructuring of the vector field precedes its appearance. The trajectories are bent in a complex manner in some region of phase space. Excess maxima and loops appear in their projections onto the $\{\rho_0, \rho_1\}$ plane. This is evident in the example of cycles shown in Fig. 16. Such complication of the cycles is not connected with bifurcations.

The influence of a stable singular point is also expressed in the quantitative characteristics of the solution. The period of the cycle shown in Fig. 16c is equal to 111.3. During time $t \approx 107$ the point describing the state of the system is located on a flat portion of it where $\rho_1 \approx 0.66$. For $c_2 = -8$, $c_1 = 1$, $k = 1$ there arise singular points whose coordinates are labeled in Fig. 16c. To such limit cycles in the region III there correspond relaxation self-oscillations.

4.4. Complex Cycles and Nonperiodic Solutions. Numerical investigation of the dynamical system (3.6) shows that in some range of parameters it has nonperiodic solutions. In this section the solution will be considered nonperiodic if after 300-400 loops about the central region (see Fig. 13) the trajectory does not contract to the limit cycle. The projection of such solutions onto the $\{\rho_0, \rho_1\}$ plane turns out to be very complex and gives no qualitative information regarding the process. Therefore, here it is convenient to use the technique applied by Lorenz [47]. We shall trace the values of the local maxima of the function $\rho_0(t) = \xi^{1/2}(t)$. Along the axis of the abscissa we plot the value of the n-th maximum and along the ordinate axis that of the (n + 1)-st. A remarkable property of the system (3.6) is that these points usually do not fill out any region on the plane. They lie near a certain curve $M_{n+1} = f(M_n)$. Within the limits of accuracy of the calculations this dependence often defines a continuous and single-valued mapping of the segment onto itself. It can be used to approximately describe the complex solutions of the system (3.6) by applying methods of the theory of one-dimensional mappings [71, 73, 77, 106].

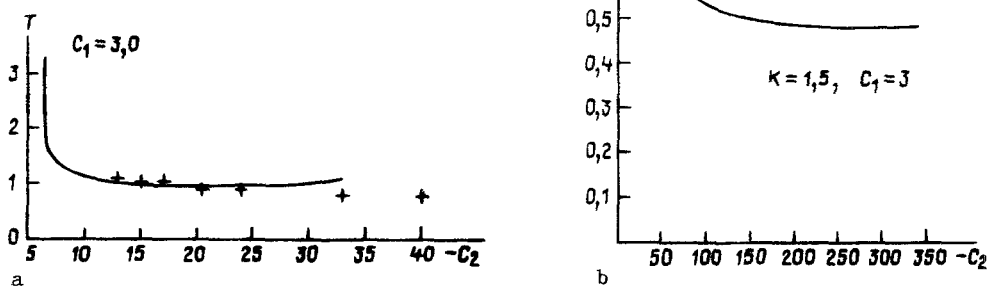

Fig. 15

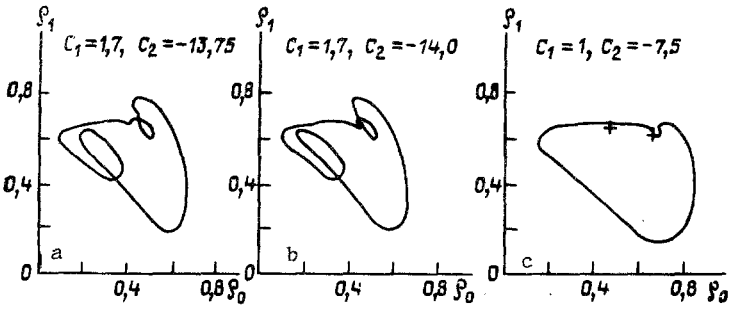

Fig. 16. Stable limit cycles in the simplified system (3.6) in which the number of turns does not coincide with the number of maxima of $\rho_0(t)$.

On the chart of attractors it is possible to distinguish three distinct regions where nonperiodic solutions exist. We consider each of them separately.

Figure 17 shows functions f(M) obtained in calculations for different values of c_2 (c_1 = 5). Over the entire range of the parameters f(M) is continuous, single-valued, and has one sharp maximum. The points usually fill out several "islands" on the curve f(M). As c_2 is reduced passage to complex cycles occurs. After several bifurcations $S^{2n} \to S^n$ a simple cycle arises.

The region of parameters II differs from the region I in that passage to nonperiodic regimes occurs on the line QNP by a jump as the value of c_2 is reduced. On this line there occurs a Hopf bifurcation. While in region I a stable limit cycle is created (the bifurcation is supercritical), in region II the bifurcation is subcritical. Hysteresis is usually a consequence of subcritical bifurcation. The calculations show that above the line QNP nonperiodic solutions and stable singular points can exist simultaneously [13].

The region of parameters III is the most complex to investigate. In this case part of the time the trajectory lies in that region of phase space where the system (3.6) is nondissipative. The function $M_{n+1} = f(M_n)$ here often turns out to be discontinuous and non-single-valued. However, even in this case it is possible to assign certain one-dimensional mappings to the solutions according to a particular algorithm [13]. As a rule, they have a "plateau" consisting of an entire interval where the derivative f'(M) is close to zero. As a consequence of this in the system there may exist several attractors for one and the same values of the parameters. In a number of chemical experiments mappings of just this type occur [25, 112]. It is possible that just they may turn out to be typical for problems where there are several interacting attractors.

The analysis of system (3.6) carried out made it possible to obtain a partition of the plane of parameters into regions in which the attractors have the same type. Figure 11 gives a classification of solutions for $k = 1$ as $t \to \infty$. By varying the initial data, it is possible to see that in certain regions of the parameters several attractors may coexist [11, 13]. However, for the system (3.6) for $k = 1$ this is more an exception than a rule.

We wish to point out that the picture obtained is rather simple. In a large part of parameter space the asymptotics is determined by singular points and simple limit cycles; the boundaries of these regions are given by comparatively simple relations. The question of the correspondence of solutions of the simplified system and of the problem in partial derivatives will be considered below.

5. A Strange Attractor in the Two-Mode System

Earlier we considered complication of the attractor on change of the parameters in the dynamical system (3.6) and the appearance of nonperiodic regimes. It would be important to investigate one such regime in detail. Analysis of a strange attractor turns out to be especially important in studying diffusion chaos in those cases where it has few modes. It would be useful to distinguish general properties of nonperiodic solutions of problem (2.1) and of the model (3.6).

On the other hand, the number of dynamical systems in which strange attractors have been studied in detail is not large. Therefore, analysis of each concrete model can play an important role in the development of theoretical concepts.

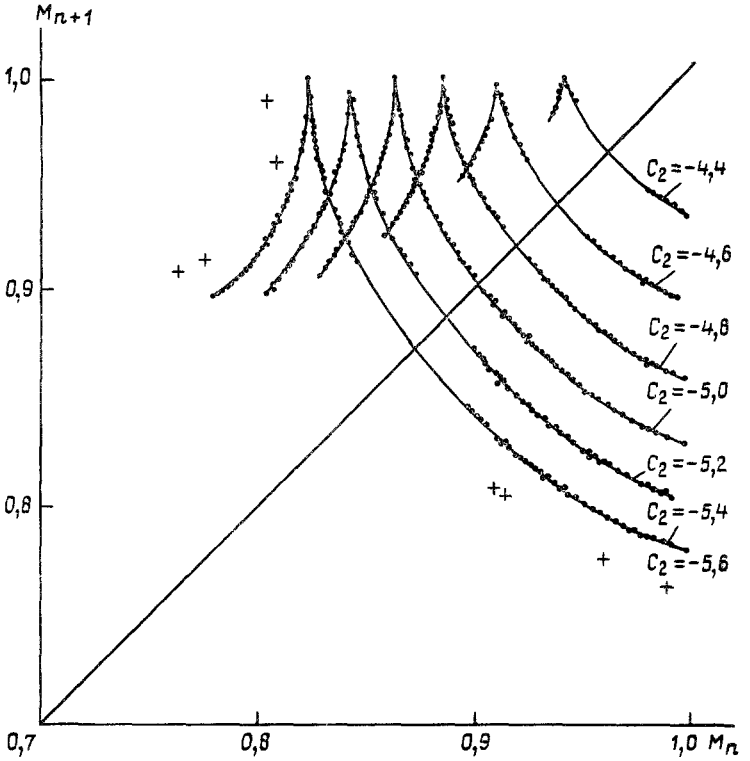

Fig. 17. One-dimensional mappings corresponding to solutions of the simplified system (3.6) for $c_1 = 5$, $k = 1$. In the case where $c_2 = -5.6$ in the system there is the stable cycle S^8.

In this section we shall give main attention below to the attractor of the system of equations (3.6) for $c_1 = 7$, $c_2 = -6$, $k = 1$. Its projection onto the $\{\xi, \eta\}$ plane is shown in Fig. 18; it lies entirely in the region where the system is dissipative. It is evident that a trajectory may land in a neighborhood of the singular point $\xi = 1$, $\eta = 0$ and thus spend a long time near it. The average time T of one turn about the central region is approximately equal to 1.63, while the average value of Ω in formula (4.3) is -4.2. Therefore, after one turn the phase volume in the motion along a trajectory is decreased by almost 900 times.

5.1. Properties of the Poincaré Mapping. We shall consider successive intersections of a trajectory with the plane $\theta = \text{const}$. Since $\dot{\xi}$, $\dot{\eta}$, $\dot{\theta}$ depend only on $\cos\theta$ and $\sin\theta$ (θ is a cyclic coordinate), it is necessary to consider intersections with all planes $\theta = \text{const} + 2\pi n$, $n = 0, 1, 2, \ldots$. The points of intersection form a certain set in the $\{\xi, \eta\}$ plane. It is shown in Fig. 19 for different values of θ. It is evident that the intersection with the plane $\theta = 0$, has the simplest form. We shall consider it in more detail.

The system of equations (3.6) uniquely defines a mapping of the plane into itself (the Poincaré mapping)

$$\begin{aligned} \xi_1 &= \bar{f}(\xi_0, \eta_0), \\ \eta_1 &= \bar{g}(\xi_0, \eta_0). \end{aligned} \tag{5.1}$$

Here ξ_1, η_1 are the coordinates of the point of first intersection of the trajectory with initial data $(\xi_0, \eta_0, 0)$ with the planes $\theta = 2\pi n$. We shall consider only intersections for which $\dot{\theta} > 0$.

It is possible to distinguish a region in the $\{\xi, \eta\}$ plane which under the mapping (5.1) goes over into itself; it contains the attractor. This is the strip ABCD in Fig. 20; its image is a narrow region whose thickness is not evident in the scale of the figure. This is caused by the strong compression of the phase volume under motion along trajectories of the system.

To investigate the Poincaré mapping it is natural to go over to new coordinates. One of them, x, we direct parallel to the side AB; the other is orthogonal to it:

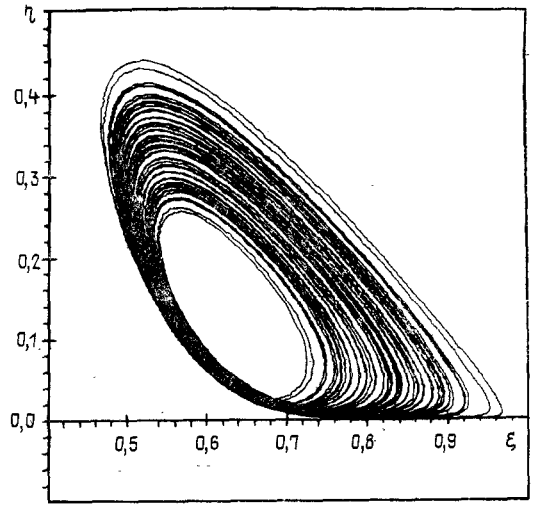

Fig. 18. Projection of the strange attractor onto the $\{\xi, \eta\}$ plane.

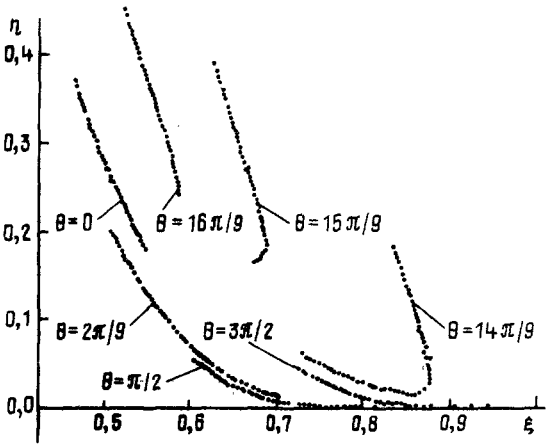

Fig. 19. The Poincaré sections for different planes.

$$x=[3(\xi-0{,}45)-7(\eta-0{,}38)]/\sqrt{58},$$
$$y=[7(\xi-0{,}46)+3(\eta-0{,}38)]/\sqrt{58}. \tag{5.2}$$

The form of the region ABCD and its image A'B'C'D' in the new coordinates is shown in Fig. 21. (We point out that Fig. 21a and b are strongly stretched in the y direction.) In these coordinates the image of the rectangle is a complex curvilinear figure consisting of two parts. The region APQD maps into its lower part. The corresponding trajectories acquire a phase increment $\Delta\theta = 2\pi$ after one turn. The upper part of the curvilinear figure is the image of the set BPQC. The phase increment for trajectories beginning here is equal to zero. The segment PQ goes entirely into the point R.

The form of the functions f and g defining the Poincaré mapping in the new coordinates x, y,

$$x_1=f(x_0, y_0),$$
$$y_1=g(x_0, y_0), \tag{5.3}$$

is shown in Fig. 22. These functions are continuous but have a discontinuity of the derivative on the line PQ. The value of the function f on this segment is equal to the x-coordinate of the point R (see Fig. 21b) and is approximately $5.4\cdot10^{-4}$; the y-coordinate of this point determines the value of g on the segment PQ and is equal to $2.77\cdot10^{-3}$. The calculations show that the partial derivatives of the functions f and g grow without bound in a neighborhood of the line PQ. These properties of the Poincaré mapping turn out to be very essential, and we shall return to them below.

We have gone over from the dynamical system (3.6) to a simpler object – the two-dimensional mapping (5.3). The section of the attractor by the plane $\theta = 2\pi n$ can be obtained as a result of an infinite number of iterations of the functions f and g:

$$x_{n+1}=f(x_n, y_n),$$
$$y_{n+1}=g(x_n, y_n),\ n=1, 2, 3, \ldots . \tag{5.4}$$

There exist simple two-dimensional mappings for which as $n \to \infty$ the points are attracted to a segment ($x_{n+1}=1-2x_n^2$, $y_{n+1}=ay_n$ $|a|<1$) or to an arc of a curve ($x_{n+1}=1-2x_n^2$, $y_{n+1}=h(x_n)$). However, for mappings generated by a system of three ordinary differential equations such a situation is not typical. The uniqueness theorem imposes restrictions on them.

The section of an attractor corresponding to a chaotic regime must possess complex internal structure. For several models calculations made it possible to find this structure [107, 113]. We shall try to do this for the system being studied.

We turn to Fig. 23. Here the distribution of points of intersections of one of the trajectories with the plane $\theta = 2\pi n$ is shown in different scales. Figure 23b shows in magnified form the rectangle labeled in Fig. 23a. In turn the rectangle labeled in Fig. 23b is

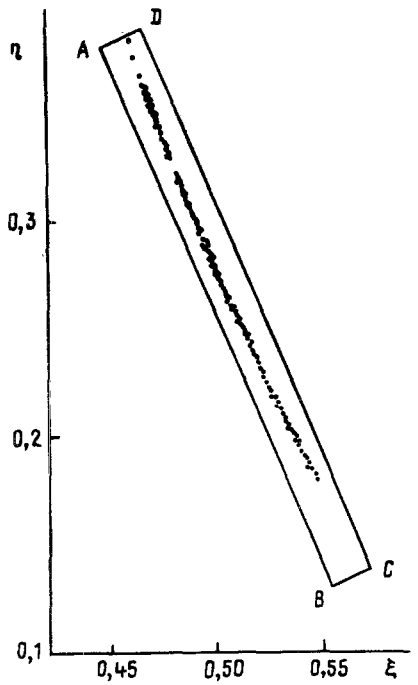

Fig. 20

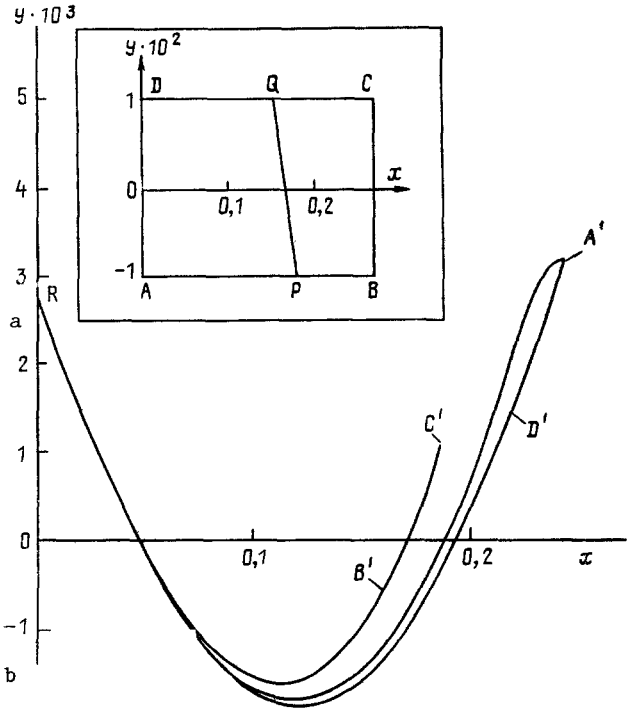

Fig. 21

Fig. 20. Poincaré section by the plane θ = 0 and the region going over into itself.

Fig. 21. The region going over into itself a) and its image b) in the new coordinates.

shown in a still larger scale in Fig. 23c. The section of the attractor on the upper figure consists of two lines. Increase of the resolution by 500 times leads to the situation that each of them splits into two more. We note that the distance between the lines is very small; it does not exceed $4 \cdot 10^{-7}$. It can be expected that this process occurs at still smaller characteristic distances. That is, the attractor in one of the directions possesses a Cantor structure.

Figure 24 shows the dependence of x_{n+1} on x_n. In the scale of the figure the points lie on a continuous, single-valued curve F. We note that $|dF/dx| > 1$ everywhere except for one part on the left end of the segment.

The one-dimensional mapping $x_{n+1} = F(x_n)$ can be considered a certain simplified model for problem (3.6). Many results of the theory of mappings of a segment into itself turn out to be useful in analyzing it [71, 73, 77].

We now consider how y_{n+1} and y_n are related. The results of the corresponding calculation are shown in Fig. 25. The picture obtained is more complex than for the coordinate x. Since to one value of y there correspond one, two, three, or four different points lying on the attractor (see Fig. 23a), the dependence of y_{n+1} on y_n will also not be single-valued. To one y_n there may correspond from one to four y_{n+1}. (Of course, all that has been said is valid on those scales where the fine structure of the attractor is not manifest.)

We compare Fig. 23a and Fig. 25. Images of points lying on the branch ABC in the first figure are determined by means of the curve A'B'C' on the second. The branch C'R' makes it possible to find where points from the portion CR go; the branch R'D'E' corresponds to the line RDE in exactly the same way. The point B in Fig. 23a lies on the intersection of the arc AC of the attractor with the segment PQ (see Fig. 21a).

Thus, the result of the action of the two-dimensional mapping (5.3) for points of the attractor can be predicted quite accurately by means of several one-dimensional mappings.

Remark. As a rule algorithms of high-order accuracy are used in the numerical solution of dynamical systems. However, successive intersections of a trajectory with a plane are usually determined by simple interpolation which sharply reduces the accuracy of the calculations. Henon's algorithm, connected with passage to new variables [91], makes it possible to

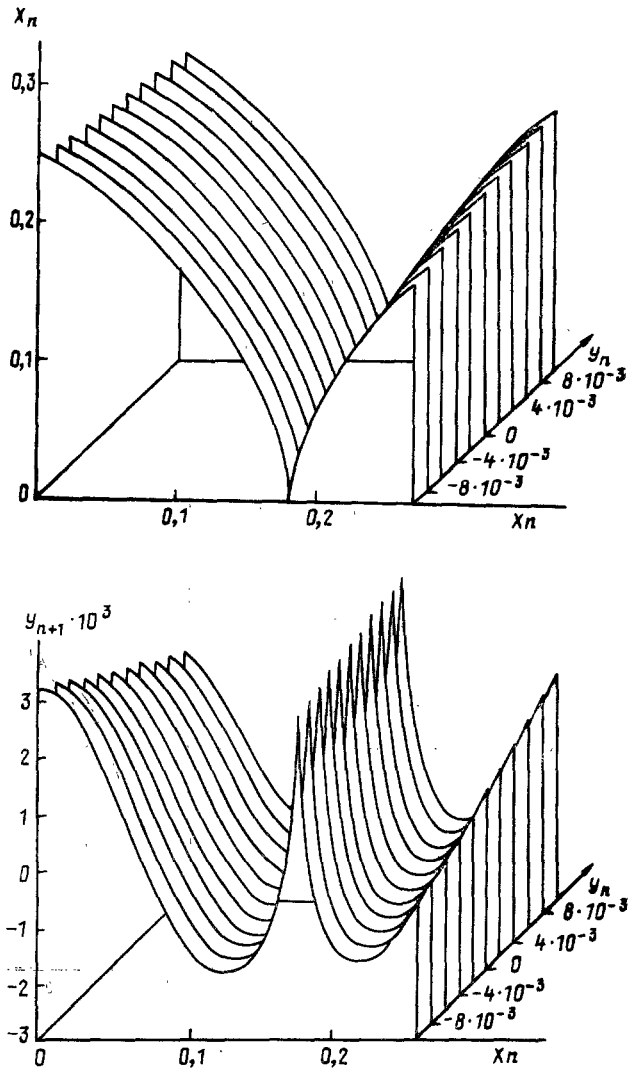

Fig. 22. The two-dimensional functions realizing the Poincaré mapping.

avoid this. It provides the possibility of constructing the Poincaré mapping with the same accuracy to which the solution is known. For analysis of the dynamical system (3.6) a Runge–Kutta method of fourth order and Henon's algorithm for constructing the Poincaré mapping are applied.

5.2. Behavior of Trajectories near Singular Points. Figure 18 shows that the projections of different loops of the trajectory onto the $\{\xi, \eta\}$ plane do not differ from one another qualitatively. However, by tracing their variation in the space $\{\xi, \eta, \theta\}$, it is possible to distinguish loops of two different types. In one type on return to the plane $\theta = 2\pi n$, $n = 0, 1, 2, \ldots$ the phase is changed by 2π, while in the other type it is unchanged. In the one-dimensional mapping F (see Fig. 24) the left part of the curve corresponds to loops of the first type, while the right part corresponds to loops of the second type. If the time of each turn were bounded above, then the functions f and g in the mapping (5.3) would be continuous and differentiable, and the increment of the phase $\Delta\theta$ could not suffer a jump. In our case this is not so. It may be supposed that the reason is the influence of one of the singular points of the dynamical system (3.6) in a neighborhood of which the time of the loop can grow without bound.

An important property of the system (3.6) is that the plane $\eta = 0$ is an invariant manifold: if $\eta(0) = 0$, then also $\eta(t) = 0$. We shall find all singular points with $\xi^2 + \eta^2 \neq 0$ lying in this plane. Judging from Fig. 18, they are precisely the ones which affect the behavior of the strange attractor. From the first equation of (3.6) it follows that $\xi = 1$, while from the third we obtain a relation for θ:

$$\sin\theta + c_2\cos\theta + c_2 + c_1k^2 = 0. \tag{5.5}$$

This equation has two solutions:

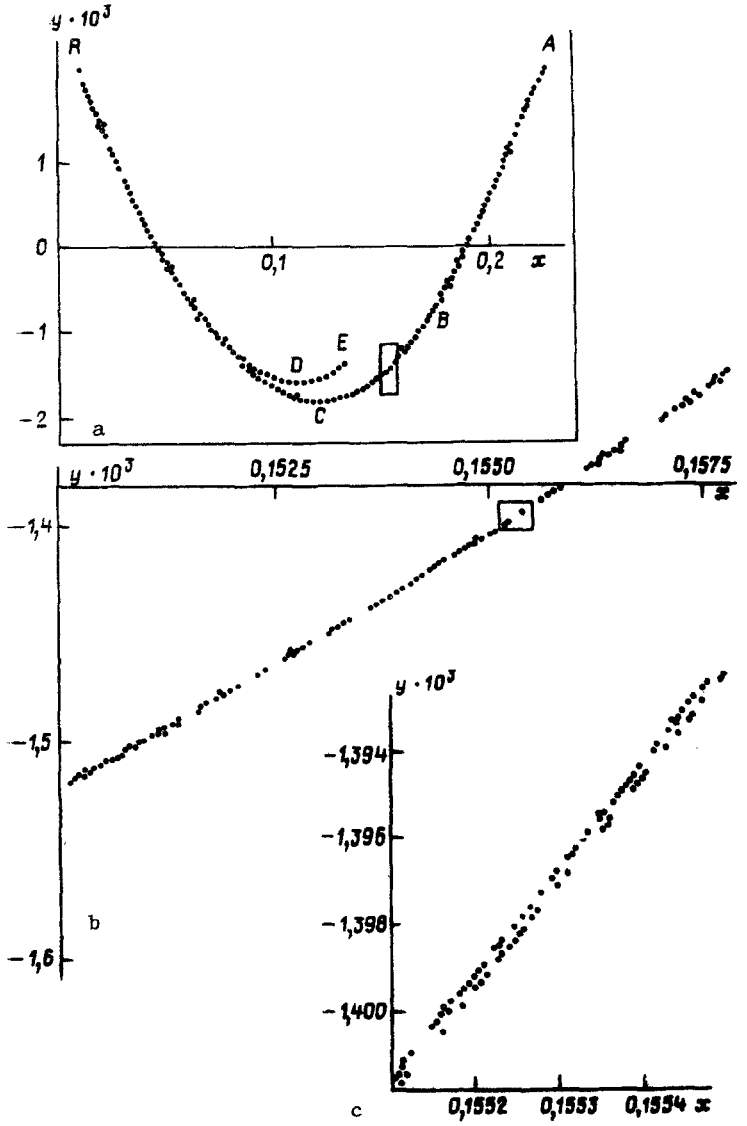

Fig. 23. A section of the attractor in different scales.

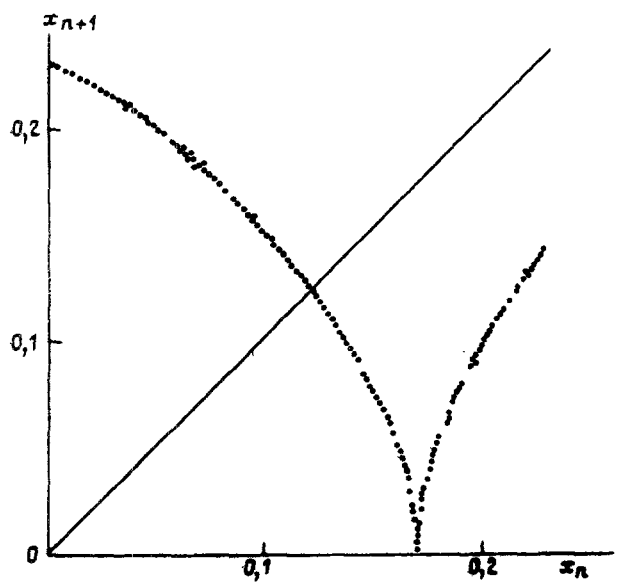

Fig. 24

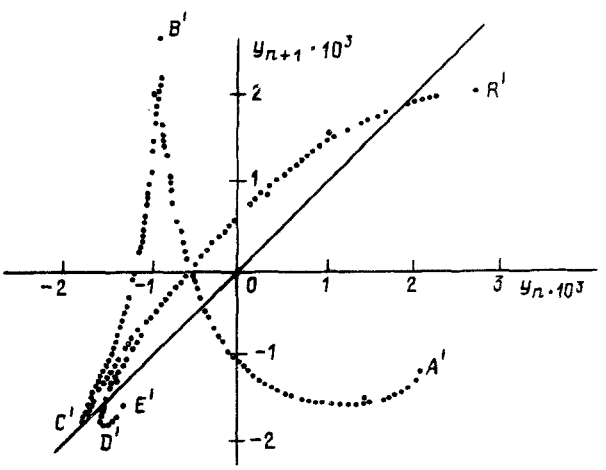

Fig. 25

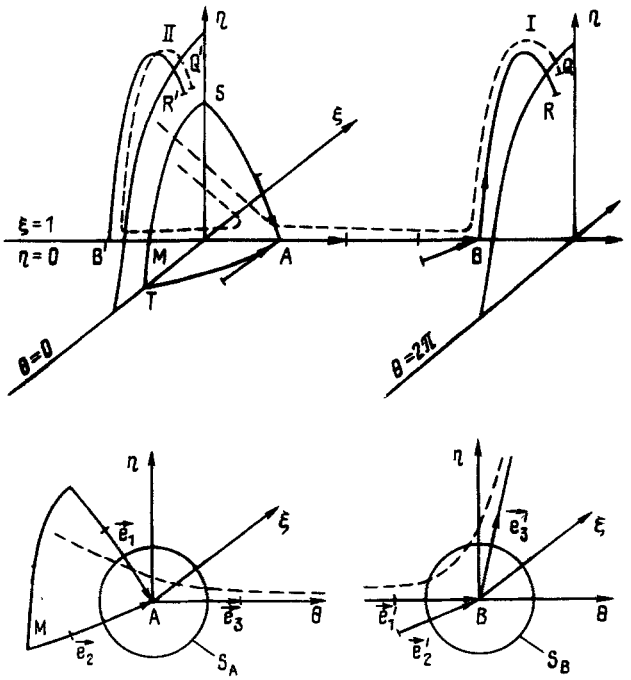

Fig. 26. Qualitative picture of the behavior of trajectories in a neighborhood of singular points.

$$\sin\theta=\left[-(c_2+c_1k^2)\mp c_2\sqrt{1+c_2^2-(c_2+c_1k^2)^2}\right]/(1+c_2^2),$$
$$\cos\theta=\left[-c_2(c_2+c_1k^2)\pm\sqrt{1+c_2^2-(c_2+c_1k^2)^2}\right]/(1+c_2^2). \tag{5.6}$$

Stability of the singular points is determined by the real parts of the eigenvalues of the matrix (4.9) of the system (3.6) linearized in a neighborhood of the singular point. For points with $\xi = 1$, $\eta = 0$ the matrix **A** simplifies:

$$\mathbf{A}=\begin{pmatrix} -2 & -2-\cos\theta-c_2\sin\theta & 0 \\ 0 & -2(1+k^2+\cos\theta-c_2\sin\theta) & 0 \\ 2c_2+2(\sin\theta+c_2\cos\theta) & -c_2/2-c_2\cos\theta+\sin\theta & 2\cos\theta-2c_2\sin\theta \end{pmatrix}. \tag{5.7}$$

This makes it possible to find its eigenvalues in explicit form:

$$\Lambda_1=-2,\quad \Lambda_2=-2\left[1+k^2\pm\sqrt{1+c_2^2-(c_2+c_1k^2)^2}\right],$$
$$\Lambda_3=\pm2\sqrt{1+c_2^2-(c_2+c_1k^2)^2}. \tag{5.8}$$

Here we have used the corollary of equality (5.5)

$$\cos\theta-c_2\sin\theta=\pm\sqrt{1+c_2^2-(c_2+c_1k^2)^2}.$$

We now substitute the values of the parameters of interest to us $c_1 = 7$, $c_2 = -6$, $k = 1$ into formulas (5.6)-(5.8). The solutions of Eq. (5.6) are hereby the following: $\theta_A \approx 1.24$, $\theta_B = 3\pi/2$. It will be convenient for us to renumber the eigenvalues in increasing order ($\vec{e}_1, \vec{e}_2, \vec{e}_3, \vec{e}_1', \vec{e}_2', \vec{e}_3'$ are the corresponding eigenvectors). For the point A we obtain

$$\lambda_1=-16,\quad \vec{e}_1=\begin{bmatrix} m \\ n \\ l \end{bmatrix};\quad \lambda_2=-2,\quad \vec{e}_2=\begin{bmatrix} a \\ 0 \\ b \end{bmatrix};\quad \lambda_3=+12,\quad \vec{e}_3=\begin{bmatrix} 0 \\ 0 \\ 1 \end{bmatrix}. \tag{5.9}$$

For the point B

$$\lambda_1'=-12,\quad \vec{e}_1'=\begin{bmatrix} 0 \\ 0 \\ 1 \end{bmatrix};\quad \lambda_2'=-2,\quad \vec{e}_2'=\begin{bmatrix} p \\ 0 \\ q \end{bmatrix};\quad \lambda_3'=+8,\quad \vec{e}_3'=\begin{bmatrix} r \\ s \\ t \end{bmatrix}. \tag{5.10}$$

Here m, n, ℓ, a, b, p, q, r, s, t are constants whose specific values are inconsequential for us.

From formulas (5.9), (5.10) it is evident that the points A and B are saddle points each having one unstable direction. The line $\xi = 1$, $\eta = 0$, $\theta = \theta(t)$ joining these points is hereby an integral curve of the system of equations (3.6) for all values of the parameters. Figure 26 shows the approximate position of the singular points A and B and also of the

eigenvectors of the matrix A corresponding to them. The surface M is a stable two-dimensional manifold of the point A. The line $\xi = 1$, $\eta = 0$ is an unstable manifold. The plane $\eta = 0$ is a stable manifold of the point B. Its unstable manifold intersects the plane $\theta = 2\pi$ at the point R.

Proceeding from Fig. 26, it is possible to represent an integral curve beginning near the surface M (above it) in the following manner. First a point on the trajectory moves near M to the point A and then along the segment $\xi = 1$, $\eta = 0$ to the saddle point B. It then passes along the arc BR and intersects the plane $\theta = 2\pi$ at a point Q located in a neighborhood of R. This is curve I in Fig. 26. We note that the trajectory cannot issue from the point B downward into the region $\eta < 0$, since for this it would have to intersect the plane $\eta = 0$ which is an invariant manifold.

Suppose now that the trajectory begins below the surface M (curve II in Fig. 26). In this case the point also moves along M but near the point A it turns to the left. It approaches the saddle point B' and then falls onto the plane $\theta = 0$ along the curve B'R'. In the first case the phase changed by 2π, while in the second it did not change. The increment of the phase on the next loop depends on the relative position of the manifold M and the points Q, Q'. The calculations carried out completely corroborate what has been said [17].

The surface M intersects the plane $\theta = 0$ along some line TS. The image of this line is the point R (or R'). Formally the Poincaré mapping is not defined on TS, since the trajectories pass through two singular points which requires infinite time. However, it can be extended by continuity. The segment PQ in Fig. 21a is part of the arc TS.

From the qualitative picture described it is clear that as an initial point on the plane $\theta = 2\pi n$ approaches the line TS the time of the loop will grow without bound. The law of growth plays an essential role in investigating stochastic properties of the attractor. We shall try to estimate it.

Let $x(t)$ be a trajectory of the dynamical system, $x(0) = x_0$, $x(t_1) = x_1$. We shall be interested in the behavior of a nearby trajectory with $\bar{x}(0) = x_0 + \varepsilon$. If $|\varepsilon|$ is small, then the difference $y(t) = \bar{x}(t) - x(t)$ will be determined by the solution of the linear problem

$$\dot{y} = \mathbf{B}(t)\, y, \quad y(0) = \varepsilon. \tag{5.11}$$

If the system is nondegenerate and the value of t_1 is finite [that is, the trajectory $x(t)$ does not pass onto the interval being studied at a singular point], then

$$\bar{x}(t_1) - x(t_1) = y(t_1) = \|\varepsilon\| \cdot Y(t_1),$$

where $Y(t_1)$ depends on the dynamical system. From this it follows that the order of the quantity $y(\varepsilon)$ can change only near singular points.

Proceeding from this, we surround the saddle points A and B by spheres S_A and S_B of small but finite radius r. We assume that inside each of them the system (3.6) is well approximated by the linear problem with matrix (5.7). Let ε be the distance from the initial point to the surface M (the stable manifold of the saddle point A), $\varepsilon \ll r$. This distance will have the same order when the trajectory intersects the sphere S_A. It is possible to determine the coordinates of the point of intersection in the basis $\vec{e}_1, \vec{e}_2, \vec{e}_3$ up to leading terms in ε:

$$\vec{s}_1 = a\vec{e}_1 + b\vec{e}_2 + c\vec{e}_3, \quad a^2 + b^2 \sim r^2, \quad c \sim \varepsilon. \tag{5.12}$$

Suppose that at time T_A the trajectory passes out of the ball S_A. The coordinates of the point $\vec{s}_2$ of exit can be written in the form

$$\vec{s}_2 = ae^{-|\lambda_1|T_A}\vec{e}_1 + be^{-|\lambda_2|T_A}\vec{e}_2 + ce^{\lambda_3 T_A}\vec{e}_3 \sim r\vec{e}_3. \tag{5.13}$$

From this it follows that

$$T_A = \frac{1}{\lambda_3} \ln \frac{1}{\varepsilon}. \tag{5.14}$$

At time T_A the distance δ from the point of exit from the ball to the plane $\eta = 0$ is

$$\delta \sim ae^{-|\lambda_1|T_A} = a\varepsilon^{|\lambda_1|/\lambda_3}. \tag{5.15}$$

It is also possible to estimate the distance from the point of exit to the line $\xi = 1$, $\eta = 0$:

$$\rho \sim be^{-|\lambda_2|T_A} = b\varepsilon^{|\lambda_2|/\lambda_3}. \tag{5.16}$$

We recall that $|\lambda_2| < |\lambda_1|$.

Between S_A and S_B the point is located in a neighborhood of the integral curve $\xi = 1$, $\eta = 0$, $\theta = \theta(t)$. Therefore, the order of smallness of the quantities δ and ρ does not change. The point $\vec{s}_1'$ at which the trajectory enters the sphere S_B is determined in the basis $\vec{e}_1'$, $\vec{e}_2'$, $\vec{e}_3'$ as follows:

$$\vec{s}_1' = a'\vec{e}_1' + b'\vec{e}_2' + c'\vec{e}_3', \tag{5.17}$$

where $a' \sim r$, $b' \sim \rho$, $c' \sim \delta$.

We now remark that δ determines the distance from the point of entry into the sphere S_B to the stable manifold of the saddle point B – the plane $\eta = 0$. Therefore, the time T_B which the point passes inside the sphere S_B can be found from a formula analogous to (5.14):

$$T_B = \frac{1}{\lambda_3'} \ln \frac{1}{\delta} = \frac{|\lambda_1|}{\lambda_3 \lambda_3'} \ln \frac{1}{\varepsilon}. \tag{5.18}$$

As $\varepsilon \to 0$ T_A and T_B tend to infinity, while the time of motion along other parts of the trajectory is bounded. Therefore, the dependence of the time of return to the plane $\theta = 2\pi n$ on ε is determined by the sum

$$T = T_A + T_B = \frac{1}{\lambda_3} \left(1 + \frac{|\lambda_1|}{\lambda_3'}\right) \ln \frac{1}{\varepsilon}. \tag{5.19}$$

Thus, the function $T(\varepsilon)$ has a logarithmic singularity. Calculations carried out [17] corroborate this. For $c_1 = 7$, $c_2 = -6$, $k = 1$ the dependence $T(\varepsilon)$ obtained in the calculation has the form $T = 0.580 \log(1/\varepsilon)$; formula (5.19) gives $0.578 \log(1/\varepsilon)$.

It is thus possible to clarify the behavior of the functions f and g near the line of discontinuity of derivatives PQ (see Fig. 21a). The values of the functions on the segment PQ itself are constant and coincide with the coordinates of the point R. The character of the singularity is determined by the dependence $\mu(\varepsilon)$, where μ is the distance from the trajectory to the curve BR at the time of exit from the sphere S_B. [The order of $\mu(\varepsilon)$ does not change further until the intersection with the plane $\theta = 2\pi n$.] Formula (5.17) makes it possible to find the coordinates of the point of exit from the sphere S_B in the basis $\vec{e}_1'$, $\vec{e}_2'$, $\vec{e}_3'$:

$$\vec{s}_2' = a' e^{-|\lambda_1'| T_B} \vec{e}_1' + b' e^{-|\lambda_2'| T_B} \vec{e}_2' + c' e^{\lambda_3' T_B} \vec{e}_3'. \tag{5.20}$$

Since $\mu \sim \max\{a' \exp[-|\lambda_1'| T_B], b' \exp[-|\lambda_2'| T_B]\}$, it follows that $\mu \sim \varepsilon^{\alpha}$, where

$$\alpha = \min\{|\lambda_1 \lambda_1'| / \lambda_3 \lambda_3', |\lambda_2| / \lambda_3 + |\lambda_1 \lambda_2'| / \lambda_3 \lambda_3'\}. \tag{5.21}$$

For $c_1 = 7$, $c_2 = -6$, $k = 1$, $\alpha = 1/2$, that is, $\mu \sim \sqrt{\varepsilon}$. In the calculation the value of the exponent α near the singularity for the function $f(x, y)$ and $y = 0$ was approximately equal to 0.51. Good agreement of the results of calculations with the estimates (5.19), (5.21) corroborate the qualitative picture of the behavior of trajectories near singular points which has been described in this section.

As we have already mentioned, projection of a trajectory onto the $\{\xi, \eta\}$ plane does not give a full idea of the geometry of the attractor in three-dimensional space. Figure 27 shows part of an integral curve of the system of equations (3.6) in the coordinates $x = \xi \cos\theta$, $y = \xi \sin\theta$, $z = \eta$. It lies on some surface, since in the scale of the figure the fine structure of the attractor is not evident. This surface consists of two parts which are "glued together" in the upper region. From this region a point begins to move in the direction of the saddle point A and then to the right or left depending on the initial data. Later, passing near the saddle point B, it again lands in the upper part of the attractor. After one such circuit the right strip is stretched and its orientation is changed. The left part of the surface is also stretched, but the orientation does not change.

From this it is clear that the attractor in this space can be represented as a Möbius strip (the right side) and an ordinary annulus (the left side) glued together. On completing a circuit about the right side of the attractor, the trajectory increases the phase by 2π, while about the left it remains unchanged.

This behavior makes it possible to give a symbolic description of a trajectory by assigning to it an infinite sequence of symbols R and L. Here R will stand at the n-th site if on the n-th loop the trajectory moved along the right portion of the surface and L if along the left. Topological methods developed in the study of the Lorentz attractor [26, 114] can apparently also be used here.

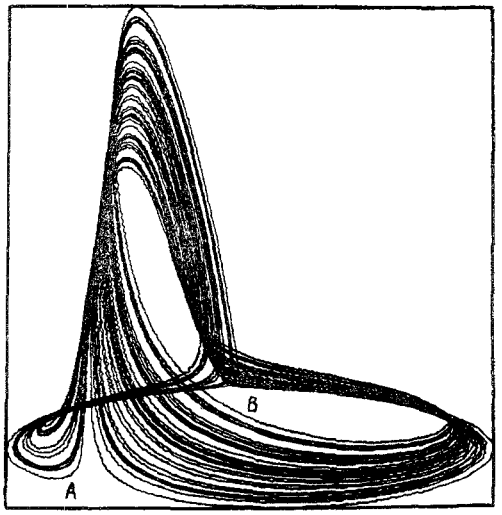

Fig. 27

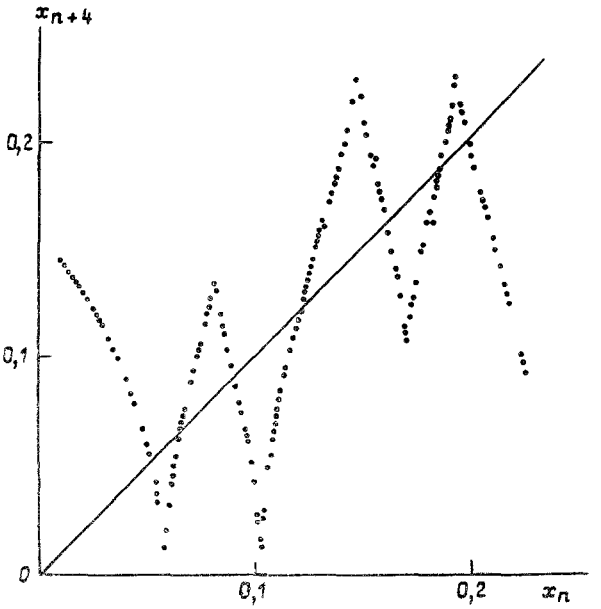

Fig. 28

5.3. Properties of Contraction and Dilation of the Mapping T^4. At the present time stochastic properties of so-called hyperbolic systems have been studied in detail. The following inequalities constitute the condition for hyperbolicity for the two-dimensional mappings $x_{n+1} = f(x_n, y_n)$, $y_{n+1} = g(x_n, y_n)$:

$$\begin{gathered}\|(f_x)^{-1}\|<1, \quad \|g_y\|<1, \quad \|a(x, y)\|=\max_{(x,y)\in G}|a(x, y)|, \\ \|(f_x)^{-1}g_x\|\cdot\|f_y\|<(1-\|(f_x)^{-1}\|)(1-\|g_y\|), \\ 1-\|(f_x)^{-1}\|\cdot\|g_y\|>2\sqrt{\|(f_x)^{-1}g_x\|\cdot\|(f_x)^{-1}\|\cdot\|f_y\|}.\end{gathered} \tag{5.22}$$

They must be valid in some region G which contains the attractor. The first two inequalities indicate the presence of everywhere contractive and everywhere dilating directions. The two others bear witness to the existence in a neighborhood of them of an entire cone of contractive and dilating directions [23, 54].

For the independent variables x and y and the functions f and g in the Poincaré mapping (5.3) inequality (5.22) are not satisfied. The derivative $|\partial f/\partial x|$ turns out to be less than one in the left part of the region ABCD. The y direction is contractive everywhere with the exception of a small neighborhood of the line PQ (see Fig. 21) on which the derivatives of f and g have a singularity.

In place of the Poincaré mapping we consider its fourth iteration $T^4: x_{n+4}=p(x_n, y_n)$, $y_{n+4}=q(x_n, y_n)$. Calculations show that $|\partial p/\partial x|>1$ in the region $G=\{0\leqslant x\leqslant 0{,}27;\ -0{,}002\leqslant y\leqslant 0.005\}$ entirely containing the attractor. We note that the corresponding one-dimensional mapping $x_{n+4}=F^4(x_n)$ is also everywhere dilating (see Fig. 28).

The function $q(x_n, y_n)$ has a singularity not only on the sequence PQ as does $g(x, y)$ in formulas (5.3) but also on some other lines $L_1, L_2, \ldots, L_5$. The derivative $\partial g/\partial y$ is small in the region G if the points $\{x_n, y_n\}$ do not lie in a neighborhood of these lines. On the lines L_i, PQ the only contractive direction is the direction tangential to them. The derivatives in all other directions tend to infinity. This follows from the form of the functions p and q in a neighborhood of L_i, PQ:

$$\begin{aligned}p(x_n, y_n)&=p_0+B(x_n, y_n)[x_n-x_0(y_n)]^\alpha, \\ q(x_n, y_n)&=q_0+A(x_n, y_n)[x_n-x_0(y_n)]^\alpha,\end{aligned} \tag{5.23}$$

where $p_0 = \text{const}$, $q_0 = \text{const}$, $B(x, y)$, $A(x, y)$ are sufficiently smooth functions, α is determined by formula (5.21), and $x_n = x_0(y_n)$ is the equation of the arc L_i, PQ.

Substituting formulas (5.23) into inequalities (5.22) and assuming that the y axis is directed along the arc L_i, PQ it is possible to verify that these conditions are satisfied near the singularity. Calculations were carried out in which one of the axes was chosen

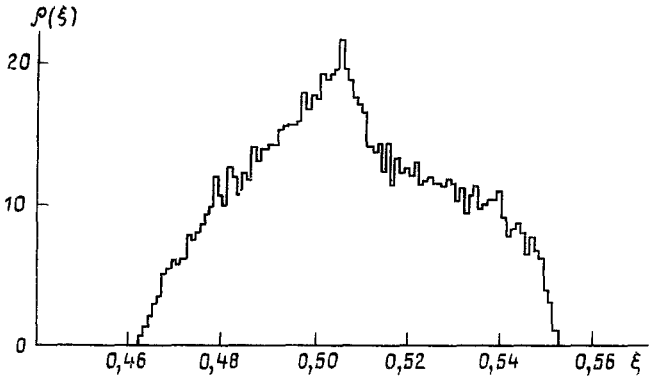

Fig. 29. Histogram constructed for a strange attractor.

along x and the other along PQ. They made it possible to verify the presence of a contractive direction for the mapping T in an entire region containing the attractor. Apparently this is also true for T^4. (Numerical verification of this fact requires the introduction of a more complex curvilinear grid.) It can be expected that, as in the Lorenz model [6, 23], ergodicity of the system will follow from the validity of conditions (5.22) away from the singularity and the existence of contractive directions along them.

5.4. Quantitative Characteristics of the Strange Attractor. The presence of a strange attractor means that the trajectories of the dynamical system behave in a stochastic manner. One manifestation of stochasticity is the existence in phase space of a stationary probability distribution or an invariant measure [65]. Such a distribution makes it possible to find the mean values of various characteristics of the system and to study its statistical properties.

We return to the dynamical system (3.6). We shall trace the values of the coordinate ξ of successive points of intersection of a trajectory with the plane $\theta = 2\pi n$ at which $\dot{\theta} > 0$. We construct a histogram on the basis of the sequence $\{\xi_n\}$ and orthonormalize it so that the area under the curve is equal to one. Calculations show that with increase of the sample length N this curve becomes smoother and smoother and ceases to change. Figure 29 shows the histogram constructed on the basis of N = 20,480 points. The number N depends on the selected interval ε along the ξ axis. The finer the step size we choose, the larger becomes the value of N for which the histogram practically ceases to change. For other initial data the same function $\rho(\xi)$ was obtained. This fact gives reason to suppose that also in three-dimensional phase space there exists an invariant measure which determines the statistical properties of all trajectories attracted to the strange attractor.

A typical property of strange attractors is the sensitivity to initial data [46, 72, 77]. The average rate at which trajectories infinitely close initially diverge is conveniently characterized by Lyapunov exponents.

Suppose that $\varphi^t(x_0)$, $\varphi^t(x_0+\Delta x)$ are two nearby trajectories of the dynamical system issuing from the points x_0 and $x_0 + \Delta x$ (see Fig. 30). The Lyapunov exponent $\chi(x_0, \vec{\omega})$ is the quantity

$$\chi(x_0, \vec{\omega}) = \lim_{t\to\infty} \lim_{d(0)\to 0} \frac{1}{t} \ln (d(t)/d(0)). \tag{5.24}$$

It can be shown that this definition is equivalent to

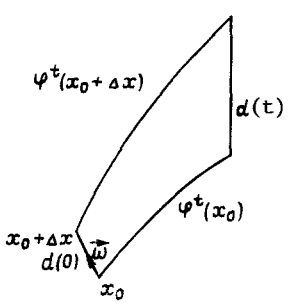

Fig. 30

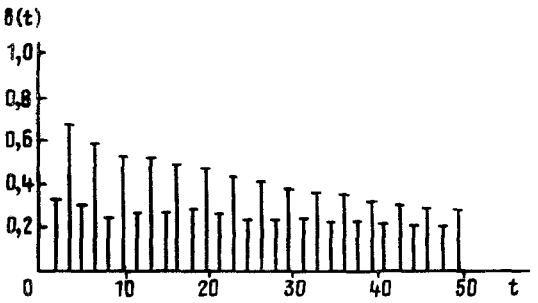

Fig. 31. Correlation function constructed for the attractor.

$$\chi(x_0, \vec{\omega}) = \lim_{t\to\infty} \frac{1}{t} \ln(\| y^t(\vec{\omega}) \| / \| \vec{\omega} \|), \tag{5.25}$$

where $y^t(\omega)$ is a solution of the problem linearized in a neighborhood of the trajectory $\varphi^t(x_0)$ and $\vec{\omega}$ is an arbitrary vector directed from x^0 to the point $x_0 + \Delta x$.

In an n-dimensional dynamical system the Lyapunov exponents $\chi(x_0, \vec{\omega})$ assume a finite collection of values $\lambda_1, \lambda_2, \ldots, \lambda_n$. In many problems these values are the same for almost all initial data x_0. In the case of a stable limit cycle $\lambda_i \leqslant 0$, $i = 1, \ldots, n$. The existence of positive Lyapunov exponents indicates that nearby trajectories diverge exponentially and that the system possesses sensitivity to the initial data. This gives reason to suppose that a strange attractor exists in the system.

To compute Lyapunov exponents it is convenient to use the technique proposed in the work [74] which requires simultaneous solution of the original system and a variational system. Renormalization and orthogonalization of solutions of the linearized problem are hereby necessary after particular time intervals.

The attractor being studied of the system of equations (3.6) ($c_1 = 7$, $c_2 = -6$, $k = 1$) is characterized by the following exponents: $\lambda_1 = +0.23$, $\lambda_3 = -4.39$, and λ_2 is close to zero within the accuracy of the computations. These values of λ_i were obtained in calculations for various initial data. The sum of the exponents gives the mean value of the quantity $\Omega: \lambda_1+\lambda_2+\lambda_3 = \langle \partial\dot{\xi}/\partial\xi + \partial\dot{\eta}/\partial\eta + \partial\dot{\theta}/\partial\theta \rangle$ which determines the rate of change of the phase volume during motion along a trajectory. An important characteristic of an attractor is its dimension. Knowing the Lyapunov exponents and using the Kaplan–Yorke formula, it is possible to estimate the probabilistic dimension of an attractor (the dimension of the natural measure) [83]. In our case this formula gives

$$D = 2 + (\lambda_1+\lambda_2)/|\lambda_3| \approx 2{,}05. \tag{5.26}$$

Since the quantity D has a small fractional part, it is natural to expect that the behavior of trajectories on the attractor is characterized by high accuracy by some one-dimensional mapping. This agrees with results of calculations (see Figs. 23, 24, 28).

Another quantitative characteristic of a strange attractor is the autocorrelation function

$$b(t) = \frac{\langle \xi(\tau)\cdot\xi(\tau+t) \rangle - \langle \xi(\tau) \rangle^2}{\langle \xi^2(\tau) \rangle - \langle \xi(\tau) \rangle^2}, \qquad \langle a(\tau) \rangle = \lim_{T\to\infty} \frac{1}{T} \int_0^T a(\tau)\, d\tau, \tag{5.27}$$

When $b(t) \to 0$, $t \to \infty$ there is mixing in the system which bears witness to the randomness of the process in question. Exponential decay of correlations turns out to be one of the strongest stochastic properties [65].

In our case the autocorrelation function has oscillating character, and the period of the oscillations is close to the average time of a loop. In order to trace the decay of correlations, along the ordinate axis we plot the local maximum of the function b(t) and along the abscissa the times at which they are achieved. The picture obtained is shown in Fig. 31.

We note that the computation of b(t) requires calculation of mean values over large portions of the trajectory. We shall clarify this with the following example. We consider a sequence $\{a_n\}$ whose terms change sign on the average every r elements. [The sequence $\xi(t_n) - \langle\xi\rangle$ of points on a phase trajectory found numerically has just such a structure.]

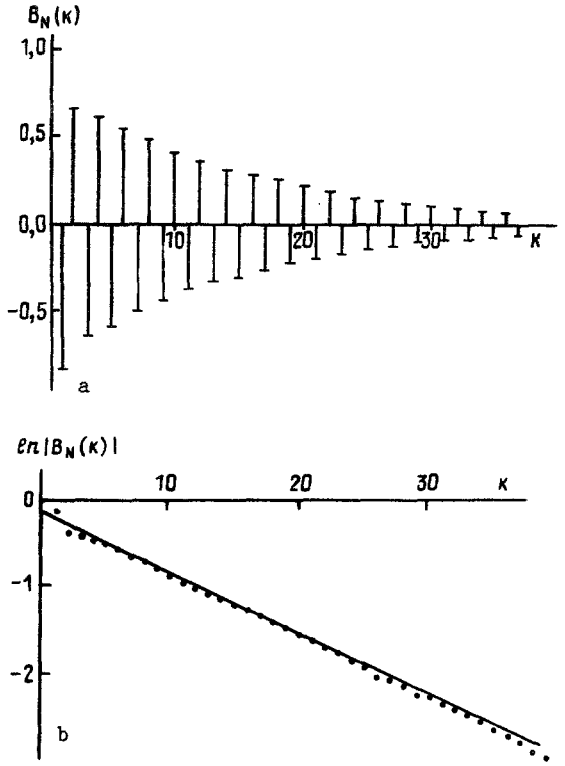

Fig. 32a, b. Correlation function construction for the Poincaré mapping.

Then

$$\langle a\rangle_N=\frac{1}{N}\sum_{n=1}^{N}a_n=\frac{N-r-1}{N}\langle a\rangle_{N-r-1}+\frac{1}{N}\sum_{n=N-r}^{N}a_n. \tag{5.28}$$

From this formula it follows that $\langle a\rangle_N$ has oscillating character, and the amplitude of the oscillations depends on N ($\approx\langle a\rangle r/N$). In order to compute $\langle a\rangle$ with accuracy ε, it is necessary to take $N > \langle a\rangle r/\varepsilon$ elements.

In our case ε should be much less than $\bar{b}(t)$; therefore, $N\gg[\langle\xi^2\rangle-\langle\xi\rangle^2]r/b(t)$. In the calculations conducted N = 106,496, and this did not make it possible to determine the decay law of the correlations.

In a quantitative investigation of correlation functions it is convenient to go over to another mathematical object connected with the dynamical system (3.6). We again consider the sequence $\{\xi_n\}$, where ξ_n is the coordinate of the n-th intersection of the trajectory with the planes $\theta = 2\pi n$, $\dot{\theta} > 0$, and the corresponding autocorrelation function $B_N(k)$. For the sequence $\{\xi_n\}$, r = 1. Figure 32a shows the dependence of $B_N(k)$, and Fig. 32b shows its logarithm. It is evident that on this interval $|B_N(k)|$ decays faster than $\text{const}\cdot e^{-\lambda k}$, where $\lambda \approx 0.0675$.

In this calculation N = 19,456. An important question in this case as well is the relation between the length of the sample N and the number of terms which we can compute with sufficient precision on the basis of it. It can be shown that the sums $I_1=\frac{1}{N}\sum_{n=1}^{N}\xi_n\xi_{n+k}$ and $I_2=\frac{1}{N}\sum_{n=1}^{N}\xi_n f^k(\xi_n)$ are connected with one another. Here f is a continuous function having one extremum [qualitatively the function f is analogous to the dependence $x_{n+1} = F(x_n)$ shown in Fig. 24].

The sum I_2 approximates the integral $I=\int_{\xi_{\min}}^{\xi_{\max}}\xi f^k(\xi)\rho(\xi)\,d\xi$, in which the integrand is rapidly oscillating. The function $f^k(\xi)=\underbrace{f(f(\ldots f}_{k}(\xi)))$ has 2^{pk} extrema where $0 < p < 1$, where p = const. (This follows from the form of the function f.) For numerical integration it is natural to require that on each extremum there should be no fewer than s points; then $N = s\cdot 2p^k$. Figure 29 gives an idea of the function $\rho(\xi)$. Thus, the number of values of the

correlation function which can be computed with sufficient precision depends on the sample length according to the logarithmic law:

$$k_{\max}=\frac{1}{p}\log_2\frac{N}{s},\quad s=4-6. \tag{5.29}$$

For $N = 19\cdot 2^{10}$ the maximal number k_{max} has order 30.

We point out that correlation functions computed along a trajectory of the dynamical system and on the basis of the Poincaré section differ substantially. It is evident that even maxima of the correlation function decay according to an exponential law, while odd maxima practically do not decay. By the Wiener–Khinchin theorem it follows from this that in the spectrum of the solution there is a sharp maximum at some frequency ω. It can be expected that $\omega = 2\pi/\overline{T}$, where $\overline{T}$ is the average time of a loop.

Study of those properties of the dynamical systems which are not fully described by the Poincaré section is now of major interest [78]. An analysis of these properties in the attractor being studied would be useful.

We have considered the behavior of the system of equations (3.6) for concrete values of the parameters. Calculations show that in the entire interval of variation of c_2 ($c_1 = 7$, $k = 1$, $-6.4 \lesssim c_2 \lesssim -5.2$) nearby trajectories of the system diverge exponentially. One of the Lyapunov exponents is positive and approximately equal to 0.2. It is natural to expect that there exists a strange attractor in this entire interval. Its statistical properties are apparently close to the properties of the attractor studied. This is indicated, in particular, by the form of the one-dimensional mappings $x_{x+1} = F(x_n)$ which are qualitatively very similar to Fig. 24.

6. Comparison of Solutions of the Kuramoto–Tsuzuki Equation and the Two-Mode System

The basic properties of the two-mode system (3.6) were investigated above. The question remains of whether the problem in particular derivatives has the same properties. It is convenient to compare the simplified system (3.6) and the original problem by comparing the types of their attractors. We earlier commented in detail on Fig. 11 in relation to the dynamical systems. Figure 33 shows the results of calculations for the problem in partial derivatives. In both cases a problem with $\ell = \pi$ ($k = 1$) is considered. In the $\{c_1, c_2\}$ plane it is convenient to distinguish several regions in which the solutions have the same type.

6.1. Class of Self-Similar Solutions. Above the line ABC both systems have the same properties. In the linear approximation the spatially homogeneous solution (2.3) is stable here. On the line ABC this solution loses stability. In the system of ordinary differential equations (3.6) the solution with $\xi = 1$, $\eta = 0$ corresponds to it. It also loses stability on passing across the line ABC, and a new stable singular point with $\xi \neq 1$ arises. Therefore, as $t \to \infty$, $\xi \to$ const, $\eta \to$ const, $\theta \to$ const. The functions x_0, x_1 and y_0, y_1 in the system (3.4) vary according to a harmonic law.

In this same range of parameters in the problem in partial derivatives passage occurs to solutions for which the quantities ρ_n, $n = 0, 1, 2, \ldots$, and the quantities Ψ_n, $n = 0, 1, 2, \ldots$, are constant. Here $a_n=\rho_n\cos\varphi_n$, $b_n=\rho_n\sin\varphi_n$, $\Psi_n=\varphi_n-\varphi_0$. This means that passage to a self-similar solution of the problem studied occurs. Indeed, we have the following lemma.

LEMMA. Suppose $W(x, t)$ is a solution of problem (2.1). A necessary and sufficient condition that it be a self-similar solution of the form (2.12) are the equalities $\rho_n(t) = \alpha_n$, $\Psi_n(t) = \beta_n$, where α_n and β_n do not depend on time.

Proof. 1. Necessity. Suppose the solution is self-similar; then

$$a_n=A_n\cos\omega t-B_n\sin\omega t,\quad b_n=B_n\cos\omega t+A_n\sin\omega t,$$

where

$$A_n=\nu_n\int_0^l R(x)\cos a(x)\cos(\pi nx/l)\,dx,$$

$$B_n=\nu_n\int_0^l R(x)\sin a(x)\cos(\pi nx/l)\,dx;\quad \nu_0=1/l,\quad \nu_n=2/l,\quad n\geqslant 1.$$

From this it follows that

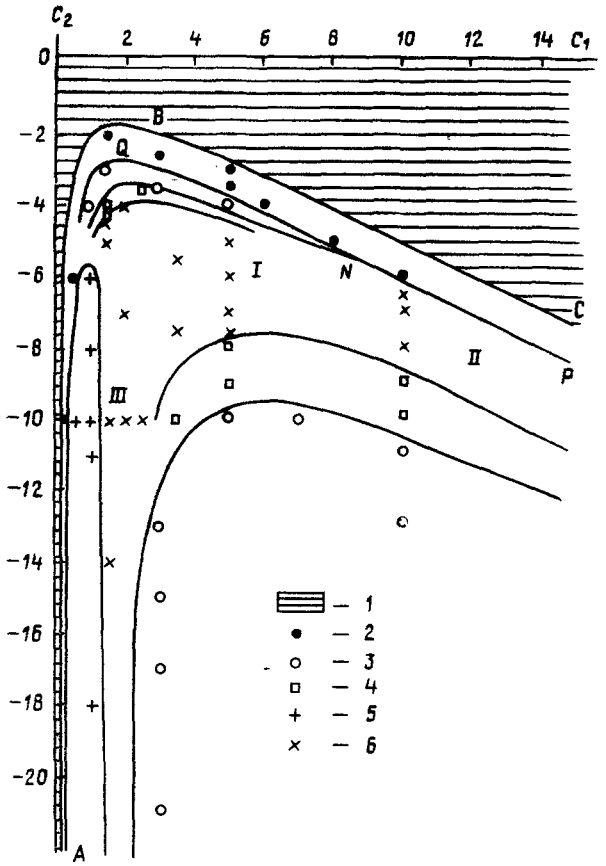

Fig. 33. Types of limit solutions (as $t \to \infty$) of the Kuramoto–Tsuzuki equation in the region $\ell = \pi$: 1) the spatially homogeneous solution is stable, 2) the solution for which the quantities $\rho_n(t)$ do not depend on time, 3) the solution for which $\rho_0(t)$ and $\rho_1(t)$ determine a simple cycle, 4) $\rho_0(t)$ and $\rho_1(t)$ determine a double cycle, 5) an even solution, 6) more complex regimes. The solid lines indicate approximately the position of the boundaries on which the solution changes its type.

$$\rho_n^2 = A_n^2 + B_n^2, \quad \Psi_n = \{\arccos(A_n/\rho_n) - \arccos(A_0/\rho_0)\}.$$

From these two equalities it follows that ρ_n and Ψ_n do not depend on time.

2. Sufficiency. We turn to the system (3.1) and write out an explicit expression for the quantity $R^2(x, t) = u^2(x, t) + v^2(x, t)$

$$R^2(x, t) = \sum_{n=0}^{\infty} r_n(t) \cos(\pi n x/l). \tag{6.1}$$

where $r_0(t) = \rho_0^2 + 0.5\sum_{m=1}^{\infty}\rho_m^2$, $r_n(t) = \sum_{m=0}^{\infty}\rho_m\rho_{m+n}\cos(\psi_m - \psi_{m+n}) + 0.5\sum_{m=0}^{n}\rho_m\rho_{n-m}\cos(\psi_m - \psi_{n-m})$, $n \geqslant 1$. Since r_n depend only on ρ_m and the phase differences Ψ_m, it follows that the quantity R^2 does not change with time.

We set $W(x, t) = R(x)e^{i\varphi}$. It can be verified that

$$\begin{aligned}\cos(\varphi - \varphi_0) &= \left[\sum_{n=0}^{\infty}\rho_n\cos(\pi n x/l)\cos\Psi_n\right] \Big/ R(x),\\ \sin(\varphi - \varphi_0) &= \left[\sum_{n=0}^{\infty}\rho_n\cos(\pi n x/l)\sin\Psi_n\right] \Big/ R(x)\end{aligned} \tag{6.2}$$

and hence $\varphi - \varphi_0 = a(x)$ does not depend on time. From formulas (3.1) it is possible to obtain the value

$$\dot{\varphi}_0 = -c_2 r_0 - \frac{1}{2\rho_0}\sum_{m=1}^{\infty}\rho_m r_m(c_2\cos\Psi_m + \sin\Psi_m) = \omega, \tag{6.3}$$

which is also constant. Therefore, $\varphi = \omega t + a(x)$ and the solution is self-similar.

We shall compare the coordinates of the singular point of the simplified system with those values of ρ_0 and ρ_1 which characterize self-similar solutions of problem (2.1) of the form (2.12). From Table 2 it is evident that these values coincide up to several percent. The calculations were carried out according to a purely implicit difference scheme with second order approximation of the boundary conditions. Thus, in this range of parameters

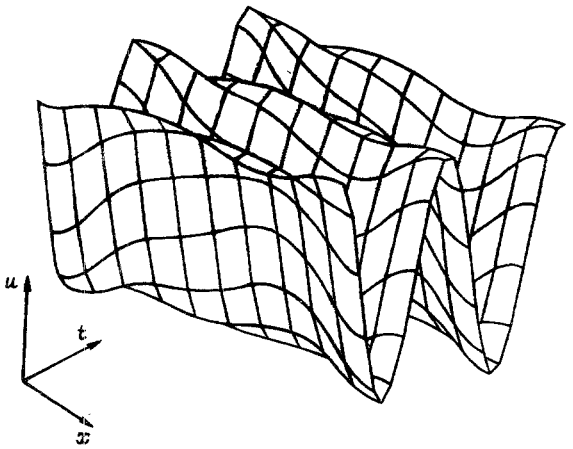

Fig. 34

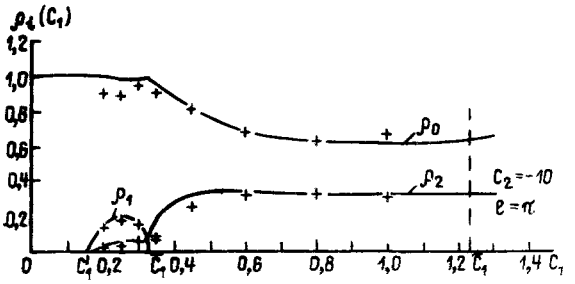

Fig. 35

Fig. 34. Function u(x, t) corresponding to a self-similar solution of the form (2.12) for $c_1 = 2$, $c_2 = -1$, $\ell = 18.6$.

Fig. 35. Variation of the parameters of the self-similar solution with increasing c_1. The step size in the parameter c_1 is equal to 0.01. The solid lines correspond to the system of five ordinary differential equations and the crosses to calculations in partial derivatives.

the approximate system gives a good quantitative description of solutions of the problem in partial derivatives.

A typical form of the function u(x, t) in the self-similar solution of the form (2.12) is shown in Fig. 34. It is evident that this solution can describe a rather complex autowave process in the course of which local extrema of the functions u and v periodically appear and vanish.

The lower boundary of the range of parameters in which the self-similar solution determines the asymptotics (the portion QNP in Fig. 33) can also be predicted with good accuracy. A Hopf bifurcation occurs on this curve. In the approximate system a limit cycle is created and in problem (2.1) a solution for which the function $R^2(x, t) = u^2(x, t) + v^2(x, t)$ is periodic in time.

6.2. Even Self-Similar Solutions. From the simplified system it follows that in the range of parameters AEF (see Fig. 11) there also exists a stable singular point. Therefore, passage to self-similar solutions occurs here also. We turn to the results of calculations. A typical picture is shown in Fig. 35.

We separate out several characteristic regions on the line c_1 and consider the behavior of the solutions.

1. $0 < c_1 < c_1'$. As follows from the two-mode system, the spatially homogeneous solution is stable here. Linear analysis of its stability makes it possible to find the value of c_1'.
2. $c_1' < c_1 < \bar{c}_1$. The solution constains a zeroth, first, and second harmonic (the others are an order less), and as $t \to \infty$ it passes to a self-similar solution of the form (2.12). The value of c_1 is close to that given by linear analysis of the stability of the spatially homogeneous solution relative to the second harmonic.
3. $\bar{c}_1 < c_1 < \tilde{c}_1$. Passage to self-similar solutions of the same form again occurs. However, they are not ordinary ones. Their Fourier series contain no harmonics with odd indices. The functions u and v as $t \to \infty$ are even in spite of the fact that the initial data possessed no symmetry. The parameters of these solutions can also be predicted with an accuracy of several percent on the basis of the two-mode system (3.6) [12]. In it it is necessary to set $k = 2\pi/\ell$, since the zeroth and second harmonics have the largest amplitude.
4. $c_1 \gtrsim \tilde{c}_1$. As $t \to \infty$ the quantities ρ_n do not approach constant values. The amplitudes of the first three modes are comparable.

TABLE 2

c_1	c_2	System of 3 ODE k = 1		The problem in partial derivatives $\ell=\pi$			
		ρ_0	ρ_1	ρ_0	ρ_1	h/π	τ
0,3	-10	0,969	0,243	0,941	0,150	1/40	$2\cdot10^{-3}$
0,5	-6,0	0,909	0,399	0,923	0,294	1/40	$2\cdot10^{-3}$
3,0	-2,5	0,857	0,337	0,845	0,331	1/30	10^{-2}
6,0	-4,0	0,901	0,262	0,891	0,227	1/30	10^{-2}
8,0	-5,0	0,919	0,234	0,909	0,229	1/40	$2\cdot10^{-3}$
10	-6,0	0,932	0,214	0,923	0,201	1/40	$2\cdot10^{-3}$

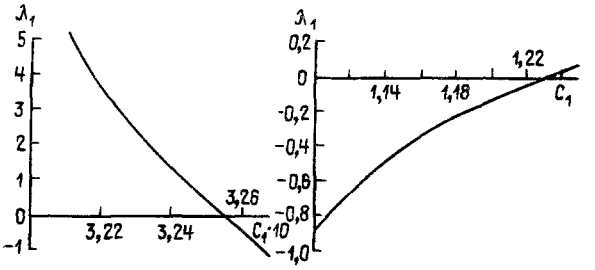

Fig. 36. Dependence $\lambda_1(c_1)$ on the boundaries of the interval of stability of the even solution.

In order to qualitatively explain the picture observed it is necessary to use a model more complex than the system (3.6). It turns out that it suffices to consider the first six equations of the system of equations (3.1), writing them in the variables $\{\rho_0, \rho_2, \Psi_2, \rho_1, \Psi_1\}$.

An even self-similar solution of the problem in partial derivatives is observed for $c_1\in(\bar{c}_1, \tilde{c}_1)$. In order to estimate the boundary of this interval we investigate the stability of the even solution of the approximate system obtained of five ordinary differential equations relative to the first harmonic. Suppose the quantities $\{\rho_0, \rho_2, \Psi_2, 0, \Psi_1\}$ determine a singular point of this system for $k = \pi/\ell$. Then $\{\rho_0, \rho_2, \Psi_2\}$ is a singular point of the system (3.6) for $k = 2(\pi/\ell)$. It can be verified that this point is stable in the range of parameters considered. The matrix **A** of the linearized system (3.6) is negatively definite. The value of Ψ_1 can be found from the condition $\dot{\Psi}_1 = 0$.

The linearized system of five equations in this case has the form

$$\begin{pmatrix}\dot{\rho}_0\\ \dot{\rho}_2\\ \dot{\Psi}_2\\ \dot{\rho}_1\\ \dot{\Psi}_1\end{pmatrix}=\begin{pmatrix} & \mathbf{A} & & a_{14} & 0\\ & & & a_{24} & 0\\ & & & a_{34} & 0\\ 0 & 0 & 0 & \lambda_1 & 0\\ a_{51} & a_{52} & a_{53} & a_{54} & \lambda_2\end{pmatrix}\begin{pmatrix}\rho_0\\ \rho_2\\ \Psi_2\\ \rho_1\\ \Psi_1\end{pmatrix}.$$

Three of its eigenvalues coincide with eigenvalues of the matrix A and have negative real parts. The two others are defined by the formulas

$$\lambda_1=P+\sqrt{Q\,(1+c_2^2)-R^2},\quad \lambda_2=-2\sqrt{Q\,(1+c_2^2)-R^2}, \tag{6.4}$$

where

$$P=1-k^2-2\rho_0^2-\rho_2^2-2\rho_0\rho_2\cos\theta_2,$$
$$Q=\rho_0^4+\rho_2^4/4+2\rho_0\rho_2\cos\theta_2\,[\rho_0^2+\rho_2^2/2+\rho_0\rho_2\cos\theta_2],$$
$$R=-c_1k^2-c_2\rho_0^2-2c_2\rho_0\rho_2\cos\theta_2+0{,}5\rho_2^2\,[\sin 2\theta_2+c_2\cos 2\theta_2].$$

The values of $\bar{c}_1$ and $\tilde{c}_1$ can be found approximately from the condition $\lambda_1(c_1) = 0$. The graph of the function $\lambda_1(c_1)$ near the boundaries of the interval of stability is shown in Fig. 36 [$\lambda_1(c_1)$ were computed both by an explicit formula and numerically on the basis of the behavior of the integral curves in a neighborhood of the singular points. The results obtained coincide to high accuracy].

Figure 35 shows that at the point $\bar{c}_1$ a solution of general form goes over continuously into an even solution; the harmonics with odd indices become equal to zero. The first solution simultaneously loses stability, while the second solution becomes stable.

The calculations show that solutions of the system of five ordinary differential equations and of the original problem are close (see Fig. 35). This gives reason to suppose that also in the problem in partial derivatives the change of type of a solution is occasioned by instability of the even self-similar solutions relative to perturbations of the first harmonic.

Usually symmetric solutions in problems of synergetics are unstable. In the problem being studied this is not so: there exists a range of parameters where the even self-similar solution is stable. In contrast to the majority of open, nonlinear systems where spontaneous loss of symmetry occurs [52, 70], here spontaneous symmetry creation is observed. As $t \to \infty$ the solution possesses symmetry not present in the initial data.

Because of the evenness of the functions u and v the nonlinear system decomposes as $t \to \infty$ into two identical noninteracting subsystems. More complex symmetric solutions correspond to decomposition of the system into a large number of noninteracting parts. They may turn out to be stable in regions of large length.

Above we have investigated the change of solutions of problem (2.1) for different values of c_1, c_2 when the length of the region was fixed. In many cases, however, it is important to know how the solution changes as ℓ is changed. Analysis of this problem for stationary dissipative structures led to the discovery of a so-called zone structure. It turned out that when the length of the region is increased structures may periodically appear and disappear (in the latter case the spatially homogeneous solution again becomes stable) [37].

We fix the parameters c_1, c_2 in the model being studied and consider how the solution of problem (2.1) changes with increasing ℓ. Figure 37 shows the dependence of the steady-state values of ρ_n on the parameter. For $\ell \approx 5$ the spatially homogeneous solution loses stability, and a self-similar solution of the form (2.12) then determines the asymptotics. At first the zeroth and first modes have largest amplitude. The first harmonic then decays, and the solution becomes symmetric. Beginning with $\ell \approx 18$, the number of harmonics with close amplitudes increases rapidly, but the solution continues to be self-similar. For $\ell >$ 22 a complex oscillatory regime is observed in the system. The question of simple and effective simplified models in this range of parameters so far remains open.

6.3. Two-Frequency Regimes. If from distinct initial data passage occurs to one and the same solution of the problem in partial derivatives in which $|W|$ depends periodically on time, then we call such a solution a cycle. We distinguish the functions $\rho_0(t)$, $\rho_1(t)$ in it and compare them with the predictions of the simplified system. Here it is again convenient to use the notation S^n, where n is the number of turns which the projection of the solution onto the $\{\rho_0, \rho_1\}$ plane makes after one period.

It can be seen that the following assertion holds [19].

LEMMA IV. Suppose the solution of problem (2.1) is such that

$$\rho_n(t+T)=\rho_n(t),\ n=0,\ 1,\ 2,\ldots,$$
$$\Psi_n(t+T)=\Psi_n(t)+2\pi m_n,\ m_n\in\{0,\ \pm1,\ \pm2,\ldots\}, \tag{6.5}$$

$\rho_0 \neq 0$ for $t\in[0, \infty)$. Then it can be represented in the form

$$W(x,\ t)=R(x,\ t)\exp[i(\omega_0 t+\omega_1(t)+a(x,\ t))], \tag{6.6}$$

where $R(x, t+T)=R(x, t)$, $\omega_1(t+T)=\omega_1(t)$,

$$a(x,\ t+T)=a(x,\ t)+2\pi p,\ p\in\{0,\ \pm1,\ \pm2,\ldots\},\ \omega_0=\text{const}.$$

Thus, a Hopf bifurcation in problem (2.1) is connected with passage from self-similar solutions of the form (2.12) to more complex solutions of the form (6.6) in which there are two frequencies that are independent in the general case.

Comparison of Figs. 11 and 33 shows that solutions of the approximate system (3.6) and of the equation in partial derivatives behave qualitatively the same as the parameters c_1 and c_2 vary. In both cases the plane of the parameters is partitioned into similar regions in which the solutions do not change their type. However, the boundaries of the regions are shifted somewhat. This is natural, since on these lines bifurcation of the solutions occurs, and the higher harmonics affect their position.

Examples of comparing simple cycles are shown in Fig. 38. In the region above the boundary of transition to complex solutions the periods of the cycles differ by no more than 10-15%. Other characteristics of the solutions, for example, the quantities $\rho_{0\min}$, $\rho_{0\max}$, $\rho_{1\min}$, $\rho_{1\max}$, are also close [12].

Examples of simple cycles for which the parameters c_1 and c_2 lie below the region of complex solutions are shown in Fig. 38b. We point out that their periods agree well, although the dimensions may differ by several times. The effect of the second harmonic is the reason for the divergence. This shows a solution of the simplified system in which not only the zeroth and first but also the second harmonic are considered (N = 3 in Fig. 38b). Its solution practically does not differ from that given by problem (2.1).

Considering the two-mode system, we focused attention on the fact that in a wide range of variation of the parameter c_2 the period of simple cycles does not depend on c_2. (We

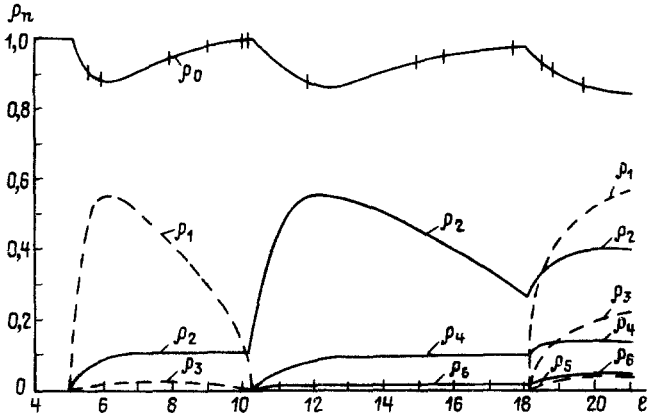

Fig. 37

recall that it is just c_2 which determines the period of spatially homogeneous solutions.) Figure 15 shows that in this same range of parameters the period of $\rho_n(t)$ practically does not depend on c_2. The values of T in the simplified system and in the original equation agree well with one another. If the parameter c_2 is reduced further ($c_2 \leqslant -35$), then solutions of the system (3.6) and of problem (2.1) begin to behave differently. In the simplified model there exists a stable singular point, while in the original equation there is a simple cycle. Its period decreases slowly with decreasing c_2, and for $c_2 \leqslant -400$ it passes to a constant value.

The amplitude of the cycle varies according to the law $\sim |c_2|^{-1/2}$. Solutions of the original equation and the problem

$$W_t = W + (1+ic_1)W_{xx} - ic_2 W|W|^2, \quad 0 \leqslant x \leqslant l,$$
$$W_x(0, t) = W_x(l, t) = 0, \quad W(x, 0) = W_0(x) \tag{6.7}$$

are close in this range of parameters. We note that in problem (6.7) only the two parameters c_1 and ℓ are essential. The change of variables $W = W' c_2^{-1/2}$ makes it possible to set $c_2 = 1$. The region of appliability of Eq. (6.7) is limited. In particular, its homogeneous solutions grow without bound as $t \to \infty$. An analysis of it may nevertheless turn out to be useful.

Since $|W| \to 0$ as $c_2 \to -\infty$, in this range of parameters $\rho_0(t)$ and $\rho_1(t)$ are also close to zero. An analogue of such a solution in the two-mode system must lie near the origin where the quantity Ω in formula (4.3) is strictly positive, and hence there are no stable cycles. This is the cause of the difference in the behavior of solutions of the original problem and of the simplified model.

Calculations show that for $c_1 = 3.0$, $c_2 \to -\infty$, $\ell \to \pi$ 3-4 of the first Fourier coefficients of the functions u, v are comparable. To describe such solutions in the system (3.1) it is necessary to consider at least four harmonics. However, in some physical problems the investigation of the two-mode system for equation (6.7) is of independent interest [55, 113]. A detailed analysis of this model is carried out in the work [113]. In it there was discovered a cascade of bifurcations with period doubling, hysteresis, strange attractors, and transitions from stochastic to regular regimes as a result of tangential bifurcations.

6.4. Some Methodological Questions. Questions of the method of calculations have major significance for the investigation of nonlinear problems. Solutions may here have involved, frequently nonperiodic character, and computational experiments are practically the only source of information regarding them.

In the numerical solution of problem (2.1) a purely implicit difference scheme with second-order approximation of the boundary conditions was used [58]. The method of simple iteration was applied with consideration of the nonlinearity, and matrix sweep-out was applied for solution of the linear system. The functions $u_0(x) = \sum_{m=0}^{3} \cos(2\pi m x/l)$, $v_0(x) = \sum_{m=0}^{3} \cos(\pi(2m+1)x/l)$ were usually used as initial data.

Approximation of the boundary conditions turned out to be a very important factor. Use of a scheme with second-order approximation of the boundary conditions improves the accuracy

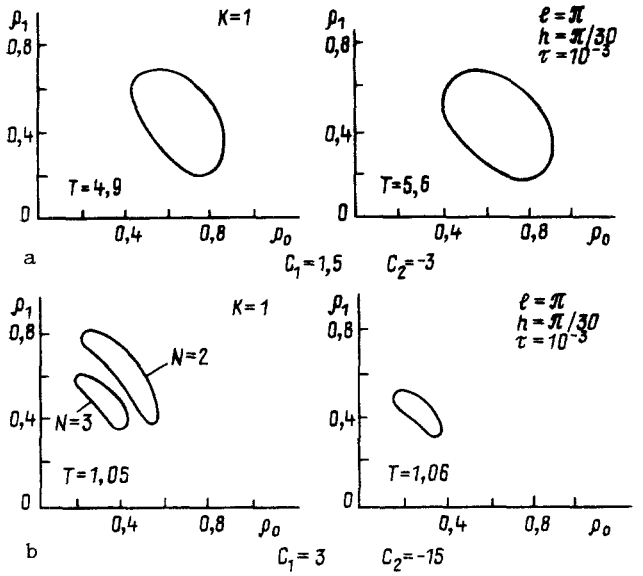

Fig. 38. Comparison of the simplest periodic solutions of the dynamical system (3.6) (on the left) and of the problem in partial derivatives (on the right).

of the calculations and makes it possible to compute with a larger step size in space. This is essential near bifurcation lines where the parameters of solutions may depend strongly on the length of the region ℓ.

For the problem being studied large computation times are usually necessary (they depend strongly on c_1 and c_2 and grow rapidly with increasing length of the region) after which the system passes to a steady-state regime. Another feature is the necessity of small step sizes in time and space. A rigorous test for the choice of the step size in time τ is the calculation of the spatially homogeneous solution whose period is equal to $2\pi/c_2$. As a rule, the step size found makes it possible to compute other solutions as well whose period is usually larger. The step size τ must decrease with increasing c_1. Increase of the step size can qualitatively change the picture of the process. An example of such behavior is shown in Fig. 39. For $\tau = 10^{-2}$, $h = \pi/30$ the calculation in partial derivatives gives a simple cycle. Reduction of the step sizes h and τ leads to a change of the type of the solution: the behavior of the system as $t \to \infty$ determines a double cycle. Results of other methodological calculations are presented in the work [12].

The Fourier coefficients of solutions of the problem studied decay rapidly with increasing index. Therefore, in a number of cases it is convenient here to use the Galerkin method and its modifications. Just such methods were used in the calculation of symmetric solutions. Figure 40 shows approximate solutions of the system of equations (2.1) in which the first N harmonics are considered. It is evident that for $N \geq 4$ the parameters of the cycles practically do not change.

The perturbations which the difference scheme and the Galerkin method cause in the solution are different. Indeed, in numerical realization of symmetric solutions of various types these solutions preserve symmetry properties as $t \to \infty$ which coincides with the properties of the original problem. Application of the difference scheme leads to a different result: a solution with symmetric initial data decays. Therefore, passage to some solution in this case bespeaks its stability which is especially important in the problems studied. A similar situation is characteristic also for media with trigger properties [45].

7. Diffusion Chaos

In this section we consider complex nonperiodic solutions of the Kuramoto–Tsuzuki equation. We shall primarily be interested in the following questions. How does the transition from simple solutions to complex solutions occur as the parameters of the problem vary? What bifurcations lead to the appearance of chaos? Is it possible to use two-dimensional and one-dimensional mappings as simplified models?

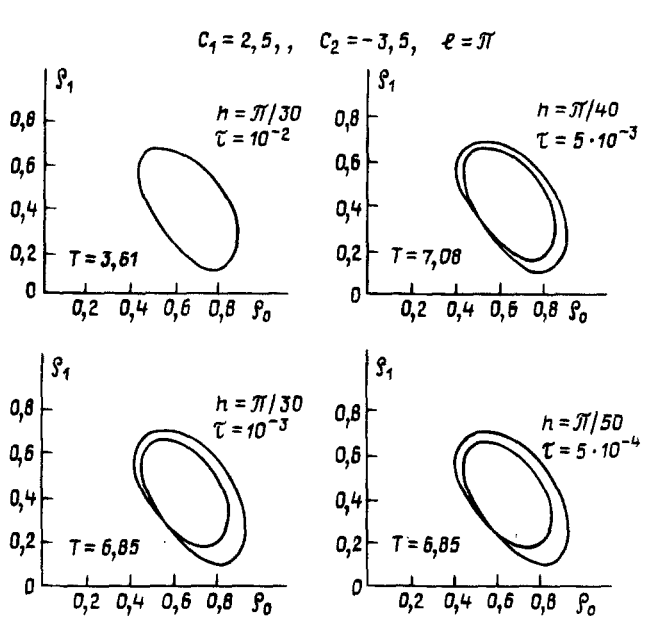

Fig. 39

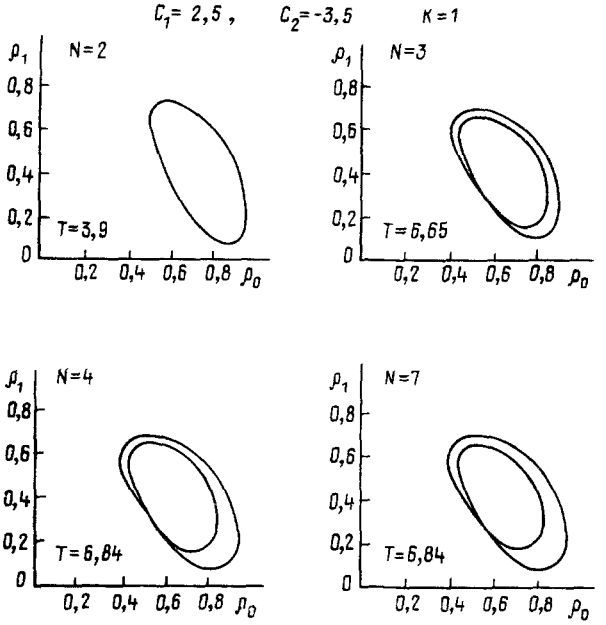

Fig. 40

Fig. 39. Effect of step sizes h and τ on the results of solving problem (2.1).

Fig. 40. Approximate solutions of the system of equations (3.1) in which the first N harmonics are considered.

We shall study the one-dimensional problem (2.1) for small regions. This case is especially interesting for the following reason. Increase of the length of the region or the dimension of the problem must lead to complication of the solutions. Therefore, if chaos is discovered in the problem being studied it can be considered a rather general property of the Kuramoto–Tsuzuki equation.

In this respect investigation of problems of hydrodynamics, where it is necessary to consider multidimensional effects, is much more complex, and this leads to the situation that "... for the complete Navier–Stokes equations we not only do not know of a single turbulent solution but it is even unknown whether such a solution exists. What the appearance of a stochastic attractor should be for a turbulent flow is also unclear" [50].

As before, we shall consider problem (2.1) for $\ell = \pi$. On the $\{c_1, c_2\}$ plane (see Fig. 33) it is possible to distinguish three ranges of parameters in each of which the passage to complex solutions and the complex solutions themselves possess a number of interesting features.

7.1. Occurrence of Nonperiodic Regimes in the Region I, II. Their Properties. We set $c_1 = 5.0$ and trace the change of solutions as the parameter c_2 is reduced (the range of parameters I). The initial data in all cases have the form $u_0(x) = \sum_{p=0}^{3} \cos(2\pi p x/l)$, $v_0(x) = \sum_{p=0}^{3} \cos[(2p+1)\pi x/l]$. From calculations carried out for the two-mode system with k = 1 it follows that the occurrence of nonperiodic solutions in this case is occasioned by a sequence of bifurcations with period doubling $S^n \to S^{2n}$. A simple cycle arises as a result of supercritical Hopf bifurcation. Qualitatively the same picture is observed in the problem in partial derivatives. Namely, for $c_1 = 5$, $c_2 = -4.1$, $\ell = \pi$ the cycle S^1 with period T = 3.00 determines the asymptotics; for $c_1 = 5$, $c_2 = -4.16$, $\ell = \pi$ there is a stable cycle S^2 in the system with period T = 5.76.

Passage to nonperiodic solutions then occurs. We therefore again consider the sequence $\{M_n\}$ of local maxima of the function $\rho_0(t)$. Along the axis of the abscissa we plot the values of the n-th maximum and along the ordinate axis the values of the (n + 1)-st maximum. In many cases the points $\{M_n, M_{n+1}\}$ lie on a curve $M_{n+1} = f(M_n)$ which with the limits of accuracy of the calculations turns out to be continuous and single-valued. It defines a one-dimensional mapping of the segment into itself.

We shall assume that the elements of the sequence $\{M_n\}$ are distinct if they differ by more than ε (ε is determined by the accuracy of the calculations and for the problem in partial

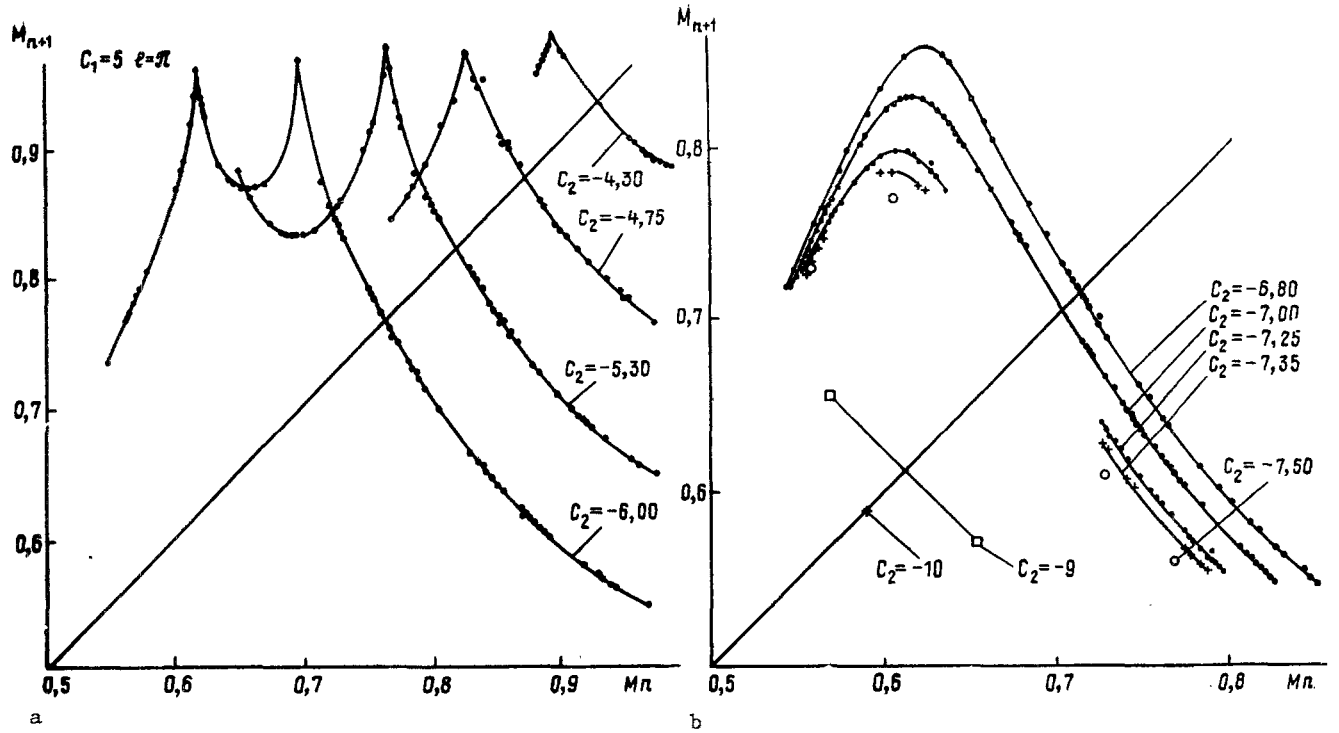

Fig. 41. a, b) Variation of the one-dimensional mappings $M_{n+1} = f(M_n)$ depending on the parameter c_2. The problem in partial derivatives was solved for $c_1 = 5.0$, $\ell = \pi$.

derivatives amounts to ~10^{-3}). The characteristic time of the computation depends on the type of solution. A sequence of 50-80 maxima was usually constructed for complex cycles. Solutions containing 100-300 distinct maxima were considered nonperiodic. As a rule, such a sequence is sufficient to determine the features of the function f(M). More than 10^4 values are needed to investigate statistical properties of the solution, for example, to construct a histogram of $N(\rho_0)$ showing how often the maxima of $\rho_0(t)$ assume some value.

We turn to the results of numerical solution of the problem in partial derivatives for $c_1 = 5.0$. At first the picture turns out to be the same as in the two-mode system (see Figs. 41a and 17). As before the function f has one sharp maximum which moves to the left with decreasing c_2. There is nevertheless no quantitative correspondence here: the scales on these figures are different.

Under further reduction c_2 a restructuring of the function f begins which is not present in the simplified model (see Fig. 41b). At first the curve f has a minimum. The solution here is also nonperiodic. However, the presence of a portion with a small derivative near the smooth minimum indicates the possibility of the occurrence of stable limit cycles. Indeed, for $c_2 = -5.6$ the limit cycle S^8 in the system is stable. The function f then acquires two sharp maxima.

In all cases considered above the mapping f was single-valued. For $c_2 = -6.3$ single-valuedness is lost; the solution is nonperiodic as before.

A further restructuring then occurs after which the function f becomes smooth and single-valued (see Fig. 41b). A complex nonperiodic regime is again observed. The points hereby lie within the limits of several "islands." Such regimes, which have received the name of semiperiodic solutions of noise cycles, are being intensively investigated at the present time [77]. The order of passage about the islands in them is fixed, but within the limits of each of them the trajectory behaves in a stochastic manner. The notation χ^n was introduced in the work [119] for a solution with n islands. In Fig. 41b we see that there is a transition $\chi^1 \to \chi^2$ and $\chi^2 \to \chi^4$. Investigation of the family of one-dimensional reflections

$$x_{n+1}=\lambda x_n(1-x_n) \tag{7.1}$$

showed that in the neighborhood of noise cycles there must be complex periodic solutions. It is natural to expect that they indeed exist in the case under investigation.

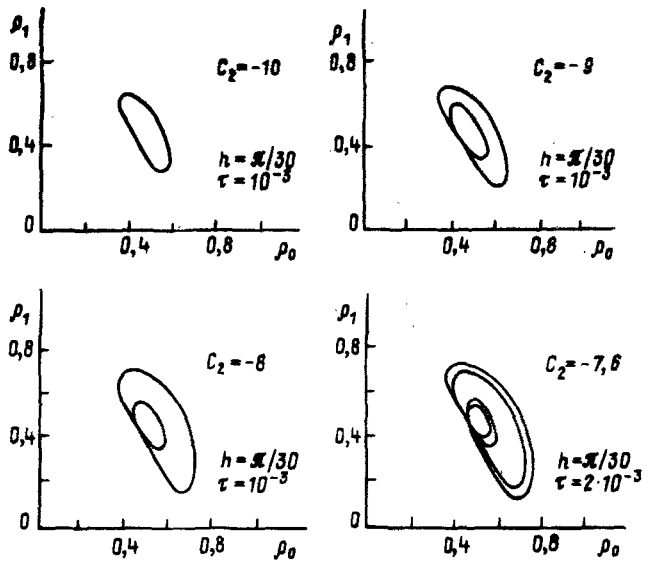

Fig. 42

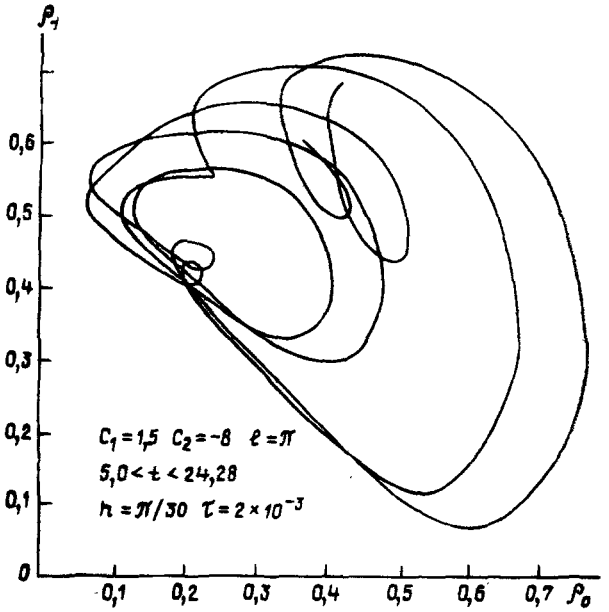

Fig. 43

Fig. 42. Complication of solutions of problem (2.1) on the line $c_1 = 5$, $\ell = \pi$.

Fig. 43. Part of a nonperiodic solution of the Kuramoto–Tsuzuki equation in the projection onto the $\{\rho_0, \rho_1\}$ plane. Range of parameters III.

If we assume that the function f(M) is continuous and single-valued, then we can consider it in the quality of a useful simplified model. In analyzing it, we can use results from the theory of one-dimensional mappings. In particular, here we used theorems of A. N. Sharkovskii [71] and Li and York [106] on the existence of cycles of different types, and a whole array of theorems from ergodic theories [73, 77, 93]. From the form of the function f(M) it is clear (see Fig. 41b) that near the peak it can be approximately a quadratic parabola. Obviously, here the theory of Feigenbaum [27, 84, 85] was used. By it, it is possible to predict the value of c_2 at which there will be consecutive bifurcations.

When $c_1 = 5$, $c_2 = -10$ the asymptotics of the solutions to problem (2.1) determine the simple cycle. If the parameter c_2 is increased, moving toward the region of diffusion chaos from below, then in the system there will also be bifurcation of the period. Cycles S^1, S^2, and S^4 are proved in Fig. 42. For $c_2 = -7.4$, we use cycle S^8, for $c_2 = -7.35$ – S^{16}.

The basic difference between the regions of parameters I and II has to do with the fact that in it there occurs a transition to the nonperiodical solutions with a decrease in the parameter c_2. Far from the curve QNP the behavior of the solutions in region I and II is qualitatively the same as for the initial system and simplified model. This shows the comparison of corresponding one-dimensional mappings [13].

In the simplified system as the parameter c_2 is reduced by a jump there occurred a transition from singular points to nonperiodic solutions. Calculations carried out indicate that an analogous picture is observed in the original problem. Transition to nonperiodic regimes occurs with a jump from self-similar solutions.

7.2. Feature of Solutions in the Range of Parameters III. The behavior of solutions of the Kuramoto–Tsuzuki and simplified model in the range III is similar in many respects. Figure 43 shows the projection of one of the nonperiodic solutions of the problem in partial derivatives onto the $\{\rho_0, \rho_1\}$ plane. It is evident that different loops differ in dimensions and in the number and position of the loops which is not observed in the ranges I and II.

We again consider the dependence $M_{n+1}(M_n)$. It can define a one-dimensional mapping (see Fig. 44a) which, however, differs strongly from the form of the function f(M) obtained in the simplified model [13]. As c_2 decreases single-valuedness is lost (see Fig. 44b). This means that an attractor of higher dimension arises in the system.

In many cases a complex transitional process precedes passage to a steady-state solution. The calculation shown in Fig. 44c corroborates this. Successive maxima here do not lie on one

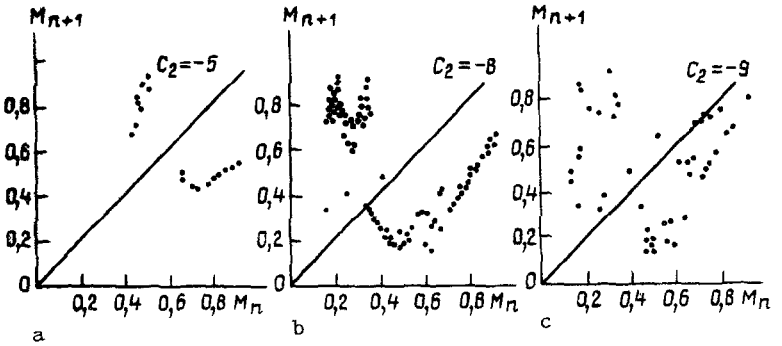

Fig. 44. Sequences $\{M_n\}$ corresponding to nonperiodic solutions of the equation in partial derivatives; $c_1 = 1.5$, $\ell = \pi$.

curve. For $0 < t < 100$ the solution changes in an irregular manner. For $t \gtrsim 100$ passage to a self-similar solution of the form (2.12) with $\rho_0 = 0.6905$, $\rho_1 = 0.0275$, $\rho_2 = 0.2939$ occurs. Apparently, it appears as a result of loss of stability of the even self-similar solution determining the asymptotics for small values of c_1. A similar behavior was observed in the Lorenz system and was called metastable chaos. This phenomenon has been studied in detail and has been observed experimentally in a number of cases [38, 114].

7.3. Other Problems Connected with Diffusion Chaos. Above we considered results of solving problem (2.1) for $\ell = \pi$. The question arises if other paths from ordered solutions to chaos are possible for other values of the parameters. Calculations show that successive Hopf bifurcations occur as the length of the region is increased [109]. If the local maximum of $\rho_0(t)$ are again selected and the graph $M_{n+1}(M_n)$ is constructed, then its typical form after two bifurcations is as shown in Fig. 45. Appearance of nonperiodic solutions as a result of several Hopf bifurcations was considered by Ruelle and Takens [57, 72]. Calculations carried out make it possible to suppose that in many other cases complication of solutions of problem (2.1) will proceed in accordance with this mechanism.

We have considered qualitative features of nonperiodic solutions of the equation in partial derivatives. An estimate of their quantitative characteristics is an important problem. At the present time algorithms have appeared which make it possible to estimate the dimension of attractors in infinite-dimensional systems [82, 87, 117]. It has been shown that for this it suffices to measure one of the variables at one point at discrete times [117]. Use of these methods in the investigation of problem (2.1) is of great interest.

Numerical calculations carried out for the Kuramoto–Tsuzuki equation showed that there exist several ranges of parameters where problem (2.1) has nonperiodic solutions. In investigating them simplified models of various types turn out to be useful: the system of three ordinary differential equations; the family of one-dimensional mappings. We shall now answer the question of the connection of diffusion chaos with the presence of a strange attractor in a finite-dimensional system. Such a connection exists. The two-mode system (3.6) makes it possible to predict many important properties of nonperiodic solutions of the Kuramoto–Tsuzuki equation.

Among them we distinguish the following. 1. The presence of three regions where transition to nonperiodic regimes occurs in a different manner. 2. A sequence of bifurcations leading to chaos. 3. The form of one-dimensional mappings corresponding to complex solutions of the problem in partial derivatives in a broad range of the parameters c_1 and c_2. All this leads to the situation that the investigation of strange attractors in the simplified model gives important information regarding diffusion chaos which is described by the original equation.

At the present time dozens of chemical reactions in which oscillatory and chaotic regimes are possible are being investigated experimentally [25, 31, 112]. Complex mathematical models are usually used to model their basic features. As a rule, they all describe the behavior of the system far from the point of loss of stability of the thermodynamic branch. A detailed investigation of them turns out to be a very complex problem.

Investigation of problem (2.1) shows that diffusion chaos can be observed in a neighborhood of a point of first bifurcation. Probably many qualitative features of oscillatory

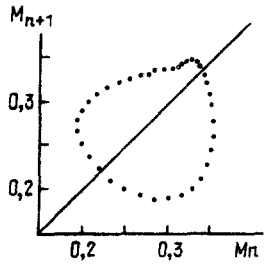

Fig. 45

reactions in which the distribution of reagents is spatially inhomogeneous can be explained on the basis of the simpler model (2.1). Therefore, the theoretical and experimental investigation of open dissipative systems in a neighborhood of a point of bifurcation is a natural and necessary step in their analysis. Experimental study of complex processes periodic in time and phenomena of diffusion chaos are of special interest.

8. Simplest Types of Order in Two-Component Systems in the Two-Dimensional Case

In many mathematical models the following two-dimensional analogue of the Kuramoto–Tsuzuki equation is a major interest:

$$W_t = W + (1+ic_1)(W_{xx}+W_{yy}) - (1+ic_2)|W^2|W. \tag{8.1}$$

These include the theory of occurrence of wind waves on water [2], investigations of dissipative structures in media and in oscillatory chemical reactions [90], and some models of morphogenesis [21]. We note that Eq. (8.1) describes a narrower class of two-component systems than the Kuramoto–Tsuzuki equation in one-dimensional problems. Since in the two-dimensional case not only the length but also the direction of the wave vector is essential, there are more unstable modes, and more complex models than Eq. (8.1) arise.

Earlier major attention was devoted to the investigation of the Cauchy problem of this equation. Spiral waves or other solutions having phase singularities were hereby usually considered [121]. However, it would be useful to study the behavior of solutions of Eq. (8.1) for the case of small two-dimensional regions. This would make it possible to carry out a more complete analysis without restricting attention to one distinguished class of solutions and to clarify the basic types of order which would be of interest in more complex problems.

We consider the following boundary value problem:

$$\begin{gathered} W_t = W + (1+ic_1)(W_{xx}+W_{yy}) - (1+ic_2)|W|^2 W, \\ 0 \leqslant x \leqslant l,\ 0 \leqslant y \leqslant l,\ W(x, y, 0) = W_0(x, y), \\ W_x(0, y, t) = W_x(l, y, t) = W_y(x, 0, t) = W_y(x, l, t) = 0. \end{gathered} \tag{8.2}$$

We shall consider the behavior of solutions of it for different values of c_1 and c_2 in the case of small regions. In the numerical calculations presented below $\ell = \pi$.

We consider the following questions. Are one-dimensional solutions of problem (8.2) stable relative to two-dimensional perturbations? Does this problem have solutions for which there is no one-dimensional analogue? How does complication of two-dimensional solutions occur as the parameters c_1 and c_2 vary?

We shall consider solutions of the boundary value problem in a square with side length ℓ. The coefficients of diffusion and cross diffusion are chosen to be the same in both directions. This leads to the situation that problem (8.2) has a broad class of symmetric solutions. For example, solutions which are even or odd relative to the axis of symmetry of the square. The evolution of such solutions may differ qualitatively from the behavior of solutions of general form, as was the case in the one-dimensional problem. They will not be considered below. In all calculations the initial data are nonsymmetric and have the form

$$u(x, y, 0) = 0{,}1 \sum_{m,n=0}^{4} \cos(\pi m x/l) \cos(\pi n y/l),$$

$$v(x, y, 0)=0{,}1\sum_{m,n=0}^{4}\cos(\pi mx/l)\cos(\pi ny/l)/(m+1).$$

In this formulation only the simplest symmetric solutions are of consequence. Namely,

a) the spatially homogeneous solution

$$W(x, y, t)=\exp(-ic_2t); \tag{8.3}$$

b) the one-dimensional solutions W(x, y, t) = W(x, t) or W(x, y, t) = W(y, t);

c) solutions symmetric relative to the diagonal of the square: W(x, y, t) = W(y, x, t) or W(x, y, t) = W(ℓ − y, ℓ − x, t).

8.1. A Simplified Finite-Dimensional System. Analysis of various simplified models plays an important role in the investigation of the one-dimensional problem (2.1). To construct such models in the two-dimensional problem it is convenient to represent a solution of it in the form $u(x, y, t)=\sum_{m,n=0}^{\infty}a_{mn}(t)\cos\left(\frac{\pi mx}{l}\right)\cos\left(\frac{\pi ny}{l}\right)$, $v(x, y, t)=\sum_{m,n=0}^{\infty}b_{mn}(t)\cos\left(\frac{\pi mx}{l}\right)\cos\left(\frac{\pi ny}{l}\right)$ and write out the system of equations connecting the Fourier coefficients a_{mn} and b_{mn}:

$$\begin{aligned}\dot a_{mn}&=a_{mn}-(a_{mn}-c_1b_{mn})k^2(m^2+n^2)-(u_{mn}-c_2v_{mn}),\\ \dot b_{mn}&=b_{mn}-(c_1a_{mn}+b_{mn})k^2(m^2+n^2)-(c_2u_{mn}+v_{mn}),\quad k=\pi/l,\end{aligned} \tag{8.4}$$

where u_{mn} and v_{mn} are known functions of $\{a_{ij}\}$, $\{b_{ij}\}$. Below we shall also use the notation $\rho_{mn}^2=a_{mn}^2+b_{mn}^2$. Simplified models can be obtained from this infinite system by leaving only a finite number of equations in it. This can be done in various ways, for example, by dropping harmonics with indices for which m ≥ p or n ≥ p. The simplified system obtained in this manner we shall call a system with N = p; it contains $2p^2$ equations.

The system (8.4) may turn out to be useful in numerical solution of problem (8.2). As methodological investigations show, in a number of cases application of the Galerkin method turns out to be more effective than use of a difference scheme. This may become especially important in studying solutions in larger regions.

Below we shall consider the simplified model with N = 2. The number of equations it contains can be reduced by one by going over to the variables ρ_{mn}, θ_{mn} according to the formulas $a_{mn}=\rho_{mn}\cos\varphi_{mn}$, $b_{mn}=\rho_{mn}\sin\varphi_{mn}$, $\theta_{mn}=\varphi_{mn}-\varphi_{00}$. The equation for φ_{00} can be solved separately. This means that the functions $a_{mn}(t)$, $b_{mn}(t)$ vary in a more complex manner than $\rho_{mn}(t)$ and $\theta_{mn}(t)$. In particular, to the singular points ρ_{mn} = const, θ_{mn} = const there correspond periodic solutions in the variables a_{mn}, b_{mn}, and to limit cycles there correspond two-frequency regimes. Therefore, below we shall call solutions of the simplified system, for which ρ_{mn} = const singular points and solutions for which ρ_{mn} are periodic, limit cycles.

In the simplified model with N = 2 there is an analogue of the simplest symmetric solutions. To the homogeneous solution (8.3) there corresponds a singular point ρ_{00} = 1, ρ_{mn} = 0, m + n ≠ 0. To one-dimensional solutions of problem (8.2) along the y axis there correspond solutions of the simplified system for which a_{mn} = 0, b_{mn} = 0 for n ≠ 0.

To solutions of problem (8.2) symmetric with respect to the diagonal of the square x = y it is possible to assign integral curves on which $a_{mn}=a_{nm}$, $b_{mn}=b_{nm}$. We shall also call them symmetric.

We shall trace how the type of solutions of the simplified system changes as the parameter c_2 decreases. We consider the line c_1 = 1.5. In the one-dimensional problem the sequence of transitions was as shown in Scheme 1. (Only the simplest attractors are represented here.)

In the model with N = 2 the point with ρ_{00} = 0, m + n ≠ 0 [it corresponds to the solution (8.3)] also loses stability; a stable point with $\rho_{00}\neq 1$ hereby appears. The value of

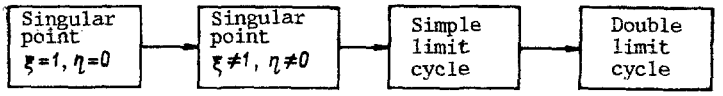

Scheme 1

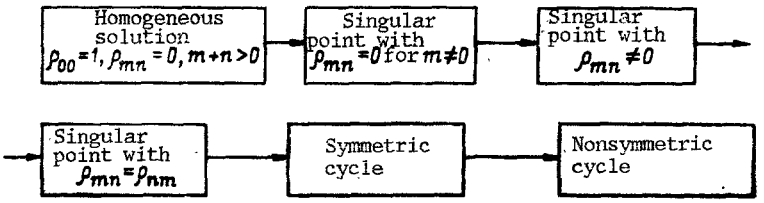

Scheme 2

c_2 for which this bifurcation occurs coincides with the critical value of the parameter for the problem in partial derivatives. In the sigular point appearing $\rho_{mn} = 0$ for $m \neq 0$. We remark that another singular point for which $\rho_{mn} = 0$ if $n \neq 0$ simultaneously appears in the system. In this case the system with N = 2 simplifies and goes over into the dynamical system (3.6).

Further complication of solutions is shown in Scheme 2. As c_2 decreases the point for which $\rho_{mn} = 0$ for $m \neq 0$ also loses stability, and the singular point with $\rho_{mn} \neq 0$ determines the asymptotics (see Fig. 46). Then for some value of c_2 ρ_{01} becomes exactly equal to ρ_{10}, and passage to a symmetric solution with $a_{01}=a_{10}$, $b_{01}=b_{10}$ is then observed in the calculations. For $c_2 \approx -3.3$ a Hopf bifurcation occurs, and a symmetric limit cycle is created [$\rho_{01}(t) = \rho_{10}(t)$]. The position of the singular point losing stability and examples of symmetric cycles are shown in Fig. 47a. For $c_2 \cong -3.7$ the cycle loses symmetry. The majority of bifurcations in Scheme 2 are connected with the loss or creation of symmetry which distinguishes the two-dimensional problem from the one-dimensional problem in an essential way.

The first transition in this sequence is connected with the appearance of a singular point with $\rho_{mn} = 0$, $m \neq 0$. As in the one-dimensional case, the critical value of the parameter is determined by equality (3.12). However, the situation may be more complex. This can be seen by tracing the variation of solutions on the line $c_1 = 3.0$ (see Fig. 46). The scheme of complication of solutions determining the asymptotics of the simplified system with N = 2 will be the following. First there appears a point with $\rho_{01} = \rho_{10}$ and then a symmetric cycle (see Scheme 3). The point and an example of a cycle are shown in Fig. 47d. After loss of symmetry the projections of the cycle onto the $\{\rho_{01}, \rho_{00}\}$ and $\{\rho_{10}, \rho_{00}\}$ planes are close (see Fig. 47e), while the projection onto the plane $\{\rho_{01}, \rho_{10}\}$ is close to a line.

It is important to note that the singular point with $\rho_{01} = \rho_{10}$ appears for the same value of the parameter c_2 where points with $\rho_{mn} = 0$, $m \neq 0$ may appear. Passage to a symmetric solution occurs from initial data of general form. It would be interesting to determine whether this phenomenon occurs in the original problem and what the reasons are for it.

8.2. Loss of Stability of the Spatially Homogeneous Solution. We consider problem (8.2) near critical values of the parameters for which the homogeneous solution (8.3) lost stability. The results of the corresponding calculations are shown by the crosses in Fig. 46. As $t \to \infty$ the solutions with ρ_{mn} = const, m, n = 0, 1, 2,... determine the asymptotics. On the line $c_1 = 1.5$, as the simplified model with N = 2 predicts, the solution arising is one-dimensional; on the line $c_1 = 3$ it turns out to be symmetric. Not only the type of the solutions of these two problems coincide; their quantitative characteristics turn out to be close.

Periodic solutions of the problem in partial derivatives are an analogue of the singular points of the simplified model. The following lemma holds.

LEMMA. If a self-similar solution of the form

$$W(x, y, t) = R(x, y)\exp[i\omega t + ia(x, y)] \tag{8.5}$$

satisfies problem (8.2), then the quantities ρ_{mn} and θ_{mn}, m, n = 0, 1, 2,... for it are constant (ρ_{mn} and θ_{mn} are determined on the basis of the Fourier coefficients a_{mn}, b_{mn} in the same way as in the simplified system). The converse assertion is also true: if the amplitudes of the harmonics and the phase shifts between them in the solution of problem (8.2) are constant, then it can be represented in the form (8.5).

It is easy to see by direct substitution that solutions of the form (8.5) can satisfy problem (8.2). The first assertion of the lemma can be verified by expanding the solution (8.5) in a Fourier series based on the system of functions $\{\cos(\pi mx/l)\cdot\cos(\pi ny/l)$; $m, n=0, 1, 2,...\}$ and computing explicitly the quantities ρ_{mn}, θ_{mn}. The converse assertion follows from the relations which connect $R(x, y, t) = |W(x, y, t)|$ and $a(x, y, t)$ with the moduli of

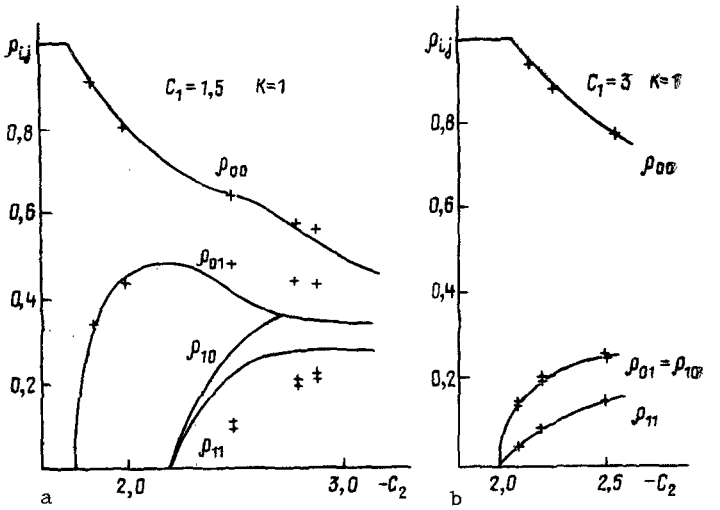

Fig. 46. Stable singular points in the simplified model with N = 2.

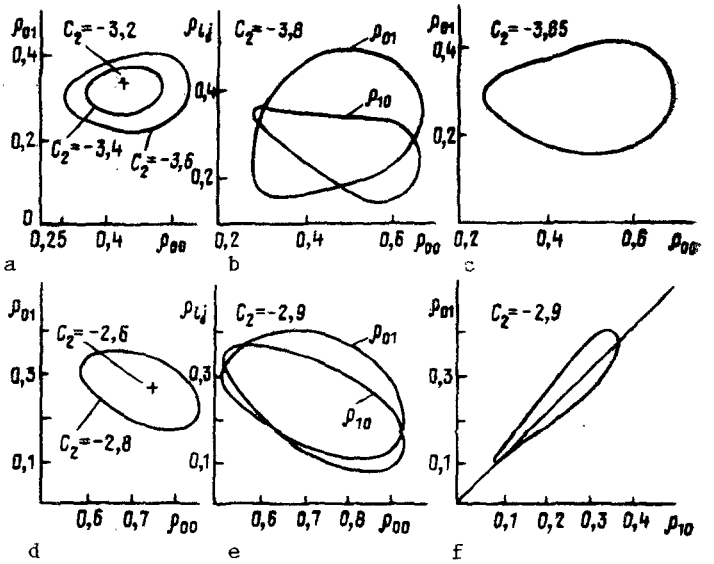

Fig. 47. Stable limit cycles in the simplified system. Above, on the line $c_1 = 1.5$; below on $c_1 = 3.0$.

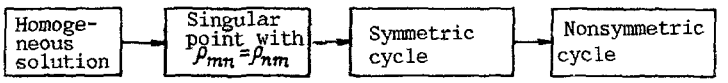

Scheme 3

the harmonics and the phase shifts. If in the system of equations (8.4) we go over to the variables $\{\rho_{mn}, \varphi_{mn}\}$, then $\varphi_{00}=\omega$. The computations here will be the same as in the one-dimensional case.

The self-similar solutions arising after the loss of stability of the homogeneous solution are close to it. Therefore, to analyze them it is natural to use asymptotic methods.

We write Eqs. (8.2) in the variables ρ, φ: $u=\rho\cos\varphi$, $v=\rho\sin\varphi$:

$$\begin{aligned}\rho_t &= \rho-\rho^3+(\rho_{xx}-\rho\varphi_x^2+\rho_{yy}-\rho\varphi_y^2)-c_1(2\rho_x\varphi_x+\rho\varphi_{xx}+2\rho_y\varphi_y+\rho\varphi_{yy}),\\ \rho\varphi_t &= -c_2\rho^3+(2\rho_x\varphi_x+\rho\varphi_{xx}+2\rho_y\varphi_y+\rho\varphi_{yy})+c_1(\rho_{xx}-\rho\varphi_x^2+\rho_{yy}-\rho\varphi_y^2).\end{aligned} \tag{8.6}$$

We seek a solution in the form of a series in the small parameter ε which characterizes the deviation of c_2 from the critical value c_2 for which the solution (8.3) loses stability:

$$\rho=1+\varepsilon r_1(x, y)+\varepsilon^2 r_2(x, y)+\varepsilon^3 r_3(x, y)+\ldots,$$

$$\varphi=(-\bar{c}_2+\varphi_1\varepsilon+\varphi_2\varepsilon^2+\varphi_3\varepsilon^3+\ldots)t+\varepsilon a_1(x,\ y)+\varepsilon^2 a_2(x,\ y)+\ldots,$$
$$c_2=\bar{c}_2+\omega_1\varepsilon+\omega_2\varepsilon^2+\omega_3\varepsilon^3+\ldots,\ \varphi_i,\ \omega_i=\text{const}. \tag{8.7}$$

We subtitute formulas (9.7) into Eqs. (9.6) and equate terms with like powers of ε. This gives a system of equations for successively determining $r_n(x, y)$, $a_n(x, y)$. In zeroth order in ε the equations are satisfied identically. In first order they can be brought to the form

$$\begin{aligned}\Delta r_1+k^2 r_1&=c_1(\varphi_1+\omega_1)/(1+c_1^2),\\ \Delta a_1&=2Lr_1+(\varphi_1+\omega_1)/(1+c_1^2),\end{aligned} \tag{8.8}$$

where $k^2=-2(1+c_1\bar{c}_2)/(1+c_1^2)$, $L=(\bar{c}_2-c_1)/(1+c_1^2)$. The structure of the equations of n-th order is analogous: r_n and a_n are contained in them just as r_1 and a_1 in formulas (8.8), but the right sides are much more complicated.

From the boundary conditions of problem (8.2) we obtain the equalities

$$\frac{\partial r_n}{\partial x}\Big|_{x=0,l}=0,\quad \frac{\partial r_n}{\partial y}\Big|_{y=0,l}=0,\quad \frac{\partial a_n}{\partial x}\Big|_{x=0,l}=0,\quad \frac{\partial a_n}{\partial y}\Big|_{y=0,l}=0. \tag{8.9}$$

It can be verified that problem (8.8), (8.9) is solvable only under the condition $\varphi_1+\omega_1=0$. A solution of it has the form

$$\begin{aligned}r_1&=\sum_{m,n}A_{mn}\cos(\pi mx/l)\cos(\pi ny/l),\\ a_1&=-2Lr_1/k^2,\quad \pi^2(m^2+n^2)/l^2=k^2,\end{aligned} \tag{8.10}$$

where m, n are integers. From the formula for k^2 it follows that at a point of first bifurcation m = 0, n = 1 or m = 1, n = 0. We henceforth assume that $k=\pi/l$, and r_1 and a_1 have the form

$$\begin{aligned}r_1&=A\cos kx+B\cos ky,\\ a_1&=-2Lr_1/k^2+\text{const}.\end{aligned} \tag{8.11}$$

The equations of higher orders will be solvable if their right sides are orthogonal to all nontrivial solutions of the corresponding homogeneous equations (the Fredholm alternative). Considering the solvability conditions for the equations of second order, we obtain

$$\omega_1=0,\ \varphi_2+\omega_2=L(A^2+B^2)(1+c_1^2)[2L^2/k^2+k^2/2]. \tag{8.12}$$

Solutions of these equations are

$$\begin{aligned}r_2&=C\cos kx+D\cos ky+Q_1\cos 2kx+Q_2\cos 2ky+Q_3\cos kx\cos ky+Q_4,\\ a_2&=-\frac{2L}{k^2}[C\cos kx+D\cos ky]+B_1\cos 2kx+B_2\cos 2ky+B_3\cos kx\cos ky,\end{aligned} \tag{8.13}$$

where

$$\begin{gathered}Q_1=A^2[0{,}25+2L^2/(3k^4)],\ Q_2=B^2[0{,}25+2L^2/(3k^4)],\ Q_3=3AB,\\ Q_4=-(A^2+B^2)(L^2/k^2+k^2/4+5/4],\ B_1=A^2[L/(4k^2)-L^3/(3k^6)],\\ B_2=B^2[L/(4k^2)-L^3/(3k^6)],\ B_3=-4ABL/k^2,\end{gathered}$$

and C and D are new unknown constants.

The solvability conditions for the equations of third order make it possible to determine the values of A and B. Earlier the small parameter ε was determined up to a factor. We shall henceforth assume that

$$\varepsilon=|c_2-\bar{c}_2|^{1/2}+\ldots. \tag{8.14}$$

This simplifies the relations for A and B:

$$\begin{aligned}A(XA^2+YB^2-\alpha Z)&=0,\\ B(YA^2+XB^2-\alpha Z)&=0,\end{aligned} \tag{8.15}$$

where

$$X=\frac{2L^4}{3k^6}-\frac{3L^2}{2k^2}+L^2+\frac{5k^2}{4}+\frac{k^4}{4},\quad Z=\frac{|c_1|}{1+c_1^2},$$
$$Y=\frac{4L^2}{k^2}+L^2-k^2+\frac{k^4}{4},\quad \alpha=\operatorname{sign}c_1\cdot\operatorname{sign}(\bar{c}_2-c_2).$$

From formulas (8.15) it is clear that $X + Y > 0$, $Z > 0$; it can also be seen that $X > 0$.

It is easy to verify that for $\alpha = -1$ the system of equations (8.15) has only trivial solutions. This corresponds to that region of the parameters where the spatially homogeneous solution (8.3) is stable. Therefore, bifurcation in the system being studied is always supercritical [39]. For $\alpha = +1$ the system of equations (8.16) has nine solutions:

$$\begin{aligned} &\text{a) } A = B = 0,\\ &\text{b) } A = 0,\ B = \pm(Z/X)^{1/2},\\ &\text{c) } B = 0,\ A = \pm(Z/X)^{1/2},\\ &\text{d) for } X \neq Y\ A^2 = B^2 = Z/(X+Y). \end{aligned} \tag{8.16}$$

The case $X = Y$ is degenerate [the system (8.15) has infinitely many solutions for which $A^2 + B^2 = Z/X$] and it will not be considered further.

Relations (8.16) show that in the general case ($X \neq Y$) the solutions arising after bifurcation will be either one-dimensional or symmetric. This conclusion is corroborated by calculations.

We consider the question of stability of the self-similar solutions arising. Suppose $\bar{r}(x, y, t)$ and $\bar{\Psi}(x, y, t)$ are small perturbations:

$$\rho = R(x, y) + \bar{r}(x, y, t);\quad \varphi = \omega t + a(x, y) + \bar{\Psi}(x, y, t). \tag{8.17}$$

Stability of the solution is determined from the problem in partial derivatives linearized with respect to $\bar{r}$ and $\bar{\Psi}$. We shall seek solutions of it in the form $\bar{r} = e^{\lambda t} r(x, y)$, $\bar{\Psi} = e^{\lambda t} \times \Psi(x, y)$. As a result an eigenvalue problem is obtained which can be brought to the form

$$\begin{aligned} \Delta r + r\left[\frac{1-c_1\omega}{1+c_1^2} - 3\frac{1+c_1c_2}{1+c_1^2}R^2 - (a_x^2 + a_y^2)\right] - 2R(a_x\Psi_x + a_y\Psi_y) = \lambda\frac{(1+c_1R\Psi)}{1+c_1^2},\\ R\Delta\Psi + r\left[\frac{-\omega-c_1}{1+c_1^2} + 3\frac{c_1-c_2}{1+c_1^2}R^2 + \Delta a\right] + 2a_xr_x + 2a_yr_y + 2R_x\Psi_x + 2R_y\Psi_y = \lambda\frac{R\Psi - c_1r}{1+c_1^2}. \end{aligned} \tag{8.18}$$

The boundary conditions for $r(x, y)$ and $\Psi(x, y)$ are the same as in formula (8.9).

Since we are interested in solutions in a neighborhood of the critical value $\bar{c}_2$, we shall assume that

$$\begin{aligned} R = 1 + \varepsilon r_1 + \varepsilon^2 r_2 + \varepsilon^3 r_3 + \ldots,\ \varphi = \omega t + \varepsilon a_1 + \varepsilon^2 a_2 + \varepsilon^3 a_3 + \ldots,\\ \omega = -\bar{c}_2 + \varphi_2\varepsilon^2 + \varphi_3\varepsilon^3 + \ldots,\ c_2 = \bar{c}_2 + \omega_2\varepsilon^2 + \omega_3\varepsilon^3 + \ldots \end{aligned} \tag{8.19}$$

Suppose first that $\varepsilon = 0$, that is, $R = 1$, $\varphi = -c_2 t$. We seek a solution of problem (8.18) in the form

$$\begin{pmatrix} r \\ \Psi \end{pmatrix} = \sum_{m,n=0}^{\infty} \begin{pmatrix} r_{mn} \\ \Psi_{mn} \end{pmatrix} \cos\frac{\pi m x}{l} \cos\frac{\pi n y}{l},$$

in order that the boundary conditions be satisfied. As a result for each pair r_{mn}, Ψ_{mn} we obtain a system of two homogeneous equations which are solvable under the condition

$$\lambda^2 + 2\lambda[\pi^2m^2/l^2 + \pi^2n^2/l^2 + 1] + [\pi^2m^2/l^2 + \pi^2n^2/l^2] \times [(1+c_1^2)\pi^2(m^2+n^2)/l^2 + 2(1+c_1c_2)] = 0. \tag{8.20}$$

Problem (8.18) has an eigenvalue which is equal to zero under the condition

$$(1+c_1^2)\pi^2(m^2+n^2)/l^2 + 2(1+c_1c_2) = 0. \tag{8.21}$$

It determines c_2 if we set $m^2 + n^2 = 1$.

Suppose now that $\varepsilon \neq 0$, relations (8.19) are satisfied, and

$$\begin{aligned} \frac{\lambda}{1+c_1^2} = \varepsilon\lambda_1 + \varepsilon^2\lambda_2 + \ldots,\ r = \rho_0 + \varepsilon\rho_1 + \varepsilon^2\rho_2 + \ldots,\\ \Psi = \Psi_0 + \varepsilon\Psi_1 + \varepsilon^2\Psi_2 + \ldots. \end{aligned} \tag{8.22}$$

We substitute the expansions (8.19) and (8.22) into Eqs. (8.18) and equate terms with like powers of ε. The equations of zeroth order give

$$\rho_0 = E\cos kx + F\cos ky,\ \Psi_0 = -2L\rho_0/k^2 + \text{const}. \tag{8.23}$$

The solvability conditions for the equations of first order lead to the equalities

$$\lambda_1=0,\ AE+BF=0, \tag{8.24}$$

where A and B are determined by formulas (8.16). Solutions of them have the form

$$\begin{aligned}\rho_1&=\xi_1\cos 2kx+\xi_2\cos 2ky+\xi_3\cos kx\cos ky+\xi_4\cos kx+\xi_5\cos ky\\ \Psi_1&=\eta_1\cos 2kx+\eta_2\cos 2ky+\eta_3\cos kx\cos ky+\eta_4\cos kx+\eta_5\cos ky,\end{aligned} \tag{8.25}$$

where $\xi_1=AE[0{,}5+4L^2/(3k^4)]$, $\xi_2=BF[0{,}5+4L^2/(3k^4)]$, $\xi_3=3(AF+BE)$,

$$\eta_1=LAE[1/(2k^2)-2L^2/(3k^6)],\ \eta_2=LBF[1/(2k^2)-2L^2/(3k^6)],$$
$$\eta_3=-4L(AF+BE)/k^2,\ \eta_4=-2L\xi_4/k^2,\ \eta_5=-2L\xi_5/k^2,$$

where ξ_4 and ξ_5 are unknown constants. The solvability conditions for the equations of second order in the parameter ε lead to the following relations:

$$E\left[\lambda_2\frac{1+k^2}{k^2}\right]=E\left[PA^2+QB^2+\alpha\frac{|c_1|}{1+c_1^2}\right], \tag{8.26}$$

$$F\left[\lambda_2\frac{1+k^2}{k^2}\right]=F\left[QA^2+PB^2+\alpha\frac{|c_1|}{1+c_1^2}\right], \tag{8.27}$$

where

$$P=\frac{25L^2}{2k^2}-\frac{2L^4}{k^6}-L^2-\frac{k^4}{4}-\frac{23k^2}{4},$$
$$Q=k^2-L^2-4L^2/k^2-k^4/4=-Y.$$

We consider the one-dimensional solution. Suppose A = 0; then $B\neq 0$, F = 0, $E\neq 0$. Equation (8.27) is satisfied identically, and from Eq. (8.26) with consideration of formulas (8.15), (8.16) we obtain

$$\lambda_2\frac{1+k^2}{k^2}=(X-Y)B^2. \tag{8.28}$$

The sign of λ_2 is determined by the sign of the quantity K = X − Y. If K > 0, then the one-dimensional solution is unstable; if K < 0, then it is stable.

Suppose the solution is symmetric: $A^2 = B^2 = Z/(X + Y)$. Here $E\neq 0$, $F\neq 0$, and Eqs. (8.26) and (8.27) coincide. After algebraic transformations we obtain

$$\lambda_2\frac{1+k^2}{k^2}=(X+P)A^2=-2KA^2. \tag{8.29}$$

The symmetric solution is unstable for K < 0 and stable for K > 0. The magnitude of K is connected with the parameters of the problem in the following manner:

$$K=\frac{2L^4}{3k^6}-11\frac{L^2}{2k^2}+\frac{9k^2}{4},\quad L=\frac{-2-k^2}{2c_1},\quad k=\pi/l. \tag{8.30}$$

It is possible to draw the conclusion that the one-dimensional solution will be stable for negative K, while for positive K the symmetric, self-similar solution will be stable.

We shall compare the results obtained with the two-dimensional calculations carried out. From formulas (8.7), (8.11)-(8.16) it follows that in a neigborhood of the bifurcation point $\bar{c}_2$ the following relations hold:

$$\begin{aligned}\rho_{00}&=1-|c_2-\bar{c}_2|(A^2+B^2)[L^2/k^4+L^2/k^2+k^2/4+5/4]+\ldots,\\ \rho_{10}&=|c_2-\bar{c}_2|^{1/2}|A|[1+4L^2/k^4]^{1/2}+\ldots,\\ \rho_{01}&=|c_2-\bar{c}_2|^{1/2}|B|[1+4L^2/k^4]^{1/2}+\ldots,\\ \rho_{11}&=|c_2-\bar{c}_2|\cdot|AB|[9+40L^2/k^4+16L^4/k^8]^{1/2}+\ldots\end{aligned} \tag{8.31}$$

For $c_1 = 1.5$, k = 1, $\bar{c}_2 = -1.75$, and L = −1. For $c_2 = -1.85$, that is $\varepsilon^2 = 0.1$, formulas (8.31) give $\rho_{00} = 0.903$, $\rho_{01} = 0.372$. We note that in this case K = −31/32; therefore, the one-dimensional solution must be stable. In calculations for the problem in partial derivatives we obtained $\rho_{00} = 0.908$, $\rho_{01} = 0.334$; the harmonics ρ_{mn}, $m > 0$ decay rapidly and tend to zero as $t\to\infty$. In the system of eight ordinary differential equations $\rho_{00} = 0.911$, $\rho_{01} = 0.333$, $\rho_{10} = 0$, $\rho_{11} = 0$.

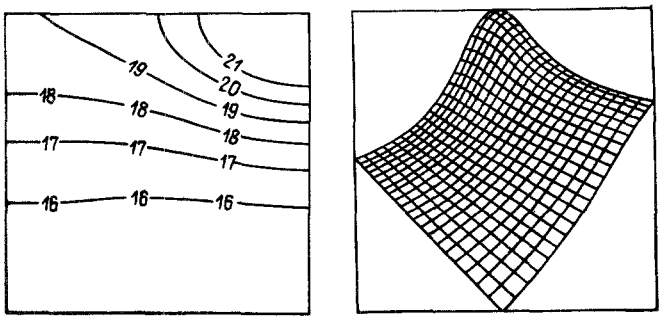

Fig. 48

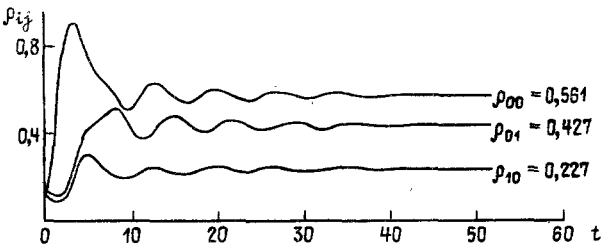

Fig. 49

Fig. 48. Function R corresponding to the nonsymmetric self-similar solution $c_1 = 1.5$, $c_2 = -2.9$, $\ell = \pi$, $h = \pi/20$, $\tau = 10^{-2}$.

Fig. 49. Process of passage to a self-similar solution.

For $c_1 = 3$, $k = 1$, $K = 11/12$; here the symmetric, self-similar solution must be stable. The critical value of c_2 is equal to -2, $L = -0.5$. For $c_2 = -2.1$, $\varepsilon^2 = 0.1$. Formulas (8.31) predict the values $\rho_{00} = 0.937$, $\rho_{01} = \rho_{10} = 0.177$, $\rho_{11} = 0.070$. In the problem in partial derivatives $\rho_{00} = 0.942$, $\rho_{01} = 0.162$, $\rho_{10} = 0.156$, $\rho_{11} = 0.057$ are obtained; in simplified system with N = 2: $\rho_{00} = 0.945$, $\rho_{01} = \rho_{10} = 0.157$, $\rho_{11} = 0.055$. This means that formulas (8.31) describe well the solutions of problem (8.2) in a neighborhood of a bifurcation point when $\varepsilon = \sqrt{0.1} \sim 0.316$.

From relation (8.30) it follows that for small values of c_1 at the time of loss of stability of the homogeneous solution symmetric solutions must also arise. The calculations corroborate this. Such a picture is observed, for example, for $c_1 = 0.4$. It can be concluded that the expansions obtained above agree well with solutions of the problem in partial derivatives and the simplified system.

8.3. Two-Dimensional Self-Similar Solutions. To the simplest attractor of the system of ordinary differential equations – a stable singular point – in the original problem there corresponds a complex self-oscillatory process which is described by a self-similar solution of the form (8.5). We note that the spiral wave is a special case of this solution. Formula (8.5) defines a spiral wave if $R(x, y) = R(\rho)$, $a(x, y) = S(\rho) + m\varphi$, $x = \rho\cos\varphi$, $y = \rho\sin\varphi$. Each of the components u(x, y, t), v(x, y, t) in the self-similar solution is periodic in time, and u(x, y, t) = v(x, y, t + T/4), where T is the period. However, the function $R = (u^2 + v^2)^{1/2}$ does not depend on time. Figure 48 shows its level lines and the type of projection for the nonsymmetric solution.

Here and below the level line with index p corresponds to the value of the function $f_p = -1 + (p - 1)/10$; the axis of the abscissa is directed horizontally, and the axis of the ordinate is directed vertically upward. All two-dimensional calculations in this section were carried out with use of the method of variable directions [58]. The step sizes in time τ and in space h are indicated in the figures. They were determined after carrying out test calculations. In those cases where in the two-dimensional problem the asymptotics is determined by the one-dimensional solution, the latter practically coincides with a solution constructed for the one-dimensional problem by another method [12].

The process of passage to a self-similar solution is shown in Fig. 49. The functions $\rho_{mn}(t)$ tend to constant values at $t \to \infty$, and $\rho_{01} \neq \rho_{10}$.

On the line $c_1 = 3$, as shown above, after loss of stability of the homogeneous solution symmetric solutions of the form (8.5) arise. Figure 50 shows the results of the corresponding calculation. It shows the function R which for sufficiently large values of t does not depend on time. The function u(x, y, t) changes with time in a complex manner, preserving symmetry relative to the diagonal of the square (see Fig. 51). It is evident that the values of the maxima and minima of the function u vary within broad limits and may be either positive or negative.

We shall consider how complication of solutions occurs in the problem in partial derivatives. The sequence on the line $c_1 = 1.5$ is shown in Scheme 4. The first two bifurcations coincide with the bifurcations in the simplified system. Here the parameters of the singular point for which $\rho_{mn} = 0$, $m \neq 0$ up to several percent coincide with the characteristics of the

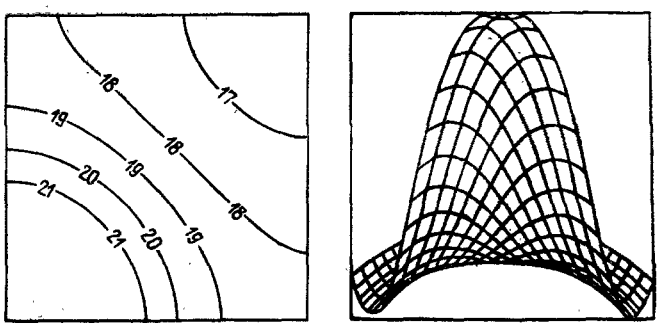

Fig. 50

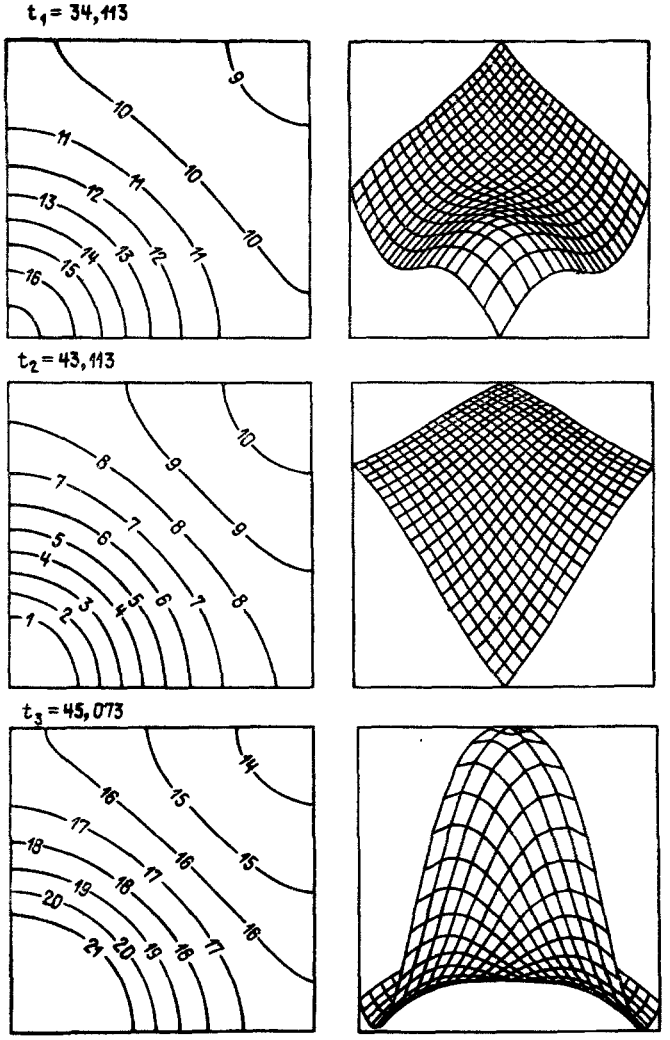

Fig. 51

Fig. 50. Function R(x, y) corresponding to a symmetric, self-similar solution: $c_1 = 3$, $c_2 = -2.5$, $\ell = \pi$, $h = \pi/20$, $\tau = 10^{-2}$.

Fig. 51. Variation of the function u(x, y, t) in the symmetric, self-similar solution; $c_1 = 3$; $c_2 = -2.5$, $\ell = \pi$, $h = \pi/20$, $\tau = 10^{-2}$.

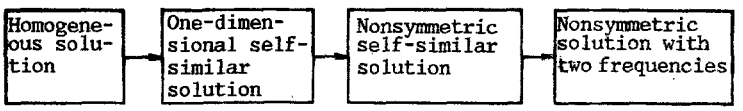

Scheme 4

one-dimensional, self-similar solutions. However, on the whole in problem (8.2) the sequence of transitions is simpler: they contain no analogues of singular points with $\rho_{mn} = \rho_{nm}$ and no symmetric limit cycles.

On the line $c_1 = 3$ the sequence of bifurcations in the simplified system and the original problem is the same as in Scheme 3. The parameters of the self-similar-solutions and the singular points here also agree well (see Fig. 46).

8.4. Two-Frequency Regimes. We shall consider solutions of the problem in partial derivatives for which the functions R and $\dot{a}$ are periodic in time. It can be seen that in this case $\rho_{mn}(t)$ are also periodic: $\rho_{mn}(t+T) = \rho_{mn}(t)$, $\theta_{mn}(t+T) = \theta_{mn}(t) + 2\pi p_{mn}$, $p_{mn} = 0, \pm 1, \pm 2, \ldots$. Such solutions are analogues of limit cycles in the system with N = 2. We note that the functions u and v are not periodic – in the system a steady-state, two-frequency regime will be observed. An analogous situation occurred in the one-dimensional problem.

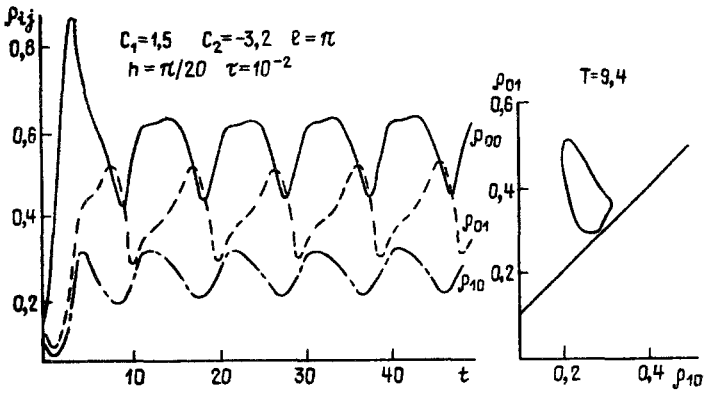

Fig. 52

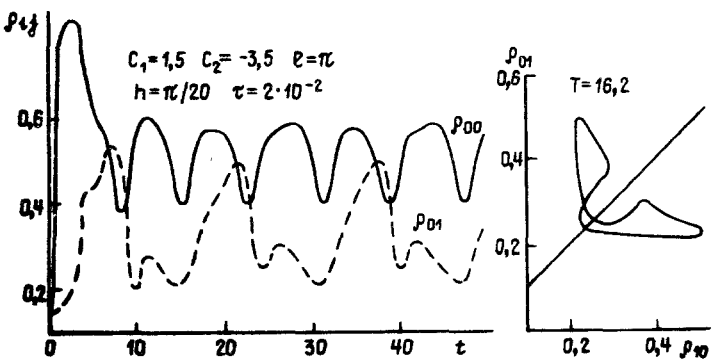

Fig. 53

Two-dimensional solutions of this type are rather complex. In order to clarify the character of the qualitative rearrangement it is necessary to consider their projections onto some finite-dimensional spaces. In the present case projections onto the plane $\{\rho_{10}, \rho_{01}\}$ are the most indicative. They are shown in Figs. 52, 53 together with graphs of the functions $\rho_{mn}(t)$.

The solution shown in Fig. 52 projects onto a curve lying entirely above the diagonal $\rho_{10} = \rho_{01}$. During the course of an entire period the directions of x and y are "not of equal influence." We call it a solution of type I. In the solution shown in Fig. 53 the projection is a closed curve which lies on both sides of the diagonal. This line is almost symmetric with respect to the line $\rho_{10} = \rho_{01}$. The directions x and y in time T/2 "change places": $R(x, y, t + T/2) \approx R(y, x, t)$. This is evident in Fig. 54 where projections of the function R(x, y) are shown at times $t_1 = 30.963$ and $t_2 = 37.333$ ($t_2 - t_1 \approx T/2$). We call such a solution a solution of type II.

It is important to emphasize that solutions of type I and type II differ qualitatively from one another. In Figs. 52 and 53 it is evident that the function $\rho_{00}(t)$ is close to $\rho_{00}(t + T/2)$. However, $\rho_{01}(t)$ and $\rho_{10}(t)$ behave differently: part of the period the function $\rho_{10}(t)$ in the bottom figure (a solution of type II) repeats the course of $\rho_{10}(t)$ in the upper figure; in the remaining part it repeats the course of the function $\rho_{01}(t)$. The period of the cycles increases abruptly as the transition point is approached. For a small change of the parameter c_2 the period of a solution increased by approximately two times (see Figs. 52, 53).

In the simplified system such transitions were not observed. However, the reason for their appearance can be explained by proceeding from features of the finite-dimensional model.

Suppose for some value of the parameter c_2 the system with a sufficiently large number N has two stable singular points situated symmetrically relative to the plane $\rho_{mn} = \rho_{mn}$ but not lying on it. As c_2 decreases a Hopf bifurcation occurs; two limit cycles arise which go over into one another on reflection in this plane. As c_2 decreases the amplitude of the oscillations will increase, and the cycles from different sides will approach the plane of symmetry. Because of the uniqueness of solutions they can touch one another, and hence also the plane $\rho_{mn} = \rho_{nm}$, only at a singlular point.

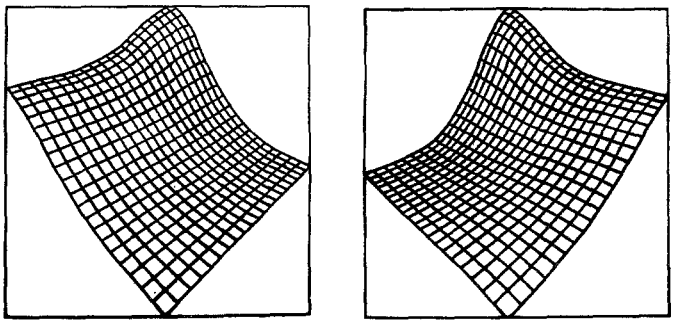

Fig. 54

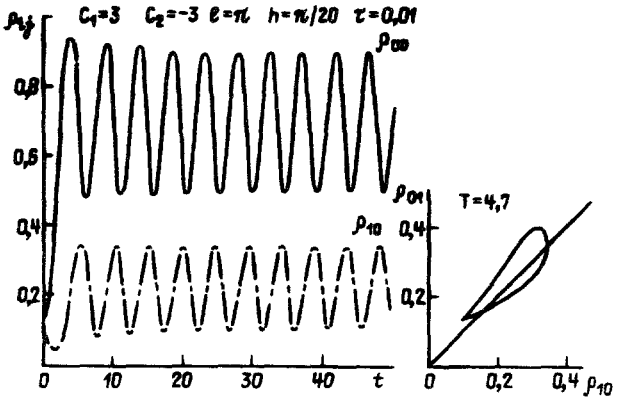

Fig. 55

The period of each of the cycles on approach to this value of the parameter $c_2 = c_2^*$ must increase without bound. After the transition $c_2 < c_2^*$ the cycles are qualitatively rearranged. If earlier, being on a limit cycle, a point rotated about one equilibrium state, now it is alternatively in a neighborhood of each of them.

We point out that for $c_2 = c_2^*$ in the finite-dimensional system a homoclinic trajectory arises, and the system itself possesses special symmetry [if $\{\rho_{mn}(t), \theta_{mn}(t)\}$ is a solution, then $\rho_{nm}(t)$, $\theta_{nm}(t)\}$ is also a solution]. This makes it possible to suppose that here methods developed in the analysis of the Lorenz system can be used effectively [114].

We recall that together with the solution shown in Fig. 53 there exists the solution $\tilde{W}(x, y, t) = W(y, x, t)$ symmetric to it. Therefore, complication of solutions of problem (8.2) can also proceed along a path connected with the symmetry in an essential manner.

A completely different picture is observed for $c_1 = 3$. This is connected with the fact that the Hopf bifurcation in this case admits a symmetric, self-similar solution as in the simplified system with N = 2. The symmetry is then lost. Figures 55 and 56 show a nonsymmetric solution with a periodic function R which cannot be assigned to either type I or type II.

The circumstance that analogues of limit cycles can determine the asymptotics of the two-dimensional problem (8.2) is very important. Indeed, there is the widespread notion that the basic forms of order in active media are guiding centers and spiral waves. In problem (8.2) they are a special case of the two-dimensional self-similar solution in which the variables are again separated. Indeed, in a particular range of parameters precisely the self-similar solutions determine the asymptotics of the process. However, in a large range of values c_1, c_2, and ℓ they are unstable, and more complicated order arises. It is described by solutions with periodically varying functions R and $\dot{a}$. It is natural to expect that such solutions will be observed in many open dissipative systems near a bifurcation point.

It can be expected that two-frequency regimes will be observed in those cases where the solution has a phase singularity. Apparently, such solutions would be similar to spiral waves in which the function $R = (u^2 + v^2)^{1/2}$ and the frequency of rotation depends periodically on time.

Spiral waves are characteristic not only for self-oscillations but also for excitable media [34, 36]. Therefore, attention should be directed to computational experiments where in the case of excitable media regimes are observed in which the instantaneous radius of rotation of a spiral changes periodically with time [35]. The model studied in this work arose in modeling processes in a heart muscle. It would be interesting to investigate such solutions in the case of Eq. (8.2) for large values of the parameter ℓ also in other models possessing self-oscillatory properties.

When the parameter ℓ is reduced further the solutions of the one- and two-dimensional problems become nonperiodic. In the one-dimensional case both on the line $c_1 = 1.5$ and on the line $c_1 = 3$ complication was connected with a sequence of bifurcations with period doubling. In the two-dimensional problem solutions were also observed in which it was not possible to observe any order during the time of the calculations. However, the mechanism of occurrence of stochastic regimes and their properties require further study.

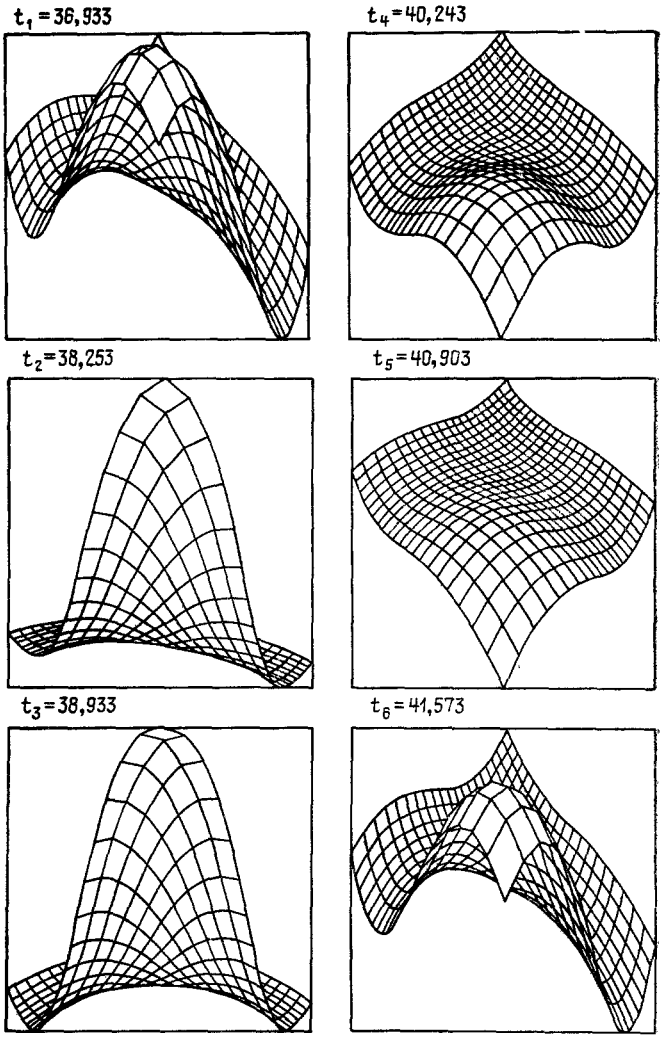

Fig. 56. Variation of the function R(x, y, t). The parameters of the calculation are shown in Fig. 55.

We shall formulate the basic results concerning the two-dimensional problem.

After loss of stability of the homogeneous solution (8.3), as analytic investigation and calculations show, in a wide range of parameters c_1, c_2, ℓ in the two-dimensional solution is stable. Such behavior of solutions should be observed also in a region of rectangular form. Hence, solutions of the one- and two-dimensional problems for certain values of the parameters coincide.

The order in the two-dimensional problem possesses features for which there is no one-dimensional analogue. New classes of symmetric solutions appear which can determine the asymptotics of the process in the case of initial data of general form. For example, solutions symmetric relative to the diagonal of the square. There also arise more complex oscillatory processes than in the one-dimensional case.

The simplified system with N = 2 in some cases correctly conveys the sequence of bifurcations leading to complication of solutions of the problem in partial derivatives. For self-similar solutions there is not only qualitative but also good quantitative correspondence with singular points in the simplified model. In a certain range of parameters (for example, on the line $c_1 = 3$) the limit cycles in the system of eight ordinary differential equations describe well the two-frequency solutions of problem (8.2).

Complication of solutions in the two-dimensional problem differs essentially from the one-dimensional case. Transitions between symmetric and nonsymmetric solutions play an important role in it. The lines on which bifurcations occur lie here much closer to one another in the space of parameters.

The analysis carried out showed that in the two-dimensional problem there exist analogues of the space–time structure which were studied in the one-dimensional formulation. These are the periodic self-similar solutions and two-frequency regimes. It is important to note that in spite of the complexity of the two-dimensional problem in partial derivatives simplified models are a great aid in investigating it.

9. Other Problems Connected with the Analysis of Dissipative Systems in a Neighborhood of a Bifurcation Point

Simplified models have been widely used in the investigation of two-component systems in a neighborhood of a bifurcation point. We see that analysis of each of them requires carrying out numerical calculations and application of various analytic methods. In the hierarchy of models represented in the scheme there are several levels. Work in studying the majority of models cannot be considered complete. We point out some questions requiring further study.

Two-dimensional self-similar solutions played a major role in the study of the two-dimensional problem. In a number of cases they were precisely the solutions which determined the behavior of the system for $t \to \infty$. At the present time many other nonlinear equations have appeared in which they play a basic role [43, 45]. Their construction is connected with solving an elliptic boundary value problem depending on a parameter. Effective methods for their numerical analysis have practically not been developed even for the case of the simplest regions.

In the one-dimensional problem it would be interesting to clarify how the number of self-similar solutions and their properties change as the parameters vary. It is unclear how it would be possible to construct a complete bifurcation diagram. The construction of such a diagram for stationary structures in a number of systems of the form (1.2) led to interesting results [37].

Above we have considered the simplest solutions of the dynamical system (3.6) and one example of a strange attractor. The majority of notions regarding stochastic regimes in systems of ordinary differential equations are connected with the results of studying the Lorenz system. It would be useful to have several more dynamical systems with stochastic behavior. In the model (3.6) it is interesting to clarify how the strange attractor arises as the parameters vary and what are the properties of the complex nonperiodic solutions in the range of parameters III.

The majority of results obtained at the present time pertain to the case of regions of small length when solutions of problem (2.1) and of the dynamical system (3.6) agree well. Increase of ℓ leads to the necessity of studying simplified models with a large number of degrees of freedom. For example, in a three-mode system it is possible to study strange attractors that have 2 positive Lyapunov indices. Analysis of the structure of the attractor carried out for one of the generalizations of the Lorenz equations [107] shows that there are a number of substantial problems here.

Analytic estimates of the dimension of an attractor have been obtained for a class of systems arising in chemical kinetics [20]. It would be interesting to apply these results to the analysis of problem (2.1) and also to clarify by means of various numerical algorithms the law of growth of the dimension with increasing ℓ.

The method of multiscale expansions by means of which Eq. (1.3) was obtained can be successfully applied in studying convective instability of a liquid [110], in the analysis of problems of plasma physics [94], and in the theory of nonlinear waves [118]. The following equation was obtained under the assumption of the closeness of a solution of Eq. (1.3) to a spatially homogeneous solution [104]:

$$\dot{v} = \nu \Delta v - \mu \nabla^2 \nabla^2 v - \lambda v (\nabla v). \tag{9.1}$$

Here v is the gradient of the phase W, $\nu = 1 + c_1 c_2$, $\lambda = 2(c_1 - c_2)$, $\mu = (1 + c_1^2)/2$. In the work [100] the problem of the instability of waves in active media in the two-dimensional case on passing from one stable background to another was posed. Application of the method of multiscale expansions also in this case leads to Eq. (9.1). In such an approach v is interpreted as the local phase velocity of a traveling wave. An analytic solution of Eq. (10.1) of the type of a traveling wave was found in the work [100].

When $\nu > 0$ (9.1) is close to the Burgers equation with regard to its properties [68]. For $\nu < 0$ this equation may have complex, apparently nonperiodic solutions [122]. Indeed,

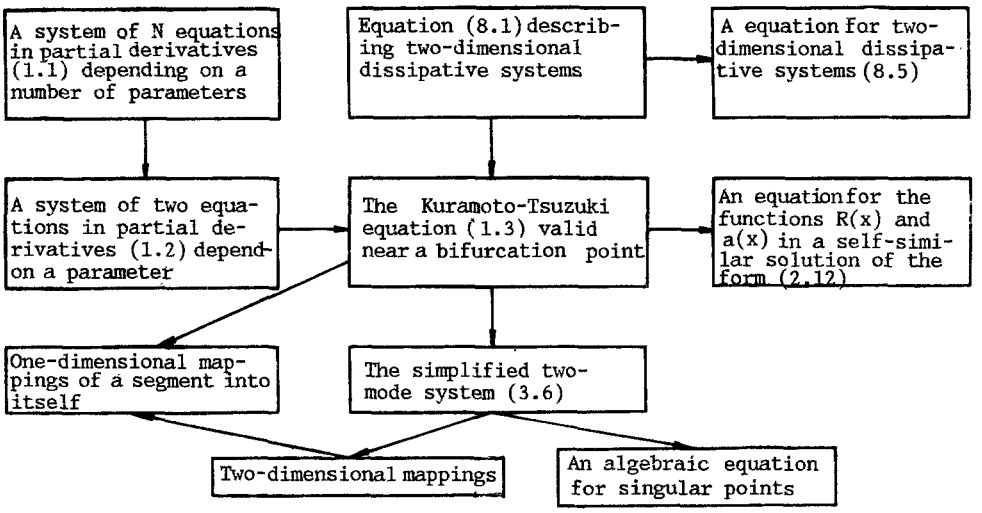

Scheme 5

in the absence of the term $\mu\nabla^2\nabla^2 v$ solutions of it may exist for a bounded time. It can be reduced to a linear equation with negative diffusion by the Hopf–Cole substitution for $\nu < 0$. The term $\mu\nabla^2\nabla^2 v$ ensures stabilization of solutions; it describes dissipation of the harmonics $\exp(i\omega t + ikx)$ for large k. Equation (9.1) is of interest as one of the simplest model equations which in the one-dimensional case can describe chaotic processes.

However, calculations show that in many ranges of the parameters the function $|W(x, t)|$ is essentially inhomogeneous in space; therefore, the range of application of Eq. (9.1) is much smaller than the original equation; this was pointed out in the works [98, 99].

In deriving Eq. (1.3) it was assumed that a Hopf bifurcation or a Turing bifurcation for $k_c \neq 0$ occurs in the system (1.2). Analysis of more complex cases (when $k_c = 0$ or more than two eigenvalues intersect the imaginary axis) leads to other equations [111],

One of the generalizations of the Kuramoto–Tsuzuki equation is connected with consideration of subsequent terms in the expansions with respect to the small parameter in problem (1.2). Suppose the nonlinear sources in this system depend on two parameters λ and μ. We write Eq. (1.3) in the form

$$W_t = d_0 W_{xx} + (a_1 + a_2|W|^2)W. \tag{9.2}$$

Suppose that for $\mu < \mu_0$ $\mathrm{Re}\, a_2 < 0$, and for $\mu > \mu_0$ $\mathrm{Re}\, a_2 > 0$. In the latter case Eq. (9.2) is not applicable: as the parameter λ varies the amplitude of the solution changes by a jump to a finite quantity. The Fitz-Hu-Hagumo model and other models where threshold effects play an essential role give examples of this behavior [66]. In order to describe these effects it is necessary to consider subsequent terms and pass to the equation

$$W_t = d_0 W_{xx} + (a_1 + a_2|W|^2 - a_3|W|^4)W, \tag{9.3}$$

where d_0, a_1, a_2, a_3, are complex constants [124]. The possibility of such a transition is connected with the presence of still another small parameter $\sim(\mu - \mu_0)^{1/2}$. Therefore, Eq. (10.3) does not possess the same generality as Eq. (1.3) and has a much more limited range of applications.

In passing from the original system (1.2) to Eq. (1.3) the one-dimensionality of the problem is essential: the form of the functions f in formula (1.4) can be uniquely determined from the linearized equation. In the multidimensional case the situation is more complicated – the linearized problem may have several solutions; the number of them depends in an essential way on the geometry of the region. For example, for a square $f_1 = \exp(ikx)$, $f_2 = \exp(iky)$, $f_3 = \alpha f_1 + \beta f_2$.

Equations describing two-component systems for a Turing bifurcation were obtained in the two- and three-dimensional case in [111]. For regions of different geometry these equations may constitute systems not of two equations, as (1.3), but of a larger number of equations. A detailed analysis of them would be very useful.

A model connected with a discrete analogue of Eq. (1.3) is used in some physical problems. A system of ordinary differential equations is obtained by replacing W_{xx} by $[W(x + h) - 2W(x) + W(x - h)]/h^2$ [3].

A number of generalizations of the Kuramoto–Tsuzuki equation arise in problems of hydrodynamics. A two-dimensional equation containing derivatives with respect to the x and y directions with different coefficients arises in the theory of wind waves on water [2]. In a number of cases it is necessary to consider the effect of low noise [80, 111]. Proceeding from the method of multiscale expansions, equations were derived which made it possible to describe a system of convector rolls for low Prandtl numbers [79]. This problem is also of interset.

Above we considered the simplest method of constructing simplified models for problem (1.2) and Eq. (1.3). In a number of hydrodynamic experiments it was found possible to estimate the dimension of the attractor and to show that the number of degrees of freedom is not large [76, 108]. However, it is usually not possible to construct a sufficiently simple model connecting these variables. The Galerkin method often gives systems of high dimension. For many concrete systems the question of constructing effective simplified models remains open.

We note a class of problems arising in nonlinear optics where the dissipative terms are small increments to the terms ic_1W_{xx} and $ic_2W|W|^2$ [75]. It is natural to expect that solutions of equations of this type at particular times will be close to solitons [66, 68]. In a number of cases it is here possible to trace the sequence of bifurcations leading to complication of solutions and chaotic regimes [75].

Thus, the results of investigating two-component systems in a neighborhood of a bifurcation point may find applications in many other problems. A number of unsolved theoretical questions concerning classification of two-component systems are of great interest. This gives reason to suppose that in the future new interesting results can be obtained in this area.

LITERATURE CITED

1. A. A. Andronov, A. A. Vitt, and S. Khaikin, The Theory of Oscillations [in Russian], Nauka, Moscow (1981).
2. A. A. Andronov, Jr. and A. L. Fabrikant, "Landau damping, wind waves, and whistle," in: Nonlinear Waves [in Russian], Nauka, Moscow (1979), pp. 68-104.
3. I. S. Aranson, A. V. Gaponov-Grekhov, and M. I. Rabinovich, "Development of chaos in ensembles of dynamical structures," Zh. Éksp. Teor. Fiz., 89, No. 1 (7), 92-105 (1985).
4. V. I. Arnol'd, "Supplementary Chapters of the Theory of Ordinary Differential Equations [in Russian], Nauka, Moscow (1978).
5. V. I. Arnol'd, Catastrophe Theory [in Russian], Moscow State Univ. (1983).
6. V. S. Afraimovich, V. V. Bykov, and L. P. Shil'nikov, "On attracting sets of the type of the Lorenz attractor," Tr. Mosk. Mat. Obshch., 44, 150-212 (1982).
7. T. S. Akhromeeva, S. P. Kurdyumov, and G. G. Malinetskii, Paradoxes of the World of Nonstationary Structures [in Russian], Znanie, Moscow (1985).
8. T. S. Akhromeeva, S. P. Kurdyumov, G. G. Malinetskii, and A. A. Samarskii, "On classification of two-component systems in a neighborhood of a bifurcation point," Dokl. AN SSSR, 279, No. 3, 591-595 (1984).
9. T. S. Akhromeeva, S. P. Kurdyumov, G. G. Malinetskii, and A. A. Samarskii, "On diffusion chaos in nonlinear dissipative systems," Dokl. AN SSSR, 279, No. 5, 1091-1096 (1984).
10. T. S. Akhromeeva and G. G. Malinetskii, "Oscillatory processes in nonlinear dissipative media. On some simplified models," Preprint, Inst. Prikl. Mat. AN SSSR, No. 53 (1982).
11. T. S. Akhromeeva and G. G. Malinetskii, "Two-component systems in a neighborhood of a bifurcation point. The behavior of solutions in small regions," Preprint, Inst. Prikl. Mat. AN SSSR, No. 29 (1983).
12. T. S. Akhromeeva and G. G. Malinetskii, "On new properties of nonlinear dissipative systems," Preprint, Inst. Prikl. Mat. AN SSSR, No. 118 (1983).
13. T. S. Akhromeeva and G. G. Malinetskii, "On diffusion chaos," Preprint No. 140, Inst. Prikl. Mat. AN SSSR (1983).
14. T. S. Akhromeeva and G. G. Malinetskii, "On symmetric solutions of the Kuramoto–Tsuzuki equation," Differents. Uravn., 20, No. 7, 1281-1283 (1984).
15. T. S. Akhromeeva and G. G. Malinetskii, "The simplest types of order in two-dimensional dissipative systems," Preprint No. 112, Inst. Prikl. Mat. AN SSSR (1984).
16. T. S. Akhromeeva and G. G. Malinetskii, "The simplest types of order in open dissipative systems," Differents. Uravn., 21, No. 4, 657-668 (1985).

17. T. S. Akhromeeva and G. G. Malinetskii, "On a strange attractor in a problem of synergetics," Preprint No. 89, Inst. Prikl. Mat. AN SSSR (1985).
18. T. S. Akhromeeva and G. G. Malinetskii, "On nonuniqueness of a class of self-similar solutions of the Kuramoto–Tsuzuki equation," Differents. Uravn., 21, No. 9, 1577-1582 (1985).
19. T. S. Akhromeeva and G. G. Malinetskii, "Periodic regimes in nonlinear dissipative systems near a bifurcation point," Zh. Vychisl. Mat. Mat. Fiz., 25, No. 9, 1314-1326 (1985).
20. A. V. Babin and M. I. Vishik, "Attractors of evolution partial differential equations and estimates of their dimension," Usp. Mat. Nauk, 38, No. 4, 133-187 (1983).
21. B. N. Belintsev, "Dissipative structures and problems of biological morphogenesis," Usp. Fiz. Nauk, 141, No. 1, 55-101 (1983).
22. V. S. Berman and Yu. A. Danilov, "On group properties of the generalized Landau–Ginzburg equation," Dokl. AN SSSR, 258, No. 1, 67-70 (1981).
23. L. A. Bunimovich and Ya. G. Sinai, "Stochasticity of the attractor in the Lorenz model," in: Nonlinear Waves [in Russian], Nauka, Moscow (1979), pp. 212-226.
24. V. A. Vasil'ev, Yu. M. Romanovskii, and V. G. Yakhno, "Self-wave processes in distributed kinetic systems," Usp. Fiz. Nauk, 128, No. 4, 625-666 (1979).
25. K. Vidal, "Dynamic instabilities observable in the Belousov–Zhabotinskii relation," in: Sinergetika [Russian translation], Mir, Moscow (1984), pp. 109-125.
26. R. Williams, "The structure of the Lorenz attractor," in: Strange Attractors [Russian translation], Mir, Moscow (1981), pp. 58-72.
27. E. B. Vul, Ya. G. Cinai, and K. M. Khanin, "Feigenbaum's universality and the thermodynamic formalism," Usp. Mat. Nauk, 39, No. 3, 3-37 (1984).
28. V. A. Galaktionov, S. P. Kurdyumov, A. P. Mikhailov, and A. A. Samarskii, "Localization of heat in nonlinear media," Differents. Uravn., 17, No. 10, 1826-1841 (1981).
29. R. Gimor, Applied Theory of Catastrophes [Russian translation], Vols. I, II, Mir, Moscow (1984).
30. G. G. Elenin, S. P. Kurdyumov, and A. A. Samarskii, "Nonstationary dissipative structures in a nonlinear, heat-conducting medium,," Zh. Vychisl. Mat. Mat. Fiz., 23, No. 3, 19-28 (1983).
31. A. M. Zhabotinskii, Concentrated Self-Oscillations [in Russian], Nauka, Moscow (1974).
32. N. V. Zmitrenko and S. P. Kurdyumov, "The N- and S-regimes of compression of a finite mass of plasma and features of regimes with peaking," Zh. Prikl. Mekh. Tekh., No. 1, 3-23 (1977).
33. N. V. Zmitrenko and A. P. Mikhailov, Thermal Inertia [in Russian], Znanie, Moscow (1982).
34. V. S. Zykov, Modeling Wave Processes in Excitable Media [in Russian], Nauka, Moscow (1984).
35. V. S. Zykov and O. A. Morozova, "Cycloid circulation of spiral waves in various models of excitable media," Pushchino, Texts of Reports of the All-Union Seminar "Mathematical and Computational Methods in Biology" (1985), pp. 76-77.
36. G. R. Ivanitskii, V. I. Krinskii, and E. E. Sel'kov, Mathematical Biophysics of a Cell [in Russian], Nauka, Moscow (1978).
37. A. N. Ivanova and N. E. Maganova, "On the nonlocal character of the behavior of dissipative structures," Zh. Vychisl. Mat. Mat. Fiz., 24, No. 8, 1217-1230 (1984).
38. J. Yorke and E. Yorke, "Metastable chaos: passage to stable chaotic behavior in the Lorenz model," in: Strange Attractors [Russian translation], Mir, Moscow (1981), pp. 193-212.
39. J. Ioss and D. Joseph, Elementary Theory of Stability and Bifurcations [Russian translation], Mir, Moscow (1983).
40. B. B. Kadomtsev, Collective Phenomena in a Plasma [in Russian], Nauka, Moscow (1976).
41. A. N. Kolmogorov, I. G. Petrovskii, and N. S. Piskunov, "Investigation of the diffusion equation combined with the growth of the quantity of matter and its application to a biological problem," Mosk. Gos. Univ., Sec. A, 1, No. 6, 1-27 (1937).
42. S. P. Kurdyumov, "Eigenfunctions of combustion of a nonlinear medium and constructive laws of constructing its organization," in: Modern Problems of Mathematical Physics and Computational Mathematics [in Russian], Nauka, Moscow (1982), pp. 217-243.
43. S. P. Kurdyumov, E. S. Kurkina, A. B. Potapov, and A. A. Samarskii, "The architecture of multidimensional thermal structures," Dokl. AN SSSR, 274, No. 5, 1071-1075 (1984).
44. S. P. Kurdyumov and G. G. Malinetskii, Synergetics – The Theory of Self-Organization. Ideas, Methods, Prospects [in Russian], Znanie, Moscow (1983).
45. S. P. Kurdyumov, G. G. Malinetskii, Yu. A. Poveshchenko, Yu. P. Popov, and A. A. Samarskii, "Dissipative structures in trigger media," Differents. Uravn., 17, No. 10, 1875-1886 (1981).

46. O. E. Lanford, "Strange attractors and turbulence," in: Hydrodynamic Instabilities and Passage to Turbulence [Russian translation], Mir, Moscow (1984), pp. 22-46.
47. E. Lorenz, "Deterministic nonperiodic flow," in: Strange Attractors [Russian translation], Mir, Moscow (1981), pp. 88-116.
48. J. Marri, Nonlinear Differential Equations in Biology. Lectures on Models [Russian translation], Mir, Moscow (1983).
49. J. Marsden and M. MacCracken, Bifurcation of Cycle Creation and Its Applications [Russian translation], Mir, Moscow (1980).
50. J. Marsden, "Attempts to establish a relation between the Navier–Stokes equations and turbulence," in: Strange Attractors [Russian translation], Mir, Moscow (1981), pp. 7-20.
51. N. N. Moiseev, Mathematics Poses and Experiment [in Russian], Nauka, Moscow (1979).
52. G. Nikolis and I. Prigozhin, Self-Organization in Nonequilibiurm Systems [Russian translation], Mir, Moscow (1979).
53. L. V. Ovsyannikov, Group Analysis of Differential Equations [in Russian], Nauka, Moscow (1978).
54. Ya. B. Pesin, "The general theory of smooth hyperbolic dynamical systems," Itogi Nauki i Tekh. VINITI, Sovr. Probl. Matem. Fundam. Napravleniya (1985), pp. 123-172.
55. M. I. Rabinovich and A. L. Fabrikant, "Stochastic automodulation of waves in nonequilibrium media," Zh. Éksp. Teor. Fiz., 77, No. 2 (8), 617-629 (1979).
56. Yu. M. Romanovskii, N. V. Stepanova, and D. S. Chernavskii, Mathematical Biophysics [in Russian], Nauka, Moscow (1984).
57. D. Ruelle and F. Takens, "On the nature of turbulence," in: Strange Attractors [Russian translation], Mir, Moscow (1981), pp. 117-151.
58. A. A. Samarskii, The Theory of Difference Schemes [in Russian], Nauka, Moscow (1977).
59. A. A. Samarskii, "Mathematical modeling and computational experiment," Vestn. AN SSSR, No. 5, 38-49 (1979).
60. A. A. Samarskii, G. G. Elenin, N. V. Zmitrenko, and S. P. Kurdyumov, "Combustion of a nonlinear medium in the form of complex structures," Dokl. AN SSSR, 237, No. 6, 1330-1333 (1977).
61. A. A. Samarskii, N. V. Zmitrenko, S. P. Kurdyumov, and A. P. Mikhailov, "Thermal structures and the fundamental length in media with nonlinear thermal conductivity and a volumetric heat source," Dokl. AN SSSR, 227, No. 2, 321-324 (1976).
62. A. A. Samarskii and S. P. Kurdyumov, "Nonlinear processes in a dense plasma and their role in the problem of laser UTS," Proc. of the Department of Wave and Gas Dynamics of the Mechanics-Mathematics Faculty of Moscow State Univ., No. 3, 19-28 (1979).
63. A. A. Samarskii, T. S. Akhromeeva, and G. G. Malinetskii, "Nonlinear phenomena and computational experiment," Vestn. AN SSSR, No. 9, 64-77 (1985).
64. A. A. Samarskii and Yu. P. Popov, Difference Schemes of Gas Dynamics [in Russian], Nauka, Moscow (1975).
65. Ya. G. Sinai, "Stochasticity of dynamical systems," in: Nonlinear Waves [in Russian], Nauka, Moscow (1979), pp. 192-211.
66. E. Scott, Waves in Active and Nonlinear Media in Application to Electronics [in Russian], Sovet-skoe Radio, Moscow (1977).
67. A. N. Tikhonov, A. A. Samarskii, L. A. Zaklyaz'minskii, P. P. Volosevich, L. M. Degtyarev, S. P. Kurdyumov, Yu. P. Popov, V. S. Sokolov, and A. P. Favorskii, "The nonlinear effect of formation of a self-sustaining, high-temperature electrically conducting layer of gas in nonstationary processes of magnetohydrodynamics," Dokl. AN SSSR, 173, No. 4, 808-811 (1967).
68. G. Whitham, Linear and Nonlinear Waves [Russian translation], Mir, Moscow (1977).
69. O. Phillips, "Interaction of waves – evolution of the idea," in: Modern Hydrodynamics. Successes and Problems [Russian translation], Mir, Moscow (1984), pp. 297-314.
70. H. Haken, Synergetics [Russian translation], Mir, Moscow (1980).
71. A. N. Sharkovskii, "Coexistence of cycles of a continuous transformation of the line into itself," Ukr. Mat. Zh., 16, No. 1, 61-71 (1964).
72. J. P. Eckmann, "Passage to turbulence in dissipative dynamical systems," in: Synergetics [Russian translation], Mir, Moscow (1984), pp. 190-219.
73. M. V. Yakobson, "Ergodic theory of one-dimensional mappings," Modern Problems of Mathematics. Fundamental Directions. Itogi Nauki i Tekh. VINITI, Vol. 2 (1985), pp. 204-226.
74. G. Benettin, L. Calgani, A. Giorgilli, and J. M. Strelcin, "Lyapunov characteristic exponents for smooth dynamical systems: a method for computing all of them," Mechanica, 15, No. 1, 9-30 (1980).
75. K. J. Blow and N. J. Doran, "Global and local chaos in the pumped nonlinear Schrödinger equation," Phys. Rev. Lett., 52, No. 7, 526-529 (1984).

76. A. Brandstarter, J. Swift, H. L. Swinney, A. Wolf, J. D. Farmer, E. Jen, Crutchfield, "Low-dimensional chaos in a hydrodynamic system," Phys. Rev. Lett., 51, No. 16, 1442-1445 (1983).
77. P. Collet and J. P. Eckmann, Iterated Maps on the Interval as Dynamical Systems, Birkhauser, Basel–Boston–Stuttgart (1980).
78. J. D. Crawford and S. Omohundro, "On the global structure of period doubling flows," Physica D, 13, No. 1, 2, 161-180 (1984).
79. M. C. Cross and A. C. Newell, "Convection pattern in large aspect ratio systems," Physica D, 10, No. 3, 229-338 (1984).
80. R. J. Deissler, "Noise strained structure, intermittency and the Ginzburg–Landau equation," J. Stat. Phys., 40, No. 3/4, 371-395 (1985).
81. J. D. Farmer, "Sensitive dependence on parameters in nonlinear dynamics," Phys. Rev. Lett., 55, No. 4, 351-354 (1985).
82. J. D. Farmer, "Chaotic attractors of an infinite-dimensional system," Physica D, 4, No. 3, 366-393 (1982).
83. J. D. Farmer, E. Ott, and J. A. Yorke, "The dimension of chaotic attractors," Physica D, 7, No. 1, 2, 153-180 (1983).
84. M. J. Feigenbaum, "Quantitative universality for a class of nonlinear transformations," J. Stat. Phys., 19, No. 1, 25-52 (1978).
85. M. J. Feigenbaum, "The universal metric properties of nonlinear transformations," J. Stat. Phys., 21, No. 6, 669-706 (1979).
86. A. Gierer and H. Meinhardt, "A theory of biological pattern formation," Kybernetic, No. 12, 30-39 (1979).
87. P. Crassberger and I. Procaccia, "Measuring the strangeness of strange attractors," Physica D, 9, No. 1, 2, 189-208 (1983).
88. C. Grebogy, E. Ott, and J. A. Yorke, "Crises, sudden changes in chaotic attractors and transient chaos," Physica, 7, No. 1, 2, 181-200 (1983).
89. J. Guckenheimer and P. Holmes, Nonlinear Oscillations, Dynamical Systems, and Bifurcations of Vector Fields, Springer-Verlag, New York–Berlin–Heidelberg (1983).
90. P. S. Hagan, "Spiral waves in reaction-diffusion equations," SIAM J. Appl. Math., 42, No. 4, 762-786 (1982).
91. M. Henon, "On the numerical computation of Poincaré maps," Physica D, 5, No. 2, 3, 412-414 (1982).
92. L. M. Hocking and K. Stewartson, "On the nonlinear response of a marginally unstable plane parallel flow to a two-dimensional disturbance," Proc. R. Soc. London A, 326, 289-312 (1972).
93. M. V. Jakobson, "Absolutely continuous invariant measures for one-parameter families of one-dimensional maps," Commun. Math. Phys., 81, No. 1, 39-88 (1981).
94. T. Kakutani, "Plasma waves in the long wave approximation," Progr. Theor. Phys., 55, 97-119 (1974).
95. S. Koga, "Rotating spiral waves in reaction-diffusion systems," Progr. Theor. Phys., 67, No. 1, 167-178 (1982).
96. S. Koga, "Schrödinger equation approach to rotating spiral waves in reaction-diffusion systems," Progr. Theor. Phys., 67, No. 2, 454-463 (1982).
97. H. Koppell and L. N. Howard, "Plane wave solutions to reaction-diffusion equations," Stud. Appl. Math., 52, No. 4, 291-328 (1973).
98. Y. Kuramoto, "Chemical waves and chemical turbulence," in: Synergetics. A Workshop, Springer-Verlag, New York–Berlin–Heidelberg (1977), pp. 164-173.
99. Y. Kuramoto, "Diffusion-induced chaos in reaction systems," Progr. Theor. Phys., 64, 346-367 (1978).
100. Y. Kuramoto, "Diffusion-induced chemical turbulence," in: Dynamics of Synergetic Systems, Springer-Verlag, Berlin–Heidelberg–New York (1980), pp. 134-153.
101. Y. Kuramoto and S. Koga, "Turbulized rotating chemical waves," Progr. Theor. Phys., 66, No. 3, 1081-1083 (1981).
102. Y. Kuramoto and T. Tsuzuki, "Reductive perturbation approach to chemical instabilities," Progr. Theor. Phys., 52, No. 4, 1399-1401 (1974).
103. Y. Kuramoto and T. Tsuzuki, "On the formation of dissipative structures in reaction-diffusion systems," Progr. Theor. Phys., 54, No. 3, 687-699 (1975).
104. Y. Kuramoto and T. Tsuzuki, "Persistant propagation of concentration waves in dissipative media far from thermal equilibrium," Progr. Theor. Phys., 55, No. 2, 356-369 (1976).
105. Y. Kuramoto and T. Yamada, "Turbulent state in chemical reactions," Progr. Theor. Phys., 56, No. 2, 679-681 (1976).

106. T. Y. Li and J. York, "Period three implies chaos," Am. Math. Mon., 82, No. 10, 982-985 (1975).
107. E. N. Lorenz, The local structure of a chaotic attractor in four dimensions," Physica D, 13, No. 1, 2, 90-104 (1984).
108. V. S. L'vov and A. A. Predtechensky, "On Landau and stochastic attractor pictures in the problem of transition to turbulence," Physica D, 2, No. 1, 38-51 (1981).
109. H. T. Moon, P. Huerre, and L. G. Redekopp, "Transition to chaos in the Ginzburg-Landau equation," Physica D, 7, No. 1, 2, 135-150 (1983).
110. A. C. Newell and J. A. Whitehead, "Finite bandwidth, finite amplitude convection," J. Fluid Mech., 38, 279-303 (1969).
111. A. Nitzan and P. Ortoleva, "Scaling and Ginzburg criteria for critical bifurcations in a nonequilibrium reacting system," Phys. Rev. A, 21, No. 5, 1735-1755 (1980).
112. J. C. Roux, "Experimental studies of bifurcations leading to chaos in the Belousof-Zhabotinsky reaction," Physica D, 7, No. 1, 2, 57-68 (1983).
113. D. A. Russell and E. Ott, "Chaotic (strange) and periodic behaviour in saturation by the oscillating two-stream instability," Phys. Fluids, 24, No. 11, 1976-1988 (1981).
114. C. Sparrow, "The Lorenz Equations: Bifurcations, Chaos, and Strange Attractors, Springer-Verlag, New York-Heidelberg-Berlin (1982).
115. K. Stewartson and J. A. Stuart, "A nonlinear instability theory for a wave system in plane Poiseuille flow," J. Fluid Mech., 48, Part 3, 529-545 (1971).
116. H. L. Swinney, "Observations of order and chaos in nonlinear systems," Physica D, 7, No. 1, 2, 3-15 (1983).
117. F. Takens, "Detecting strange attractors in turbulence," in: Dynamical Systems and Turbulence, Warwick 1980, Springer-Verlag, Berlin-Heidelberg-New York (1980), pp. 366-381.
118. T. Taniuti, "Reductive perturbation method and far fields of wave equations," Suppl. Progr. Theor. Phys., 55, 1-35 (1974).
119. K. Tomita and I. Tsuda, "Towards the interpretation of the global bifurcation structure of the Lorenz system," Suppl. Progr. Theor. Phys., 69, 183-199 (1980).
120. A. Turing, "The chemical basis of morphogenesis," Phil. Trans. R. Soc. London B, 237, 37-72 (1952).
121. A. T. Winfree, "The geometry of biological time," Springer-Verlag, Berlin-Heidelberg-New York (1980).
122. T. Yamada and Y. Karamoto, "A reduced model showing chemical turbulence," Progr. Theor. Phys., 56, No. 2, 681-682 (1976).
123. T. Yamada and Y. Karamoto, "Breakdown of synchronized state in a self-oscillatory chemical reaction systems," Progr. Theor. Phys., 60, No. 6, 1935-1936 (1978).
124. K. Yamafuji, K. Toko, J. Nitta, and K. Urahama, "Reductive perturbation approach to hard-mode instabilities of inverted-type bifurcations," Progr. Theor. Phys., 66, No. 1, 143-153 (1981).
125. N. J. Zabusky, "Computational synergetics and mathematical innovation," J. Computat. Phys., 43, No. 2, 195-249 (1981).